

**METHODS FOR THE EVALUATION OF  
MELANIN AS A SUNSCREEN AGENT**

Martin Daniel Bleasel, B.Pharm. (Hons.)

Submitted in fulfilment of the requirements for the degree of Doctor of  
Philosophy

UNIVERSITY OF TASMANIA

March, 1999.

This thesis contains no material that has been accepted for the award of any other degree or graduate diploma in any tertiary institution, except by way of background information and duly acknowledged in the text of the thesis.

To the best of my knowledge and belief, this contains no material previously published or written by another person, except when due reference is made in the text of this thesis.

Martin Bleasel

This thesis may be made available for loan and limited copying in accordance with the Copyright Act 1968.

Martin Bleasel

## **Acknowledgments**

Firstly, I would like to thank my supervisor Dr Stephen Aldous for his guidance throughout the course of this study

I would also like to thank Associate Professor Stuart McLean, and Dr Stephen Aldous, Directors of the School of Pharmacy, University of Tasmania, for kindly making available to me the facilities of the department.

Thank you also to the Royal Hobart Hospital, Acute Care Program for the Research grant which provided financial support towards all the studies undertaken.

From the Central Science Laboratory (CSL), University of Tasmania I would like to thank Dr Noel Davies and Dr Ross Lincolne for their assistance with different studies in this thesis.

The following people also assisted with different studies in this thesis, and I wish to thank them:

Rosie Ashbolt, Menzies Center, University of Tasmania at Hobart

Gina Haddolt, Tasmanian School of Pharmacy, University of Tasmania at Hobart

Glen Haddolt, Leslie Vale, Tasmania

Omar Hasan, Pharmacy Department, University of Tasmania at Hobart

David Blackburn , Tas Paints, Hobart

Andrew Revill Commonwealth Scientific & Industrial Organisation, Hobart

# TABLE OF CONTENTS

<i>Acknowledgments</i> .....	<i>iii</i>
<i>Abbreviations</i> .....	<i>vi</i>
<i>Summary</i> .....	<i>viii</i>
1) Reproducible synthesis of melanins .....	ix
2) Characterisation of melanin .....	x
3) Measurement of skin colour by diffuse reflectance .....	x
4) <i>In vitro</i> evaluation of topical sunscreens .....	xi
<b>CHAPTER 1: BACKGROUND</b> .....	<b>1</b>
SUNSCREENS .....	1
<i>Sunscreen agents</i> .....	1
<i>Sunscreen efficacy</i> .....	2
<i>Skin types</i> .....	5
<i>Sun Protection Factor and skin types</i> .....	6
<b>CHAPTER 2: SYNTHESIS OF MELANINS</b> .....	<b>7</b>
BACKGROUND .....	7
<i>Melanin</i> .....	7
<i>Pigment content and protection against UV damage</i> .....	8
<i>Photoprotection of melanin – mode of action</i> .....	9
<i>Synthesis of melanins</i> .....	9
<i>Development of synthetic procedure</i> .....	12
PREPARATION OF MELANINS .....	13
Aim .....	13
Materials and Methods .....	14
Results .....	18
Discussion .....	19
<b>CHAPTER 3: CHARACTERISATION OF MELANINS</b> .....	<b>22</b>
BACKGROUND .....	22
<i>Overview of analysis methods</i> .....	22
Background to pyrolysis .....	22
<i>Interpretation of pyrolysis results</i> .....	27
PYROLYSIS ANALYSIS OF MELANINS .....	29
Aim .....	29
Materials and Methods .....	29
Results .....	42
Discussion .....	57
<b>CHAPTER 4: <i>IN VITRO</i> EVALUATION OF SUN PROTECTION FACTORS OF SUNSCREEN AGENTS</b> .....	<b>68</b>
BACKGROUND .....	68
<i>Theory</i> .....	70
<i>In vivo</i> determination of SPF values .....	70
<i>In vitro</i> determination of SPF values .....	71
The need for <i>in vitro</i> techniques to measure SPF values greater than 30 .....	73

<i>IN VITRO</i> SPF DETERMINATION PROCEDURE .....	74
Aim .....	75
Materials and methods .....	75
Results .....	93
Statistical analysis of <i>in vitro</i> SPF results .....	96
Discussion .....	100
<b>CHAPTER 5: THE CHARACTERISATION OF SKIN COLOUR BY DIFFUSE REFLECTANCE</b> .....	<b>106</b>
BACKGROUND .....	106
<i>The need for colour measurement</i> .....	106
<i>Theory of Colour Perception</i> .....	107
Colour .....	107
<i>The optics of human skin</i> .....	112
Logarithm of the inverse reflectance .....	113
<i>Other instrumentation for the determination of diffuse reflectance</i> .....	114
EXPERIMENTAL PROCEDURE: DETERMINATION OF DIFFUSE REFLECTANCE .....	115
Aims .....	115
Materials and Methods .....	115
Results .....	124
Discussion .....	139
<b>CHAPTER 6: GENERAL CONCLUSION</b> .....	<b>147</b>
<i>Synthesis of melanins</i> .....	147
<i>Characterisation of melanins</i> .....	147
<i>Characterisation of skin colour by diffuse reflectance</i> .....	148
<i>In vitro evaluations of Sun Protective Factors of sunscreen agent</i> .....	149
APPENDICES .....	151
<i>Appendix 1: Computer software</i> .....	152
Melanin analysis software .....	152
Diffuse reflectance software .....	156
<i>In vitro</i> SPF determination software .....	160
Miscellaneous .....	168
<i>Appendix 2: Tables</i> .....	172
REFERENCES .....	174

## Abbreviations

°C	degrees Celsius
3D	three dimensional
µg	microgram
µL	microlitre
mm	millimetre
µm	micrometre
ADL	Applications Development Language
APTF	Australian Photobiology Testing Facility
ASTM	American Society for Testing and Materials
ASCII	American Standard Code for Information Interchange
CIE	Commission Internationale de l'Eclairge (International Commission on Illumination )
cm	centimetre
DF	degrees of freedom
DNA	deoxyribonucleic acid
EMR	electromagnetic radiation
g	gram
GC	gas chromatography
HP	Hewlett-Packard®
IR	infrared
kg	kilogram
kPa	kilopascal
L	litre
LIR	logarithm of the inverse reflectance
M	molar
MSD	mass selective detector
mA	milliamps
mg	milligram
min	minute
ml	millilitre
MS	mass spectrometry
m/z	mass-to-charge ratio
NIR	near infrared
NIST	National Institute of Standards and Technology (USA)
n	sample size
nm	nanometre
PC	personal computer (IBM compatible)
PLSD	probability of least significant difference
psi	pounds per square inch
PVC	polyvinyl chloride
PY/GC/FID	pyrolysis/gas chromatography/flame ionisation detection
PY/GC/MS	pyrolysis/gas chromatography/mass spectrometry
R <sup>2</sup>	correlation coefficient
RSD	relative standard deviation
SCC	squamous cell carcinoma

<b>SD</b>	standard deviation
<b>SGE</b>	Scientific Glass Engineering
<b>SPF</b>	sun protection factor
<b>SSB</b>	skin surface biopsy
<b>TIC</b>	total ion chromatogram
<b>UV</b>	ultraviolet
<b>UVA</b>	ultraviolet A
<b>UVB</b>	ultraviolet B
<b>UVC</b>	ultraviolet C
<b>UVR</b>	ultraviolet radiation
<b>v</b>	volume
<b>w</b>	weight

This thesis outlines the development of four new procedures (1) to synthesise melanins reproducibly, (2) to objectively determine the degree of structural similarity between melanins (3) to use diffuse reflectance to objectively measure skin colour and (4) to evaluate the SPF of melanin and other sunscreen formulations using *in vitro* methods.

### 1) Reproducible synthesis of melanins

Melanins were synthesised from the precursors adrenaline, dopamine and DL-dopa under controlled conditions. The synthesis procedure outlined was simple and inexpensive and the variables were easily monitored and controlled. The method also allowed for the synthesis of multiple batches of melanin simultaneously in a reproducible fashion.

### 2) Characterisation of melanin

The synthesised melanins were characterised by objective comparison of pyrograms. This was achieved by conversion of the pyrograms to “pseudo-mass spectra” and objective comparison using NIST software that is readily and widely available for the comparison of mass spectra.

The method indicated that the melanin batches, synthesised by the methods outlined in this thesis and later analysed by the methods described, were synthesised in a reproducible manner.

### 3) Measurement of skin colour by diffuse reflectance

A commercially available spectrophotometer was modified to objectively characterise skin colour and changes in skin colour by the determination of the diffuse reflectance of the skin.

This device developed compares favourably with similar devices described in the literature in terms of reproducibility and has the advantages of shorter scan times and a higher resolution. It was simple to construct and at about A\$600 was approximately one tenth the cost of similar commercial devices.

#### 4) *In vitro* evaluation of topical sunscreens

The aim of this work was to develop an improved technique for the *in vitro* determination of SPF values of sunscreens. The method outlined differs from other *in vitro* techniques in that it utilises a standard spectrophotometer operated in a pseudo-double beam mode. The pseudo-double beam mode compared detector responses taken at different gains in single beam mode, and was used to increase the linear range of the spectrophotometer detector, allowing the measurement of SPF values greater than 30 which is difficult using standard *in vitro* techniques. In theory, SPF values greater than > 1000 could be measured by this method.

The value of this technique was subsequently demonstrated when it correctly measured the SPF value of a commercially available sunscreen that had been assigned an incorrect SPF value from earlier *in vivo* testing. The corrected value was subsequently confirmed by independent *in vivo* testing.

## Summary

Australia has the highest incidence of skin cancer in the world with almost 1000 cases of non-melanoma cancer per year in 1990. Melanoma rates in 1989 were 30.2 cases per 100,000 in men and 23.9 per 100,000 in women. Between 1960 and 1989, there was an average increase in melanoma mortality of 6.3 % in men and 2.9 % in women [1-3]. While there are indications that mortality rates from melanomas have decreased in recent years, it is still a significant cause for concern [4].

As sun exposure is the principal cause of skin cancer [5-7], the use of sunscreens, which act as UV filters to decrease the skin exposure to the sun, would be expected to decrease skin cancer mortality. There is a body of evidence to suggest that this hypothesis is true. However, controversy surrounding the use of sunscreens has arisen for a number reasons; (1) the unknown detrimental effects of the long term application of sunscreen chemicals to the human skin, (2) the inability of some sunscreens to protect against UVA radiation and (3) the lack of widely accepted testing methods for sunscreen protection against UVA radiation and immunosuppression and (4) (for the general public) from media coverage of controversial interpretations of scientific studies [8-12].

Melanin is a natural polymer produced in the skin and is widely believed to be the principal agent responsible for the prevention of ultraviolet damage from the sun, not only in humans, but also in other species [13-22].

The widely believed significant role of natural melanin in protecting the skin from damage due to solar radiation, and the clear link between the amount of melanin in the skin and a reduced likelihood of skin cancer, indicate that melanin may be an useful sunscreen agent. While, to the author's knowledge, there is as yet no widely available melanin containing sunscreen, there have been number of patent applications in recent years [23-28], suggesting that sunscreens containing melanin may eventually become readily available.

As a result, there will be an increasing need for methods to synthesise melanin in a reproducible fashion and for methods to test the effectiveness of sunscreens containing melanin or other sunscreen agents.

This thesis outlines the development of four new procedures (1) to synthesise melanins reproducibly, (2) to objectively determine the degree of structural similarity between melanins (3) to use diffuse reflectance to objectively measure skin colour and (4) to evaluate the SPF of melanin and other sunscreen formulations using *in vitro* methods.

### 1) Reproducible synthesis of melanins

Melanins were synthesised from the precursors adrenaline, dopamine and DL-dopa under controlled conditions. The dopamine and DL-dopa syntheses relied on auto-oxidation while the formation of melanin from adrenaline required light as a catalyst. The synthesis procedure outlined was simple and inexpensive and the variables were easily monitored and

controlled. The method also allowed for the synthesis of multiple batches of melanin simultaneously in a reproducible fashion.

## 2) Characterisation of melanin

The synthesised melanins were characterised by objective comparison of pyrograms. This was achieved by conversion of the pyrograms to “pseudo-mass spectra” and objective comparison using software commercially available for the comparison of mass spectra.

The method could be used to differentiate between melanins produced from different precursors on the basis of statistically significant differences between their pyrograms. Conversely, no statistical differences between pyrograms of different batches of melanins produced under the same conditions from the same precursors could be detected. The analytical technique in this study could be used in combination with other analytical techniques to determine if the melanins synthesised by the methods outlined in this thesis were reproducible. It could also form the basis of future studies examining differences between melanins synthesised from the same precursor but under different conditions.

## 3) Measurement of skin colour by diffuse reflectance

A commercially available spectrophotometer was modified to objectively characterise skin colour and changes in skin colour by the determination of the diffuse reflectance of the skin. Results obtained with the modified

spectrophotometer were compared with results obtained from a commercial colour-measuring device.

This section of work was undertaken to provide a method for assessing the ability of sunscreen formulations to adhere to the skin. As a melanin containing sunscreen is likely to be brown, the ability of a formulation to adhere to skin could be monitored by objectively measuring changes in the skin colour as the product was washed or worn off the skin.

This device developed compares favourably with similar devices described in the literature in terms of reproducibility and has the advantages of shorter scan times and a higher resolution [17, 29-31]. It was simple to construct and at about A\$600 was approximately one tenth the cost of similar commercial devices.

#### 4) *In vitro* evaluation of topical sunscreens

The aim of this work was to develop an improved technique for the *in vitro* determination of SPF values of sunscreens. The method described determines the relative amount of UV light, at 5 nm intervals between 290 and 400 nm, that is transmitted through an applied layer of sunscreen and calculates an *in vitro* SPF. This differs from other *in vitro* techniques in that it utilises a standard spectrophotometer operated in a pseudo-double beam mode. The pseudo-double beam mode compared detector responses taken at different gains in single beam mode and was used to increase the linear range of the spectrophotometer detector.

The advantage of the pseudo-double beam mode, over the double beam mode, was that it was many times more sensitive, allowing the measurement of SPF values greater than 30. Evaluating products with SPF values greater than 30 is difficult using standard *in vitro* techniques due to the large light intensity range that is required to be measured.

The substrates used in the *in vitro* SPF evaluations were human stratum corneum and Transpore™ surgical tape. The substrates were easily obtained and the method was fast, simple and capable of measuring high SPF sunscreens (>70). The value of this technique was subsequently demonstrated when it correctly measured the SPF value of a commercially available sunscreen that had been assigned an incorrect SPF value from earlier *in vivo* testing. The corrected value was subsequently confirmed by independent *in vivo* testing.

# CHAPTER 1: BACKGROUND

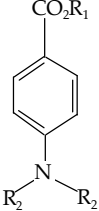
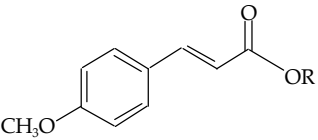
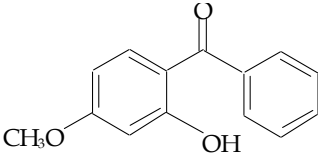
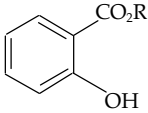
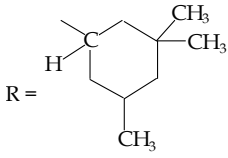
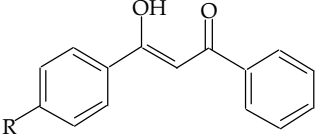
## SUNSCREENS

Sunscreens were developed to prevent UVR induced damage . The first reported use of sunscreens in the world was in 1928, in the United States with the commercial introduction of an emulsion containing two sunscreen chemicals, benzyl cinnamate and benzyl salicylate. In the early 1930s, a product containing 10 % salol (phenyl salicylate) appeared on the Australian market [32].

### **Sunscreen agents**

Sunscreens can be broadly classified into physical blockers and chemical absorbers [33]. The physical blockers include zinc oxide, titanium dioxide and red petroleum. Physical blockers reflect or scatter incident radiation across the UV, visible, and infrared part of the electromagnetic spectrum [33, 34]. Most of the chemical absorbing sunscreens belong to one of five structural categories containing conjugated bonds; para-amino benzoates (PABA), cinnamates, benzophenones, salicylates and dibenzoyl methanes, see Table 1-1. These sunscreens absorb photons of UV radiation. They release the energy gained by the photon thermally through vibrational relaxation of the sunscreen molecule enabling it to absorb another photon of UV radiation and repeat the process [34]. The PABA derivative sunscreens cause a photoallergic response in 1-2 % of the population and are now not widely used [34].

**Table 1-1: Structures and examples of the substances most commonly used in commercial sunscreen preparations [34, 35].**

Category	Structure	Examples	UV Absorption $\lambda_{\max}$ (nm)
Para amino benzoates (PABA derivatives)		PABA $R_1 = R_2 = H$	283-289
		2-ethylhexyl- <i>p</i> -dimethylaminobenzoate (Padimate O) $R_1 = -CH_2CH(C_2H_5)C_4H_9$ $R_2 = -CH_3$	310
Cinnamates		2-ethylhexyl- <i>p</i> -methoxycinnamate (Parsol <sup>®</sup> MCX) $R = -CH_2CH(C_2H_5)C_4H_9$	310
		2-ethoxyethyl- <i>p</i> -methoxycinnamate (Giv Tan F) $R = -C_2H_4-O-C_2H_5$	310
Benzophenones		(2-hydroxy-4-methoxy)-benzophenone (oxybenzone)	288-290 & 325
Salicylates		Homomenthyl salicylate $R =$ 	309
		Octyl salicylate $R_1 = -C_8H_{17}$	310
Dibenzoylmethanes		Avobenzene (Parsol <sup>®</sup> 1789) $R = -C(CH_3)_3$	358
		4-isopropyl-dibenzoylmethane $R = -CH(CH_3)_2$	315

### Sunscreen efficacy

The efficacy of a sunscreen is often described in terms of a sun protection factor or SPF. The SPF is defined as the duration of a constant UV exposure

required to produce minimal erythema in sunscreen protected skin divided by the duration of UV exposure required to produce erythema in skin that is not protected by sunscreen. The determination of SPF values is covered in more detail in Chapter 4.

By the Australian and New Zealand sunscreen standard a sunscreen can also be classified as a broad-spectrum product if it can be demonstrated, by one of the *in vitro* tests specified, to provide protection against UVA radiation [36].

The SPF of a sunscreen is a measure of how well a sunscreen can protect skin from UV induced erythema (sunburn). However, it is not necessarily a measure of how well a sunscreen prevents other forms of skin damage such as wrinkling, solar keratoses, basal-cell and squamous-cell carcinomas and melanomas.

Two recent studies have examined the beneficial effects of sunscreen application in reducing UV induced photoaging in albino mice. One study examined the benefits of a new sunscreen agent Mexoryl® SX. Mexoryl® SX is a sunscreen which absorbs radiation between 290 and 400 nm with a single peak at 345 nm. In comparison with age-matched controls changes in many of the biochemical, histological and visible signs of photoaging were significantly reduced with topical application of the sunscreen prior to UV irradiation [37]. The other study using a low SPF sunscreen consisting of a UVB screen (Parsol® MCX; maximum absorbance at 310 nm) and a UVA screen (Parsol® 1789; maximum absorbance at 355 nm) showed similar

results. Compared to aged-matched non-irradiated controls, the skin of irradiated mice was thickened and erythematous with coarse, rigid wrinkles on the exposed areas. The UVB sunscreen reduced these effects, with a decrease in skin-fold thickening. With the addition of the UVA sunscreen at 2% the visually assessed protection was enhanced, as the skin appeared normal with no wrinkling or erythema [38].

Another study has shown that daily application of a broad-spectrum sunscreen with an SPF of 17 during an Australian summer (September 1991 to March 1992) reduced the mean number of solar keratoses by 0.6. The control group who applied base cream only had a mean increase of 1.0 in the number of solar keratoses (difference, 1.53; 95 percent confidence interval, 0.81 to 2.25). The study also showed that the sunscreen group had fewer new lesions (rate ratio, 0.62; 95 percent confidence interval, 0.54 to 0.71) and more remissions (odds ratio, 1.53; 95 percent confidence interval, 1.29 to 1.80) than the base-cream group. While solar keratoses are not cancerous they are a risk factor for basal-cell carcinoma and a precursor of squamous-cell carcinoma (although the rate of malignant transformation is low) [39].

Damage to DNA is believed to be one of the principal etiological factors in the formation of skin cancer. Topical application of sunscreens has been shown both *in vitro* and *in vivo* to reduce DNA damage from UV radiation [40-42]. The immune system is believed to play a key role in preventing or delaying the formation of tumour metastasis. The use of broad-spectrum

sunscreens has been shown to decrease UV induced immunosuppression of the skin both *in vitro* and *in vivo* [11, 43, 44].

Animal studies have demonstrated that UVB suncreening agents can protect against the development of UV-induced nonmelanoma skin tumours [43].

Furthermore, analysis of skin cancer mortality in Australia for 1990 – 1994 showed a distinct reduction in the rate of increase for men (5.00 per 100 000 person years, an increase of 3.7 %) and a small fall in mortality for women (2.38 per 100 000, a decrease of 5.2 %) [4]. The analysis also showed a decrease in mortality for the younger age group (those born after 1950). Early detection could partly explain this trend. However, as the mortality rate correlates better to year of birth than year of death this would be more consistent with a changing pattern of sun exposure [4].

The changing pattern of sun exposure, and corresponding changes in mortality, may be due to the major national education campaigns started in the 1980's by the Australian government. The campaigns encouraged the early detection and prevention of skin cancer and the use of sunscreens [1].

This campaign is still ongoing.

### **Skin types**

The colour of a person and/or their ability to tan is often used as a measure of how reactive the skin is to UV radiation. The sun-reactive skin typing was originally developed to determine initial doses of UVA in the treatment of

psoriasis with oral methoxsalen. Skin typing is also widely used as a measure of sunburn sensitivity. A number of studies and standards classify skin types from I to VI based on the criteria in Table 1-2 [18, 36, 44].

**Table 1-2: Sun-reactive skin types adapted from Fitzpatrick 1988, the Australian/New Zealand standard AS/NZS 2604:1997 and Cripps 1981 [18, 36, 44]**

Skin Colour (unexposed skin)	Skin Type	Erythema and tanning reactions	Examples
White	I	<i>Always</i> burn, <i>never</i> tan	Redhead, freckled, Irish-Scots
	II	<i>Always</i> burns easily and tans <i>minimally</i>	Fair-skinned, fair-haired, blue-eyed Caucasians
	III	<i>Burns</i> moderately and tans <i>gradually</i> (to a light brown)	Darker Caucasians
	IV	Burns <i>minimally</i> , <i>always</i> tans (to a moderate brown)	Mediterranean type Caucasians
Brown	V	Rarely burns, tans profusely (to a dark-brown)	Mid-Eastern, some Latin American types
Black	VI	<i>Never</i> burns, deeply pigmented	Black skinned Negroids

### Sun Protection Factor and skin types

In order to assess the degree of protection each skin type has in relation to a conventional sunscreen, Cripps (1981) determined the SPF of each skin type. Using skin type I one as a baseline having an SPF of 1.0, type II had an SPF of 1.67, type III an SPF of 2.5, types IV-V had an SPF of nearly 4, whereas the darker Negroid skin (type VI) had an SPF of 9.68 or nearly 10 times that of type I [18].

## CHAPTER 2: SYNTHESIS OF MELANINS

### BACKGROUND

#### Melanin

The term "melanin" (Gr. *melas* = black) denotes a "complex polymeric, amorphous pigment of biological origin, that is usually dark in colour" [45].

Melanins are found across the plant and animal kingdom [21, 46-50]. Few naturally occurring pigments command more widespread interest than melanins [22]. There are many different types of melanins. They are subdivided on the bases of chemical structure or the tissue or species from which they originate. As eumelanin is the melanin that provides photoprotection in the skin of humans it will be discussed here. Reviews on the origins, nature and chemical structure of the various other melanins can be found elsewhere [20 , 22].

Eumelanins are nitrogen containing, dark brown and black pigments. They are practically insoluble in all solvents and arise by the oxidative polymerisation of 5,6-dihydroxyindole and 5,6-dihydroxyindole-2- carboxylic acid, derived biosynthetically from tyrosine via dopa (see Figure 2-1, for the structure of these compounds) [[22, 51]. Eumelanins usually occur bound to proteins and are responsible for the brown to black coloration of human skin.

## **Pigment content and protection against UV damage**

While melanin is not the only line of defence against UV induced damage to skin, it is generally well accepted that black and brown skin is well-protected against UV induced inflammation and degradation. It is also well accepted that a person's skin colour and/or ability to tan is a major determining factor in the development of skin cancers [16, 19, 52-55].

Melanoma is primarily a disease of lightly pigmented individuals. In India, a country with the majority of the population belonging to skin types IV and V, the incidence of melanoma has been estimated at approximately 0.2 cases per 100,000. Conversely, in Australia the melanoma incidence in a population of predominantly skin types I to III at an equivalent subequatorial latitude has been estimated at around 30 cases per 100,000 people, a 150-fold greater incidence [8, 56].

Other factors involved in protecting the skin from UV induced damage include: the thickness of the stratum corneum (contains UVB absorbing amino-acids), the formation and accumulation of urocanic acid with its ability to undergo cis-trans isomerisation and oxidation, the presence of other pigments such as b-carotene and the enzyme systems which repair UV damage once it has occurred [16].

### **Photoprotection of melanin – mode of action**

Melanin, unlike conventional sunscreens absorbs broadly across the UVB, UVA and visible parts of the electromagnetic spectrum [35, 57]. Melanin is also unique in that it acts both as a chemical sunscreen blocker and a physical sunscreen blocker. As a chemical sunscreen blocker melanin absorbs electromagnetic radiant energy and subsequently dissipates the energy as heat, in a similar fashion to conventional sunscreen chemical blockers. As a physical sunscreen blocker melanin scatters impinging radiation away from the skin's surface reducing the amount of light penetrating into the skin layers. Furthermore, melanin has the ability to act as a free radical scavenger for minimising the harmful effects of other free radicals generated by UV radiation [52, 58].

### **Synthesis of melanins**

Synthetic melanins can be prepared by:

- incubation of one or more monomeric precursors with an enzyme (eg. mushroom polyphenol-oxidase) in a buffered solution. Some commonly used monomeric precursors are shown in Figure 2-1.
- passing air through a buffered solution of one or more of the monomeric precursors. Some precursors can also undergo oxidation in solution with the aeration caused by stirring alone (autoxidation) [59].

- Oxidation of one or more of the monomeric precursors with oxidising agents such as persulphate, peroxide or potassium iodide [20, 26, 54].

Table 2-1 outlines some studies using various precursors and methods of polymerisation or extraction to obtain melanin.

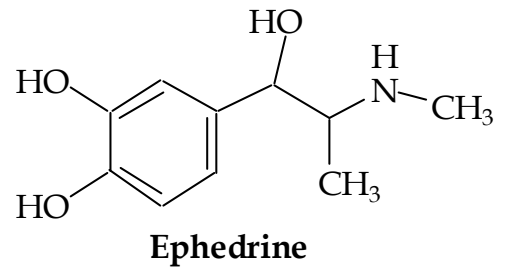
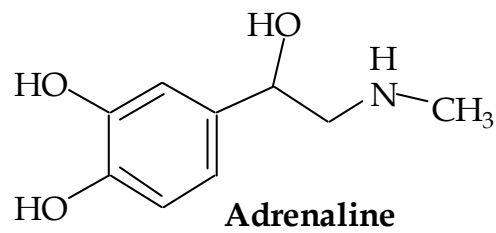
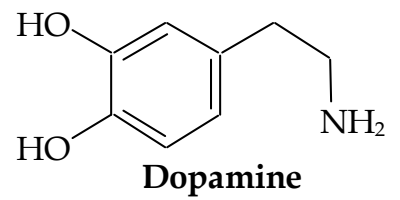
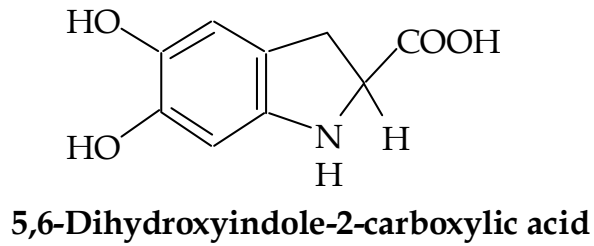
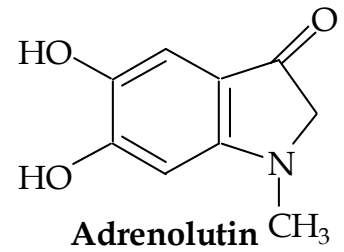
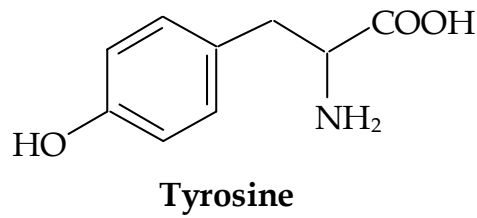
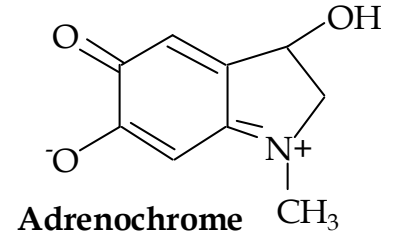
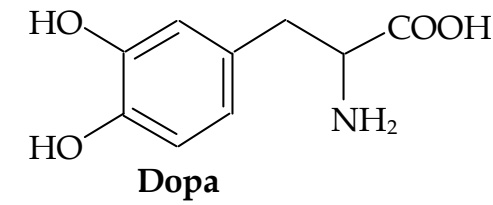
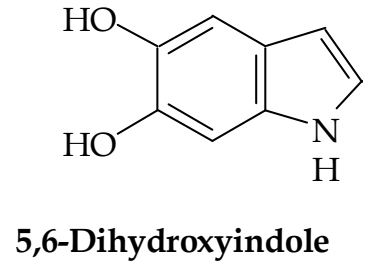
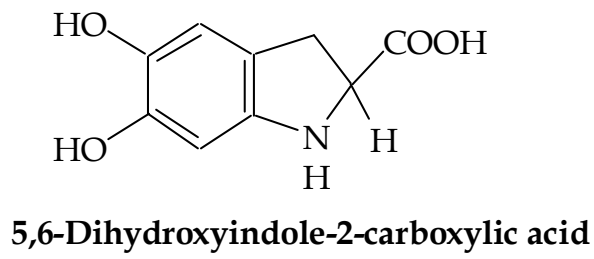


Figure 2-1: Examples of monomeric precursors of melanin.

**Table 2-1: Summary of studies on the synthesis of melanins.**

<i>Melanin Precursor/Type</i>	<i>Method</i>	<i>Agent/Source</i>	<i>Reference</i>
5,6-Dihydroxyindole	enzymatic	tyrosinase	[51]
5,6-Dihydroxyindole-2-carboxylic acid	enzymatic	tyrosinase	[51]
Adrenolutin	auto-oxidation	air	[60]
Catechol	auto-oxidation	air	[59]
Dopa	enzymatic	mushroom tyrosinase	[61]
Dopa	auto-oxidation	air/agitation	[59]
Dopa & Cys-dopa; 5-S-cysteinyl-dopa, varying %'s	enzymatic	mushroom tyrosinase	[62]
Dopamine	auto-oxidation	air/agitation	[59]
Adrenaline	photochemical	UV-Vis Light	[63]
Adrenaline	auto-oxidation	air	[60]
Hair	extraction	human/animal hair	[64, 65]
Melanoma	extraction	Fortner malignant melanoma	[66]
Neuromelanin	extraction	human midbrain / substantia nigra	[67]
Noradrenaline	auto-oxidation	air/agitation	[59]
Sepia	extraction	<i>Sepia officinalis</i>	[68, 69]
Serotonin	auto-oxidation	air/agitation	[59]
Tryptophan	Chemical oxidation	formic acid	[70]
Tyrosine	oxidation	horseradish peroxidase / mushroom tyrosinase	[71, 72]

### **Development of synthetic procedure**

Auto-oxidative methods of melanin synthesis were used for this study due to the high cost, difficult extraction procedures, variable activity and instability of enzyme systems [73, 74].

Initial synthesis of melanins involved passing compressed air at a known rate through a buffered aqueous solution of dopamine.

A number of sources of compressed air were investigated. Air from a piston driven compressor was found to contaminate the solution with oil. An activated charcoal filter was used to try to eliminate the oil residue from the air but it was found that the filter could not remove all oil residues. Use of commercially available cylinders of high purity compressed air, free of oil and particulate matter, was prohibitively expensive. No visible oil residues were found in solutions aerated by rubber diaphragm pumps and these were subsequently used as ready sources of compressed air.

A number of reaction vessel designs were investigated. Vessels open to the atmosphere were found to be unsuitable because of loss of water by evaporation when maintained at elevated temperatures for extended periods.

The reaction vessel finally adopted consisted of a Drechsel bottle with a sintered-glass aerator head and condenser. The airflow through the sintered aerator provided sufficient agitation to ensure adequate mixing of the Drechsel bottle contents.

## **PREPARATION OF MELANINS**

### Aim

The aim of this study was to develop a method for synthesising melanins reproducibly. The method should be simple, with the conditions easily

monitored and allow for the simultaneous production of multiple batches of melanins.

## Materials and Methods

### *Melanin precursors*

Sepia melanin, DL-dopa, dopamine and adrenaline were all purchased from Sigma Aldrich Pty Ltd (Australia). All were of analytical grade.

### *Melanin Synthesis*

Each reaction vessel consisted of a modified Drechsel bottle (250 ml) fitted with a modified head, containing a sintered aerator of porosity grade 0 and a 30 cm Quickfit<sup>®</sup> Graham condenser. Air was supplied by diaphragm pump. Airflow was regulated by a two-way line divider and measured with a gas flow meter.

Five such reaction vessels were connected in series to allow the simultaneous synthesis of five batches of melanin under the same conditions. The apparatus was connected as shown in Figure 2-2 and Figure 2-3.

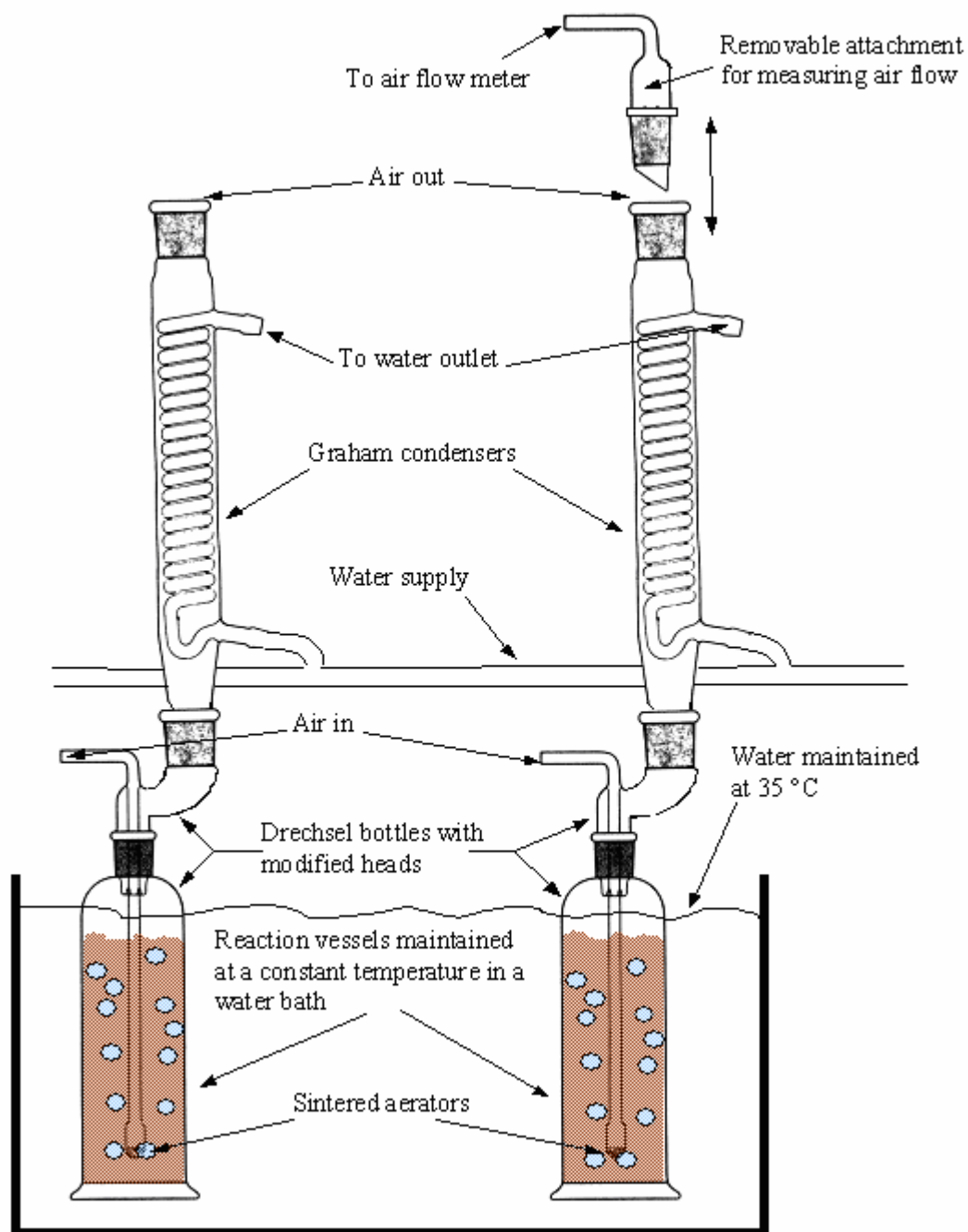


**Figure 2-2:** Schematic representation of the melanin synthesis apparatus showing two of the five reaction vessels.

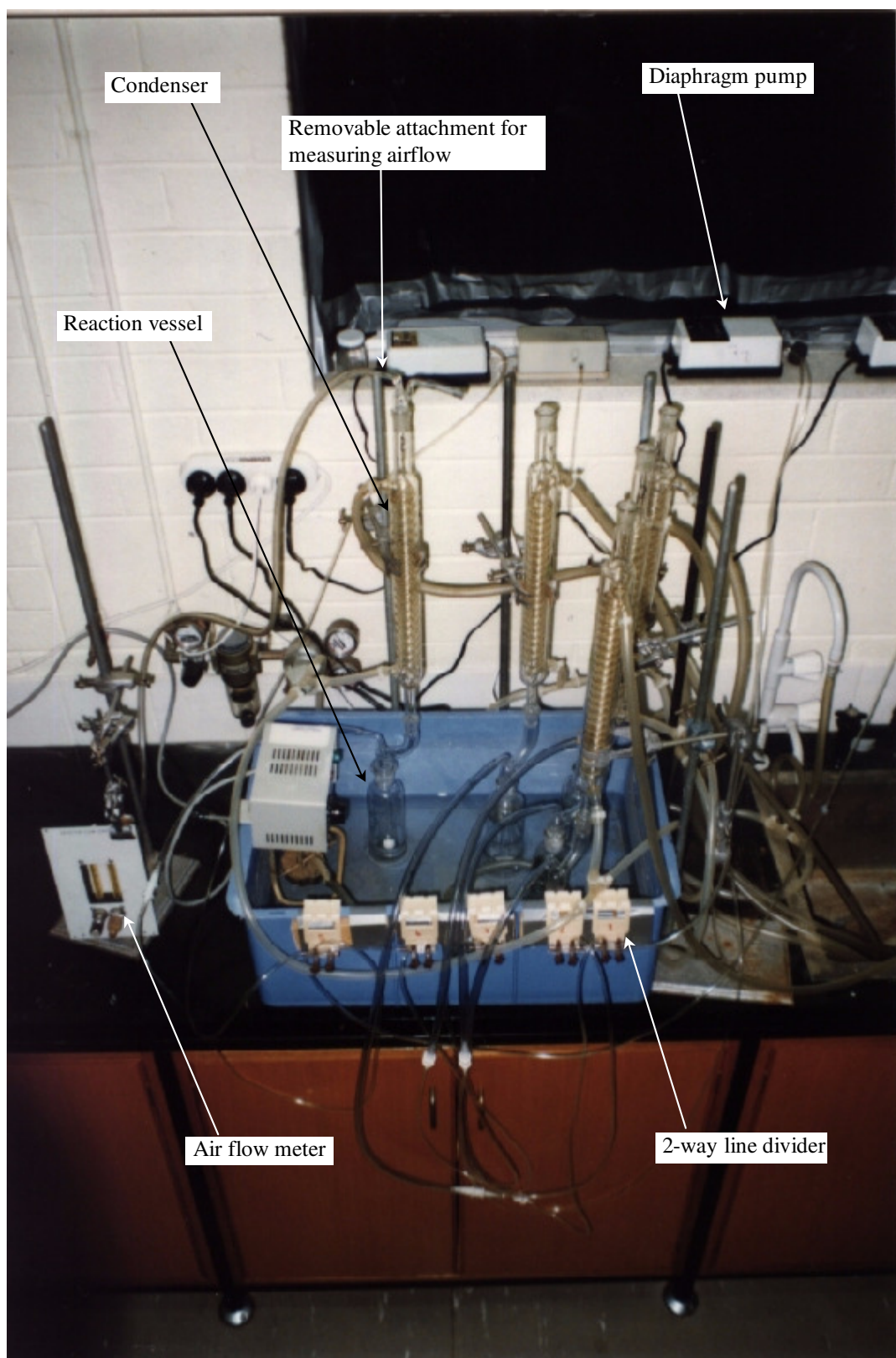


Figure 2-3: Melanin synthesis apparatus.

Periodic measurements of the rate of airflow for each reaction vessel and the water bath temperature were recorded manually.

Batches of dopamine, DL-dopa and adrenaline melanin were synthesised in lots of five.

### *Dopamine, DL-dopa melanin*

Conditions for the synthesis of dopamine and DL-dopa melanin were adapted from that used by Crescenzi [61] and Swan [20].

Dopamine and DL-dopa solutions (0.05 M, adjusted to 200 ml with Sorensen's Phosphate Buffer (0.067 M; pH 8.4)) were refluxed at 35 °C for three days. Air at a flow rate of 1.6 L/min perfused the solutions for the duration of the synthesis.

The volume of each reaction mixture at the end of three days was recorded. Each solution was filtered with a 0.45 micron hydrophilic filter. The solid residue was then dried in an oven at 37 °C for three days. The weight of the residue at the end of the three days was recorded. The residue and filtrate from each sample were stored at -18 °C until required for analysis.

As there was negligible residue after filtering the DL-dopa melanin solution the filtrate was evaporated to dryness with a rotary evaporator and the remaining solid was stored at -18 °C until required for analysis.

### *Adrenaline melanin*

The procedure for the synthesis of adrenaline melanin was adapted from that used by Chirila *et al* [63]. For each vessel adrenaline (1.83 g) was dissolved in 3.6 % HCl (50 mL). Forty five mL of a 2 % ammonia solution was then added and adjusted to 195 mL with Sorensen's Phosphate Buffer (0.201 M; pH 7.3). Air at a flow rate of 1.6 L/min perfused the solutions for three days. The reaction solution was maintained at 35 °C.

The polymerisation of adrenaline to melanin was catalysed by light. Two 75 W tungsten filament bulbs were placed 30 cm above the water bath containing the five reaction vessels.

The volume of each reaction mixture at the end of three days was recorded. Each solution was filtered through a 0.45 micron hydrophilic filter. The residue was then dried in an oven at 37 °C for three days. The weight of the residue at the end of the three days was recorded. The residue and filtrate from each sample were stored at -18 °C until required for analysis.

### Results

Results from the synthesis of melanins are shown in Table 2-2.

Table 2-2: Percentage yields and reaction variables for the synthesis of melanins.

<i>Precursor</i>	% Yield* Mean (n; RSD)	<i>Experimental variables</i>		
		Reaction temperature (°C) Mean (n; RSD)	Air flow (L/min) Mean (n; RSD)	Reaction volume, prior to filtration / evaporation (% of initial) Mean (n; RSD)
<b>Dopamine</b>	45.2 (5; 4.3)	35.0 (11; 1.9)	1.60 (52; 1.22)	94.2(5; 0.47)
<b>DL-Dopa</b>	N/A <sup>†**</sup>	35.2 (9; 0.41)	1.60 (45; 1.1)	94.3 (5; 0.47)
<b>Adrenaline</b>	42.2 (5, 15.2)	34.9 (6; 0.43)	1.60 (30; 0.55)	87.2 (5; 0.83)

\* % Yield (weight of dried melanin/weight of precursor)\* 100.

\*\* Filtration yielded no solid residue.

## Discussion

Although the apparatus was simple in design and construction, a number of design factors were considered. These included the supply, adjustment and measurement of airflow and the water flow to the condensers.

A separate diaphragm pump supplied air to each reaction vessel. Individual pumps allowed for the separate control of the airflow to each reaction vessel. When a single pump supplied air to multiple vessels, changing the airflow to one vessel unavoidably changed the airflow to other vessels, due to changes in the flow resistance of the system. While it is possible to use mass flow controllers to overcome this problem this is relatively expensive when compared with using individual pumps and two-way line dividers.

Controlling airflow with two-way line dividers had two advantages. With ordinary restriction valves, reducing the diameter of the air path reduces the airflow but also increases the back pressure on the pump. A two-way line divider has two restriction valves both supplied by the one air inlet. To decrease the airflow to a reaction vessel the second restriction could be opened to atmosphere, consequently reducing airflow through the other restriction valve without increasing the back pressure on the pump. The ability to control the airflow to the reaction vessels with two restriction valves also allowed for finer adjustment of airflow.

Airflow was measured at the top of each condenser. A Quickfit<sup>®</sup> fitting was attached to the end of the flow meter so that it could be attached and

removed from each condenser quickly and easily. This meant that only one flow meter was required to take measurements from the five reaction vessels.

Requiring only one flow meter reduced the cost of the apparatus.

Furthermore, any variability in flow rates from the reaction vessels could not then be attributed to differences in the measuring apparatus.

There were limitations with the air supply. In this procedure, there was no means of removing chemical residue from the air. As melanin binds to many chemicals [75-78] it may prove necessary, in the future, to remove chemical and particulate residue from the air prior to introduction into the reaction chamber. This could be achieved with the use of an appropriate filter eg. a charcoal filter.

In this study the condensers were connected in parallel, with the water inlet to the condensers forming an unbroken loop, see Figure 2-2 and Figure 2-3. Alternatively, the output and inputs of the condensers could have been connected in series. The advantage of connecting the condensers in series would have been that the flow rate through each condenser would be equal. However, as the water passes through each condenser the water temperature would rise, resulting in less efficient heat exchange between the water vapour and the condensing coils. With the condensers connected in parallel the water temperature passing through each condenser is equal but the flow rate potentially different, due to minor differences in the condensers and tubing. Using PVC tubing of equal diameter and lengths between condensers, variances in the flow rates was minimised. On this scale, the

choice between the two arrangements was arbitrary. On a larger scale, the differences between the two methods would be more pronounced and the flow rate and water temperature through the condensers would need to be monitored and controlled.

The yield of dopamine melanin was significantly higher than DL-dopa and adrenaline melanin. Initial melanin synthesis was done with dopamine as the precursor. Therefore, the conditions for melanin synthesis were optimised for the synthesis of dopamine melanin.

There have been many studies concerned with factors affecting the kinetics of melanin synthesis, such as the influence of pH [51] and the presence or absence of metal ions [60, 79, 80]. The conditions in this study were kept as simple as possible. However, if necessary, various synthesis conditions could be tried simultaneously to determine optimum synthesis conditions or the influences that these conditions have on the kinetic pathways of melanin synthesis.

The synthesis procedure outlined was simple and inexpensive and the variables were easily monitored and controlled. This method also allowed for the synthesis of multiple batches of melanin simultaneously in a reproducible fashion. If necessary, synthesis conditions could be easily modified to produce melanins of different types or higher yields through the modification of reaction conditions.

# CHAPTER 3: CHARACTERISATION OF MELANINS

## BACKGROUND

Melanins have a complex, heterogeneous, polymeric structure, making them difficult to characterise. Many techniques have been tried previously: ultraviolet/visible/IR spectroscopy; nuclear magnetic resonance, electron paramagnetic resonance spectroscopy, photoacoustic phase angle spectroscopy, X-Ray diffraction, laser desorption, PY/GC/FID and PY/GC/MS [67, 69, 78, 81-94].

This chapter details the use of PY/GC/MS and the NIST mass spectral search program for the analysis of melanins, to distinguish between melanins synthesised from different precursors and as a possible means of determining if synthesis is reproducible. The batches of melanins synthesised by the techniques outlined in Chapter 2 were analysed by the method described in this chapter. Due to the complex nature of the structure of melanins it is unlikely a single technique would be sufficient to determine if melanin synthesis was reproducible.

### Overview of analysis methods

#### Background to pyrolysis

Pyrolysis chromatography is useful for the analysis of large molecules and polymers that are not amenable to usual methods. Pyrolysis gas

chromatography involves the breakdown of compounds by heat into a series of volatile products which are subsequently introduced into a gas chromatograph. The volatile products are characteristic of both the sample and the experimental conditions. There are three principle types of pyrolysis units for gas chromatographs;

### 1) The filament pyrolyser

A filament type pyrolyser is resistively heated. Samples are generally placed directly onto a filament or crucible prior to heating. The filament is contained within a chamber with a low dead volume through which carrier gas flows see (Figure 3-1).

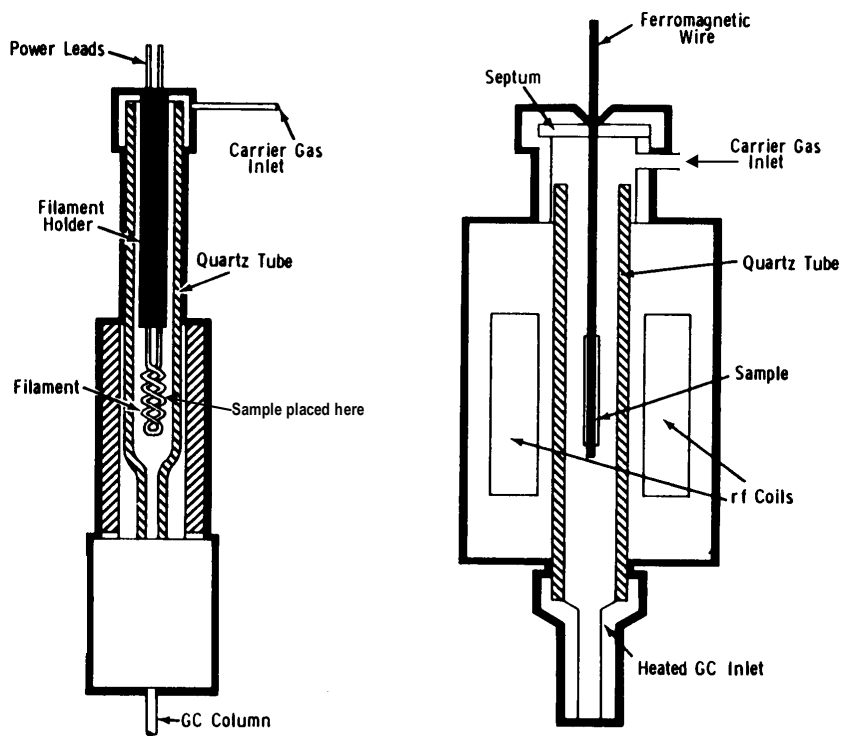
### 2) The Curie-point pyrolyser

This consists of a ferromagnetic wire on which the sample to be analysed is placed. The wire is heated inductively by placing it in a radio frequency field. The final temperature of a Curie-point pyrolyser depends on the composition of the ferromagnetic material. The ferromagnetic wire, with the sample to be analysed, is centred in a quartz tube which is connected to the inlet of a gas chromatograph and through which the carrier gas flows (see Figure 3-1).

### 3) The furnace pyrolyser

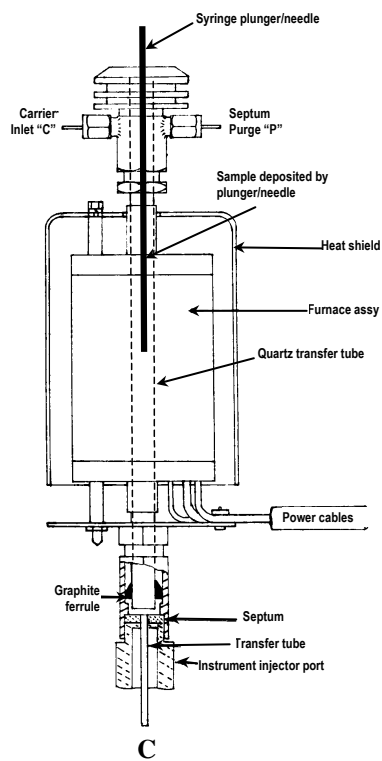
Furnace pyrolysers are also resistively heated. They consist of a quartz tube maintained at a constant pyrolysis temperature. Samples to be analysed are

injected into the heated quartz tube and the volatile decomposition products are passed onto the column by a carrier gas passing through the pyrolysis chamber (see Figure 3-1).



A

B



C

Figure 3-1: A) filament or ribbon type pyrolyser B) Curie-point pyrolyser [95] C) A furnace-type pyrolyser (adapted from [96]).

The pyrolysis products generated from the three types of pyrolysers are often different. This is due not only to the structural differences between the pyrolysers but to the manner in which the samples are heated. With filament and Curie-point pyrolysers, the sample is in intimate contact with the heating source. Once the sample starts to pyrolyse the pyrolysis products will be carried to relatively cooler regions of the pyrolysis chamber by the carrier gas flow. This reduces the formation of secondary pyrolysis products. However, with the furnace-type pyrolyser, as the sample is placed on a plunger it is supported away from the walls, which serve as the primary heat source for the pyrolysis process. As pyrolysis products form, they are carried by the carrier gas from a relatively cool region (the sample support) to hotter regions closer to the heated walls. This increases the probability of secondary pyrolysis products forming. Therefore, the extent of formation of secondary products in a furnace-type pyrolyser is more dependent on the residence time than Curie-point or filament type pyrolysers.

Reproducibility can be poor, not only from one type of pyrolyser to another but also between pyrolysers of the same type. Minor differences in the furnace temperature, sample preparation/introduction and chromatography parameters all contribute to poor reproducibility between pyrolysers of the same or different make [70, 93, 95, 97].

## Interpretation of pyrolysis results

Due to the large number of products generated by the pyrolytic process the chromatograms created are very difficult to interpret and compare. Factors affecting the reproducibility of melanin pyrolysis chromatograms (pyrograms) for comparative purposes include; difficulty in identifying specific peaks in different chromatograms, slight variations in elution times resulting in apparently different peak areas due to a variation in the coelution of two or more peaks and difficulty in differentiating peaks arising from the pyrolysis of melanins from those peaks arising from the pyrolysis of septum fragments unavoidably introduced during sample injection.

These problems can largely be overcome or minimised with the use of a MSD. By monitoring specific target ions it is possible to identify particular peaks in different chromatograms and co-eluting peaks can also be identified and quantified. Similarly, peaks arising from the pyrolysis of silicon-containing septum fragments can be identified and excluded for the purposes of comparison.

Statistical methods and pattern recognition techniques have been used for the comparison of complex variables [98-103], for the comparison of pyrograms [97, 104] including comparison of melanin pyrograms [78, 84, 93].

In the same way that a mass spectrum can be represented as a row vector composed of peak intensities (ion abundances) ordered along an axis (mass/charge ratio), a pyrogram can be analogously represented as a row

vector of peak intensities (detector response) ordered along an axis (retention time).

The National Institute of Standards and Technology (NIST; United States of America) mass spectral search program has been used widely as an objective measure of the degree of similarity between mass spectra of different compounds.

It should therefore be possible to utilise the NIST program to objectively compare chromatograms by converting them into “pseudo-mass spectra”. Because of the wide use and acceptance of the NIST program, this method was chosen to compare the chromatograms created from the pyrolysis of melanins.

The NIST program imports the mass spectrum of a particular compound as a table of values of mass to charge ratio ( $m/z$ ) and their corresponding abundance values. The program then compares the table with other tables in a library, and objectively determines the degree of similarity, which is then represented as both direct and reverse match factors. The program then generates from its library a list of compounds in a decreasing order of the degree of similarity, as represented by the generated match factors.

The match factors are integers ranging from 0 to 1000, with the higher numbers indicating a closer match. The direct match factor is obtained from the comparison of the unknown and the library spectrum. The reverse match factor is obtained from the comparison between the unknown and the library

spectrum ignoring any peaks in the unknown spectrum that are not in the library spectrum [105].

Development language software supplied with the mass spectrometer was used in this study and allowed almost complete automation of the analysis of the pyrolysis data. The details of the process are outlined below in the experimental procedure for the pyrolysis of melanins.

## **PYROLYSIS ANALYSIS OF MELANINS**

### Aim

The aim of this section of the work was to examine the use of the PY/GC/MS and the NIST mass spectral search program for the characterisation of melanins, to distinguish melanins synthesised from different precursors and as a possible means of determining if synthesis was reproducible.

### Materials and Methods

#### *Melanins*

Five batches of each of DL-dopa melanin, dopamine melanin, and adrenaline melanin were synthesised from their respective precursors as described in Chapter 2. Sepia melanin was purchased from Sigma Aldrich Pty Ltd (Australia).

### PY/GC/MS

The pyrolysis unit was an SGE (Australia) Pyrojector furnace-type pyrolyser. The unit was connected to a Hewlett-Packard (HP) 5890 gas chromatograph equipped with a HP 5970 MSD. Data was collected using a PC with HP G1034C data acquisition program. The carrier gas was helium. A 29 m, BP-1 column with an internal diameter of 0.25  $\mu\text{m}$  was used for chromatographic separation.

The syringes used were;

- i) a 1  $\mu\text{L}$  plunger-in-needle syringe with a 70 mm cone-tipped needle, with the plunger abraded with a jewellers cloth to prevent the binding of the plunger to the needle at pyrolysis temperatures
- ii) a solids injector with a spiral needle (SGE; Australia).

The pyrolysis unit was maintained at a constant temperature of 850°C. The head pressure in the pyrolysis unit was adjusted to exceed the injector head pressure of the gas chromatograph so that a split flow of 10-12 ml/min was obtained.

The injector head pressure was 15 psi at 250°C with the detector at 290°C. The oven temperature program consisted of a 2 minute isothermal period at 40°C followed by a 10°C/minute ramp to 300°C.

Blank injections indicated that no residual compounds from previous runs were detected by the analysis system.

A Sanophone<sup>®</sup> ultrasonic bath (IMBROS Scientific; Australia) was used to suspend melanin particles in methanol and clean syringes between runs.

#### *Sepia & dopamine melanin*

Separate suspensions of sepia & dopamine melanin (250 mg/ml) in methanol were sonicated for approximately 30 seconds. Immediately following sonication 1  $\mu$ L of the suspension was drawn up in a plunger-in-needle syringe and injected.

#### *Adrenaline & DL-dopa melanin*

Suspensions of DL-dopa melanin (500 mg/ml) and adrenaline (165 - 250 mg/ml\*) in methanol were sonicated for 30 seconds in an ultrasonic bath then vortexed for 30 sec. A 10  $\mu$ L aliquot of the solution was then spread evenly over the spiral plunger of the solids injector. This was achieved by placing a small droplet of the 10  $\mu$ L aliquot on the spiral plunger, moving the syringe in a rocking motion. The droplet moved over the spiral plunger leaving an even film of melanin over the surface as the methanol evaporated. This procedure was repeated until all of the 10  $\mu$ L aliquot was deposited over the plunger

---

\* The absolute yield of adrenaline melanin ranged from 33 mg-50 mg. All of the

surface. The outer sheath of the spiral plunger was slid over the plunger. The solids injector was then ready to be inserted into the pyrolysis unit.

### *Reproducibility studies*

To measure the within-day variability of the method, dopamine melanin from the same batch was analysed by PY/GC/MS five times within the same day. To measure the inter-day variability method, dopamine melanin from the same batch was analysed by PY/GC/MS on five different days.

### *Analysis of pyrograms*

The NIST mass spectra search program was used as a means of objectively determining the degree of similarity between chromatograms arising from the pyrolysis of the same and different types of melanins.

Custom comparison software was written (Appendix 1-1) to automate the process of;

1. identifying and recording a pyrogram as a table of retention times versus peak abundances and then,
2. converting the table into a pseudo-mass spectral table of pseudo m/z ratios and abundances that could be analysed by the NIST mass spectral search program.

---

final product was added to 200  $\mu$ L of methanol.

The software was written in the development language supplied as part of the Hewlett Packard integration module.

There were three main processes involved in the analysis of pyrograms.

1. The determination of parameters required by the comparison software to identify peaks within a TIC pyrogram (see Figure 3-2).
2. Converting pyrograms into pseudo-mass spectra (see Figure 3-3).
3. Using the NIST mass spectral search program to compare the resulting pseudo-mass spectra (see Figure 3-4).

*Determination of parameter values for comparison software to identify TIC peaks*

To acquire information that would be used by the software to compare pyrograms, TIC peaks were selected and data required for the later identification of these peaks was recorded. TIC peaks were selected by a systematic manual search of pyrograms from different types of melanin. The basic criteria for the selection of TIC peaks within pyrograms were:

- TIC peaks had to originate from pyrolysis of melanin and not as artefacts from pyrolysis of the septum. This distinction was achieved by manual inspection and exclusion of all TIC peaks showing mass spectral evidence of the presence of silicon, such as typical silicon ion clusters of  $m/z +1$  and  $m/z +2$  for ions such as 73, 193, 207, 267 and 281,

- TIC peaks had to chromatograph well as indicated by the shape, width and degree of tailing of the peak,
- TIC peaks had to be of sufficient intensity for reliable quantitation of peak area, evaluated visually by a favourable signal to noise ratio,
- TIC peaks had to be sufficiently resolved from large artefact peaks which may have distorted the mass spectrum of the TIC peak of interest.

As each TIC peak satisfying these criteria was identified, two ions from the mass spectrum of that peak were selected. Criteria for the selection of the two ions were;

- The ions originated from the same TIC peak. This was demonstrated by the abundances of the two ions showing identical time courses when plotted together,
- The ions were major contributors to the overall TIC peak intensity as determined by visual inspection of the mass spectrum of the TIC peak,
- The ions selected were not common ions found in many other pyrogram TIC peaks. This was verified by plotting the abundance time course of the selected ions,
- The more intense of the two ions was designated as the target ion and the less intense as the confirmation ion.

For the two ions selected the parameters required by the comparison software for identifying TIC peaks were recorded:

- The target ion (m/z),
- The confirmation ion (m/z),
- The ratio of target/confirmation ion abundances,
- The time window of the TIC peak, ie. retention time of the target ion  $\pm 2$  minutes.

Information relating to the 38 peaks selected from the melanin pyrograms examined by applying these criteria was entered into the software. The information gathered is given in Appendix 2-1.

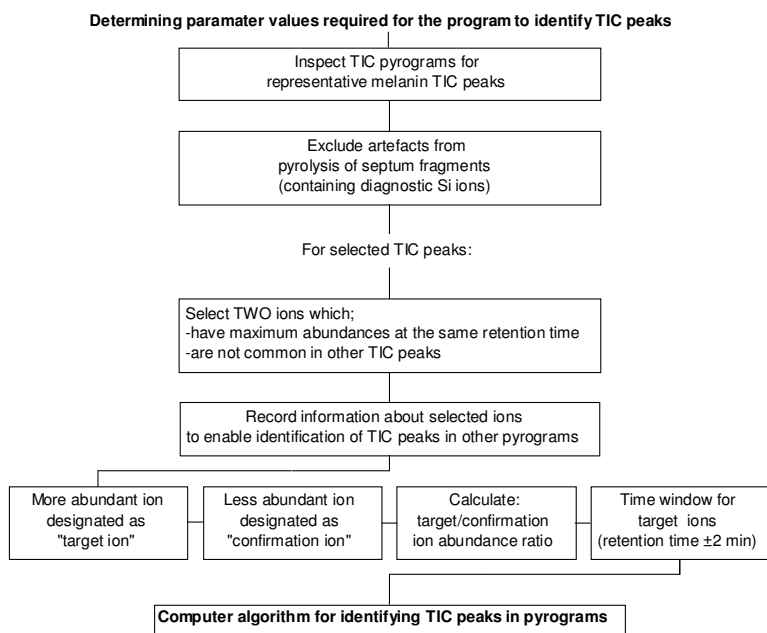


**Figure 3-2: Flow diagram for the determination of parameter values for the identification of TIC peaks within pyrograms.**

*Algorithm for identifying TIC peaks within a pyrogram & converting pyrograms into pseudo-mass spectrums*

The parameter values required (described above) to identify TIC peaks within pyrograms were entered into the comparison software in the form of one dimensional arrays at the start of the program (see Appendix 1-1). Each set of parameter values was assigned a unique identifier which was an integer starting at 100 and increasing in steps of 1.

Figure 3-3 describes the process by which the comparison software identified TIC peaks based on the parameter values defined in the array blocks.

The three ASCII files generated by the software were:

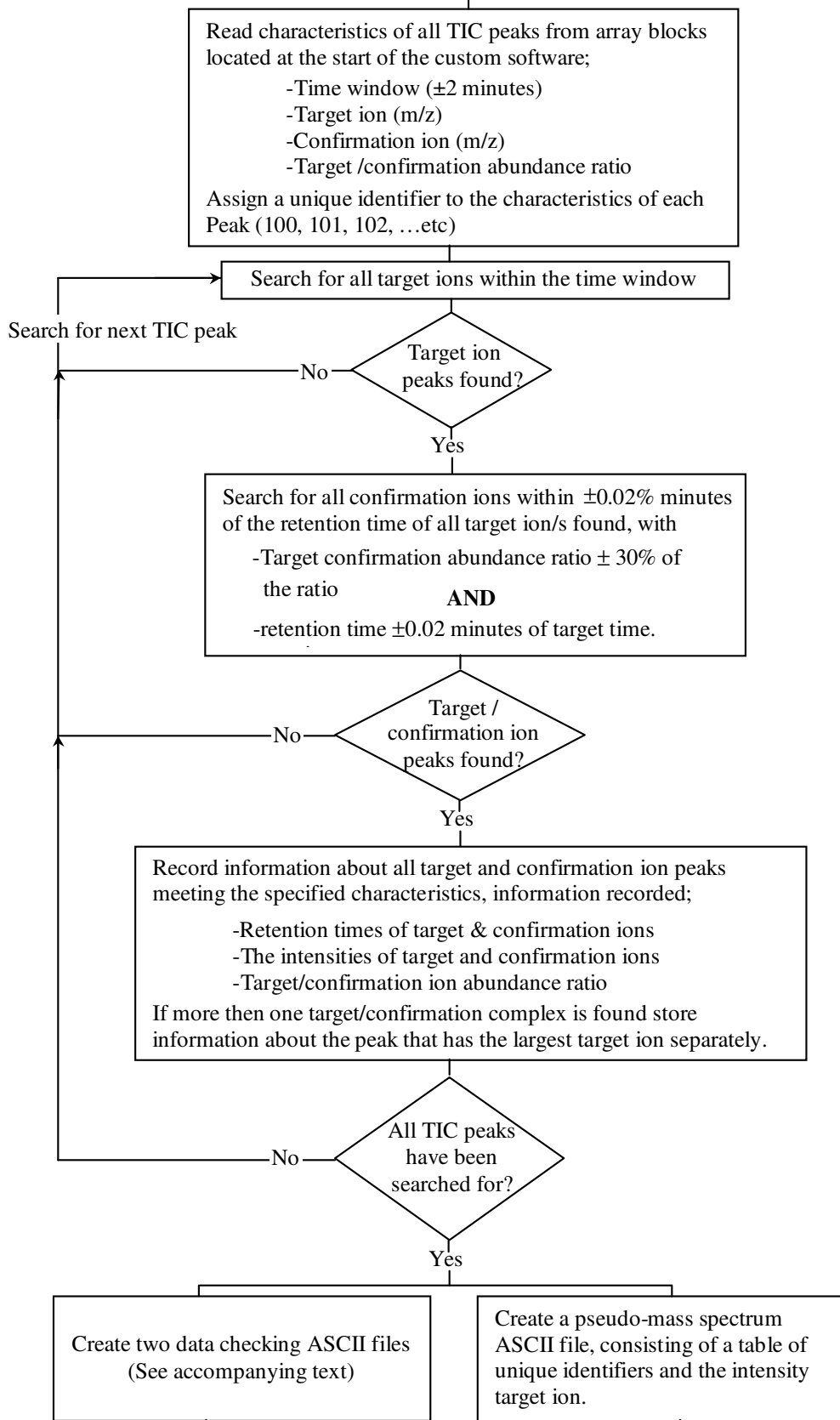
ASCII file (1) The pseudo-mass spectrum ASCII file, analogous in structure to a normal mass-spectral data file, consisting of a

table of unique identifiers and associated target ion abundances. The table was ordered from lowest to highest unique identifier. If there was more than one target/confirmation complex found for a set of parameter values, then the largest target ion intensity was used in the pseudo-mass spectrum file.

ASCII file (2) An error checking ASCII file consisting of a table of unique identifiers and associated target ion abundances and the retention time of the target ion (described later).

ASCII file (3) A second error checking ASCII file contained information relating to any peak that met all the criteria required for the identification of a peak. This ASCII file consisted of a table of unique identifier, target ion, confirmation ion, the start and end time of the 4 minute time window of the target ion, the abundance of the target ion, retention time of the target ion, the expected target/confirmation ratio and the measured target/confirmation ratio (described later).

**Computer algorithm for identifying TIC peaks pyrograms**



NIST mass spectral search program for the comparison of pyrograms

**Figure 3-3: Flow diagram of the algorithm for identifying TIC peaks in pyrograms**

### *Error checking*

Due to the large number of products generated during the pyrolysis of melanin, it was possible that a number of peaks satisfying the selection criteria would be found in any 4 minute time window. As there was a possibility of an incorrect TIC peak selection by the software, methods for the identification of such errors were developed.

Importation of ASCII file **(2)** into Microsoft Excel<sup>®</sup> allowed the percentage area of each target ion intensity, relative to the area of all the target ion intensities for that sample, to be calculated. For each type of melanin and the within-day and inter-day variation studies, the RSD for the percentage target ion intensities and the average target ion intensities were calculated. The average target ion intensities calculated were later reformatted to create average pseudo-mass spectra used for NIST chromatogram comparison (see below).

The custom software searched for TIC peaks in order of the retention times of the TIC peaks it was designed to detect. By visual inspection of the column of retention times of ASCII file **(2)**, any retention time that was out of sequence indicated the mis-identification of a TIC peak. High RSD values for the percentage target ion intensities could also indicate an error. Inspection of the individual percentage target ion intensities could indicate the source of variation. If a mis-identification was thought to have been made, ASCII file **(3)** was used to identify all TIC peaks with the same

parameters and the pyrogram and TIC peak/s visually examined to determine if an error had been made.

#### *Importation of data into NIST program*

ASCII files (1) created by the comparison software were formatted as NIST mass spectrum tables so that it was possible to import them directly into the NIST mass spectral search program.

#### *NIST chromatogram comparison*

The average pseudo-mass spectra, created from the importation of ASCII file (2) into Microsoft Excel<sup>®</sup> during the data checking process, for each type of melanin and the within-day and inter-day variation studies were formatted for importation into the NIST program as average pseudo-mass spectra files. The six reformatted files were imported into the NIST program as “unknowns”. All 30 individual pseudo-mass spectra were imported into the NIST program and stored as a NIST mass spectral library.

In normal operation, to compare true mass spectra the known compounds would form the NIST library with spectra of individual unknowns being compared against this. Reversing the roles of the unknowns and library spectra within the NIST mass spectral search program dramatically reduced the amount of manual data entry required. While reversing of the roles of the unknown and the library spectra does change the absolute values of the match factors, it does not change the relative magnitude of the match factors obtained from the different melanins.

Each of the 6 average pseudo-mass spectra files was then compared against the 30 individual melanin pseudo-mass spectra that were imported into the NIST program as the mass spectra library.

For each comparison between the 30 individual pseudo-mass spectra files and an average pseudo-mass spectrum file a table of direct and reverse match factors was created. As there were 6 average pseudo-mass spectrum files there were 6 match tables of direct and reverse match factors created (see Figure 3-4).

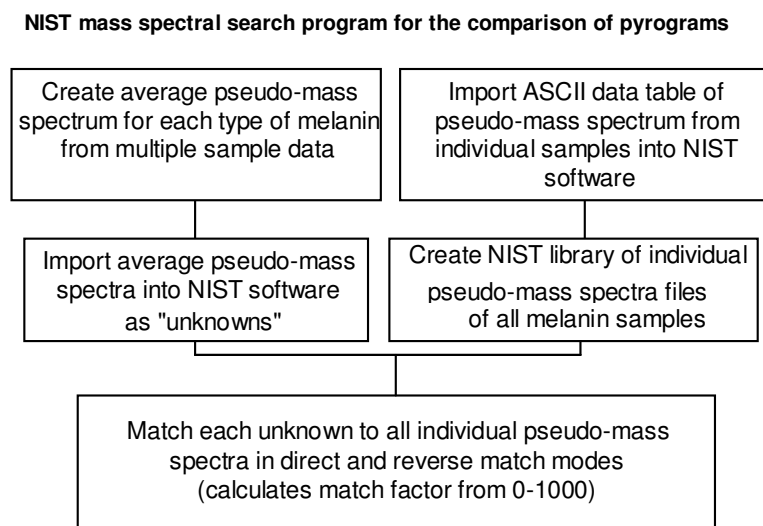


**Figure 3-4:** Flow diagram of the use of the NIST mass spectral search program to compare pyrograms.

### Statistics

The means of the direct and reverse match factors, from each match table, for each type of melanin and within-day and inter-day dopamine melanin samples were compared against each other using Fisher's probability of least significant difference (PLSD) test.

Individual match factors from each match table were plotted separately and against each other (Figures 3-6 to Figure 3-10).

### Results

Representative pyrograms are given in Figure 3-5.

Statistical comparisons of the mean direct and reverse match factors for each type of melanin and within-day and inter-day samples, from each match table, are shown in Tables 3-1 to 3-5.

From these tables it can be seen that the values of the match factors for each melanin type were similar, with the majority of RSD values being below 10 %. Mean match factors from melanins synthesised from different precursors from those used to create the average pseudo-mass spectra were significantly lower than the mean match factors of the melanin types used to create the average pseudo-mass spectra. These statistics are highlighted in bold. Low P-values ( $< 0.05$ ) indicate that the means of the match factors are significantly different. Mean match factors from melanins synthesised from the same precursors<sup>†</sup> as those used to create the average pseudo-mass spectra were not significantly different ( $p > 0.05$ ). These statistics are highlighted in Tables 3-1 to 3-5 in italics.

---

<sup>†</sup> Dopamine was used as a precursor for all within-day and inter-day studies as well the batches of dopamine melanin.

A summary of the statistical comparisons from Tables 3-1 to 3-5 is given in Table 3-7 and Table 3-8. Table 3-7 lists the probability that the mean direct and reverse match factors from the comparison of each different type of melanin to an average pseudo-mass spectrum are the same. Table 3-8 is the same as Table 3-7 except that it compares the mean direct and reverse match factors of melanins synthesised from the same precursor (Dopamine) as the average pseudo-mass spectrum to which it was compared.

Figures 3-6 to 3-10 plot the direct and reverse match factors from the comparison of all individual pseudo-mass spectra to each of the average pseudo-mass spectra for each match table. These figures are visual representations from the corresponding statistics in Tables 3-1 to 3-5.

From Table 3-6 the within-day variations (RSD) for the direct and reverse match factors were 7.3 and 1.7 respectively. From Table 3-5 the inter-day variations for the direct and reverse match factors were 2.7 and 3.0 respectively.

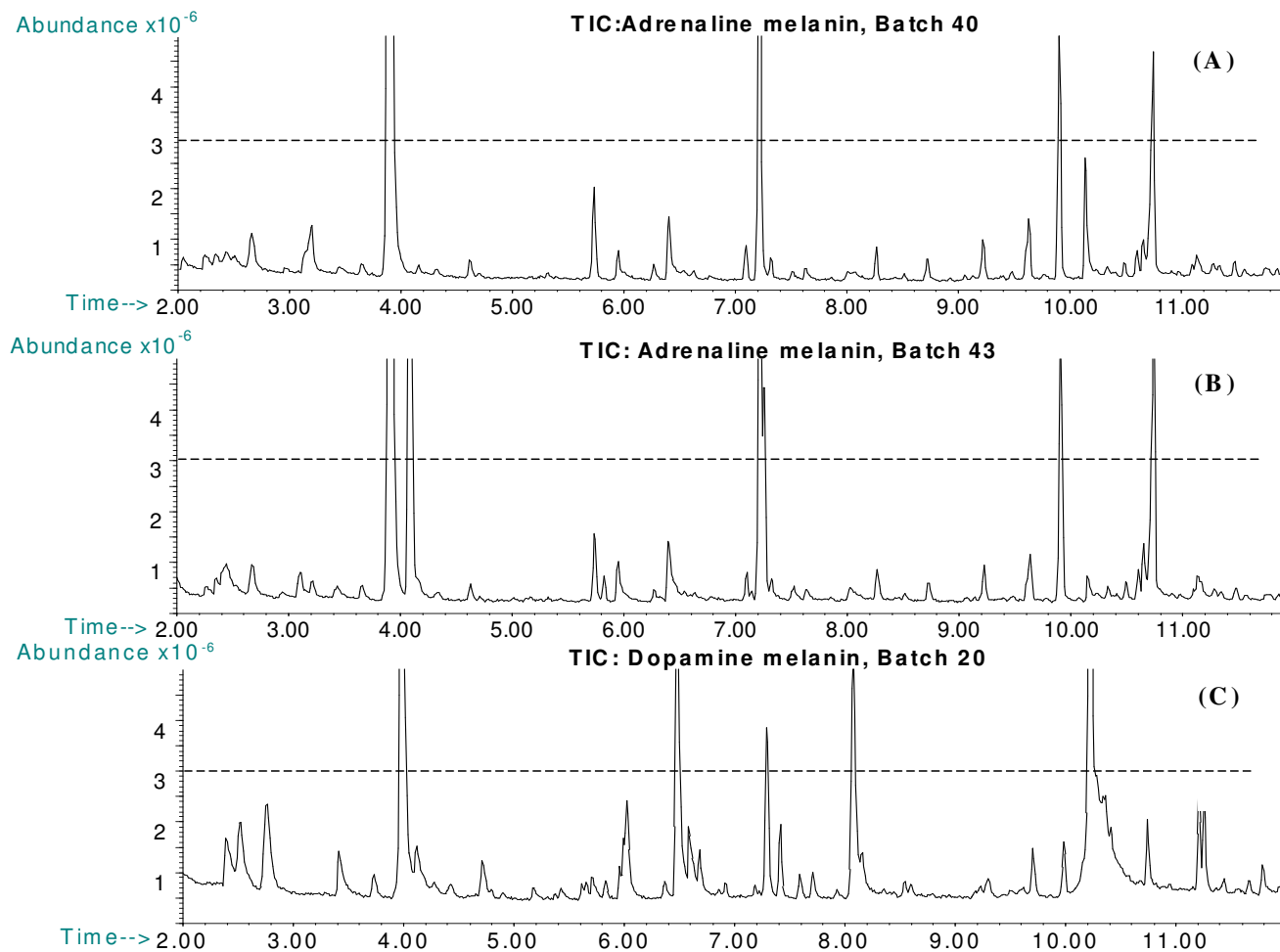


**Figure 3-5:** Pyrograms of two different batches of adrenaline melanin (A & B) and a single batch of dopamine melanin (C). Most of the very large peaks (eg. abundance  $> 3 \times 10^6$ ) are from the pyrolysis of septum fragments.

**Table 3-1: A) Table of means for the direct matching factors from the comparison of all individual pseudo-mass spectra to the average pseudo-mass spectrum of adrenaline melanin.**

Melanin	Mean (n=5)	Std. Dev.	Std. Error	RSD
Adrenaline	847	50	22	5.1
DL-dopa	581	34	15	5.9
Sepia	592	30	14	4.8
Dopamine	636	26	12	5.9
Inter-day dopamine	642	31	14	4.1
Within-day dopamine	657	31	14	4.7

ANOVA: DF=5 & 24, F-Value=38.2, P-Value < .0001

**B) Table of means for the reverse matching factors from the comparison of all individual pseudo-mass spectra to the average pseudo-mass spectrum of adrenaline melanin.**

Melanin	Mean (n=5)	Std. Dev.	Std. Error	RSD
Adrenaline	862	39	17	5.5
DL-dopa	686	81	36	4.5
Sepia	704	39	18	3.4
Dopamine	764	29	13	11.8
Inter-day dopamine	766	26	18	3.8
Within-day dopamine	787	23	10	2.9

ANOVA: DF=5 & 24, F-Value=10.2, P-Value < .0001

**C) Probability that the mean match factors are the same. Lines in bold compare the mean match factors of adrenaline to the mean match factors of other melanins. D = direct match factor, R = reverse match factor.**

Adrenaline	D					
	R					
DL-dopa	D	<b>&lt;0.0001</b>				
	R	<b>&lt;0.0001</b>				
Sepia	D	<b>&lt;0.0001</b>	0.6			
	R	<b>&lt;0.0001</b>	0.5			
Dopamine	D	<b>&lt;0.0001</b>	0.02	0.06		
	R	<b>0.002</b>	0.01	0.04		
Inter-day dopamine	D	<b>&lt;0.0001</b>	0.01	0.03	0.8	
	R	<b>0.002</b>	0.008	0.03	0.9	
Within-day dopamine	D	<b>&lt;0.0001</b>	0.002	0.007	0.4	0.5
	R	<b>0.01</b>	0.001	0.006	0.4	0.5
		<b>Adrenaline</b>	DL-dopa	Sepia	Dopamine	Inter-day Dopamine
						Within-day dopamine

### Adrenaline: Direct versus Reverse Match Factors

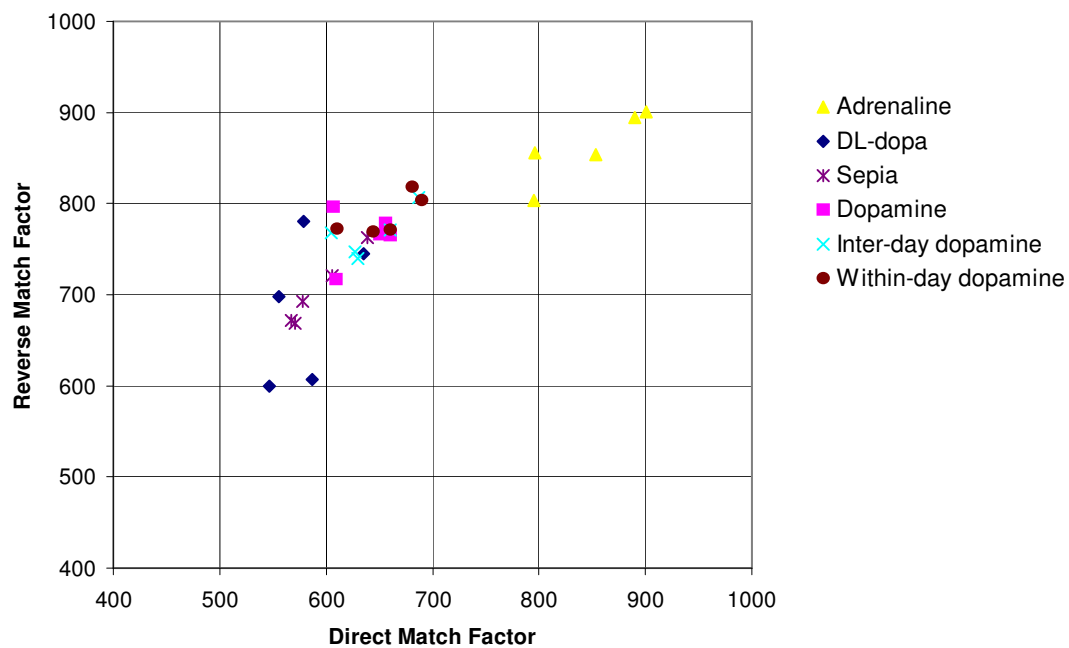


**Figure 3-6:** Plot of the direct and reverse match factors from the comparison of all individual pseudo-mass spectra to the average pseudo-mass spectrum of adrenaline.

**Table 3-2: A) Table of means for the direct matching factors from the comparison of all individual pseudo-mass spectra to the average pseudo-mass spectrum of DL-dopa melanin.**

Melanin	Mean (n=5)	Std. Dev.	Std. Error	RSD
Adrenaline	611	60	27	7.0
DL-dopa	842	40	18	9.8
Sepia	642	45	20	8.1
Dopamine	649	36	16	4.8
Inter-day dopamine	670	54	24	5.5
Within-day dopamine	722	47	21	6.5

ANOVA: DF=5 & 24, F-Value=15.4, P-Value < .0001

**B) Table of means for the reverse matching factors from the comparison of all individual pseudo-mass spectra to the average pseudo-mass spectrum of DL-dopa melanin.**

Melanin	Mean (n=5)	Std. Dev.	Std. Error	RSD
Adrenaline	617	53	24	7.2
DL-dopa	879	58	26	8.6
Sepia	652	47	21	2.3
Dopamine	662	51	23	6.6
Inter-day dopamine	701	16	7	7.7
Within-day dopamine	737	47	21	6.4

ANOVA: DF=5 & 24, F-Value=19.6, P-Value < .0001

**C) Probability that the mean match factors are the same. Lines in bold compare the mean match factors of DL-dopa to the mean match factors of other melanins. D = direct match factor, R = reverse match factor.**

Adrenaline	<b>D</b>					
	<b>R</b>					
<b>DL-dopa</b>	<b>D</b>	<b>&lt;0.0001</b>				
	<b>R</b>	<b>&lt;0.0001</b>				
Sepia	<b>D</b>	0.3	<b>&lt;0.0001</b>			
	<b>R</b>	0.3	<b>&lt;0.0001</b>			
Dopamine	<b>D</b>	0.2	<b>&lt;0.0001</b>	0.8		
	<b>R</b>	0.15	<b>&lt;0.0001</b>	0.7		
Inter-day dopamine	<b>D</b>	0.06	<b>&lt;0.0001</b>	0.4	0.5	
	<b>R</b>	0.01	<b>&lt;0.0001</b>	0.1	0.2	
Within-day dopamine	<b>D</b>	0.001	<b>0.0005</b>	0.01	0.02	0.1
	<b>R</b>	0.0005	<b>&lt;0.0001</b>	0.009	0.02	0.24
		Adrenaline	<b>DL-dopa</b>	Sepia	Dopamine	Inter-day Dopamine
						Within-day dopamine

### DL-dopa: Direct versus Reverse Match Factors

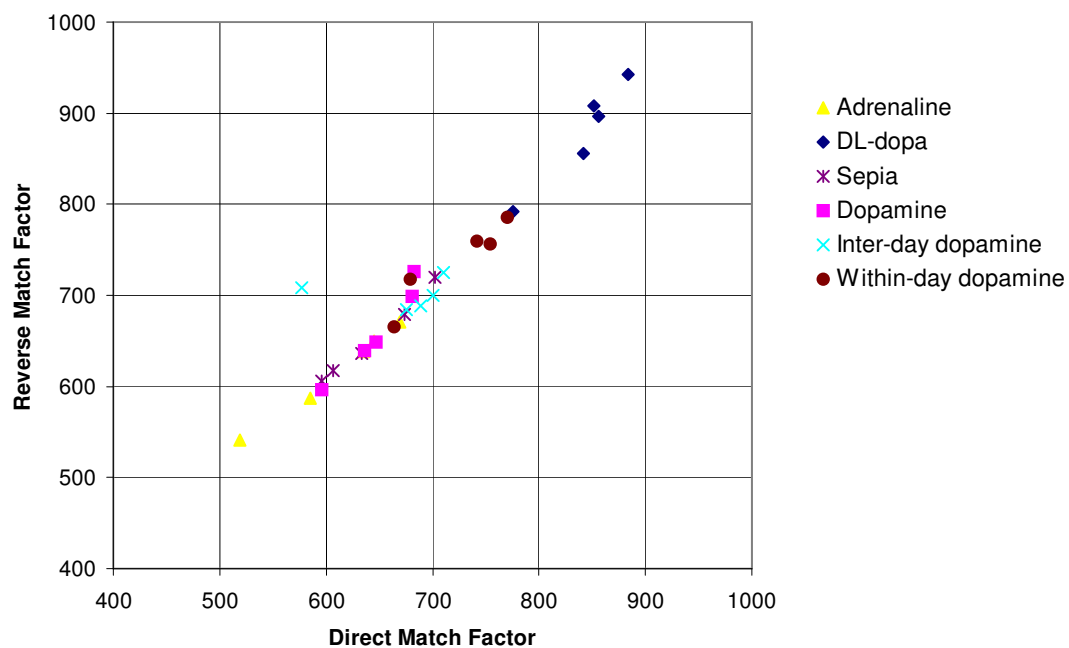


Figure 3-7: Plot of the direct and reverse match factors from the comparison of all individual pseudo-mass spectra to the average pseudo-mass spectrum of DL-dopa.

**Table 3-3: A) Table of means for the direct matching factors from the comparison of all individual pseudo-mass spectra to the average pseudo-mass spectrum of sepia melanin.**

Melanin	Mean (n=5)	Std. Dev.	Std. Error	RSD
Adrenaline	550	71	32	2.6
DL-dopa	563	115	51	12.9
Sepia	938	24	11	10.2
Dopamine	735	20	9	20.4
Inter-day dopamine	709	72	32	2.7
Within-day dopamine	701	78	35	11.1

ANOVA: DF=5 & 24, F-Value=19.6, P-Value < .0001

**B) Table of means for the reverse matching factors from the comparison of all individual pseudo-mass spectra to the average pseudo-mass spectrum of sepia melanin.**

Melanin	Mean (n=5)	Std. Dev.	Std. Error	RSD
Adrenaline	571	51	23	2.4
DL-dopa	674	106	47	8.9
Sepia	940	23	10	3.7
Dopamine	743	13	6	15.7
Inter-day dopamine	736	27	12	1.7
Within-day dopamine	732	16	7	2.2

ANOVA: DF=5 & 24, F-Value=27.9, P-Value < .0001

**C) Probability that the mean match factors are the same. Lines in bold compare the mean match factors of sepia to the mean match factors of other melanins. D = direct match factor, R = reverse match factor.**

Adrenaline	D						
	R						
DL-dopa	D	0.8					
	R	0.004					
<b>Sepia</b>	D	<b>&lt;0.0001</b>	<b>&lt;0.0001</b>				
	R	<b>&lt;0.0001</b>	<b>&lt;0.0001</b>				
Dopamine	D	0.0004	0.0008	<b>0.0001</b>			
	R	<.0001	0.04	<b>&lt;0.0001</b>			
Inter-day dopamine	D	0.002	0.003	<b>&lt;0.0001</b>	0.6		
	R	<.0001	0.06	<b>&lt;0.0001</b>	0.8		
Within-day dopamine	D	0.003	0.005	<b>&lt;0.0001</b>	0.500	0.9	
	R	<.0001	0.09	<b>&lt;0.0001</b>	0.7	0.9	
		Adrenaline	DL-dopa	<b>Sepia</b>	Dopamine	Inter-day Dopamine	Within-day dopamine

### Sepia: Direct versus Reverse Match Factors

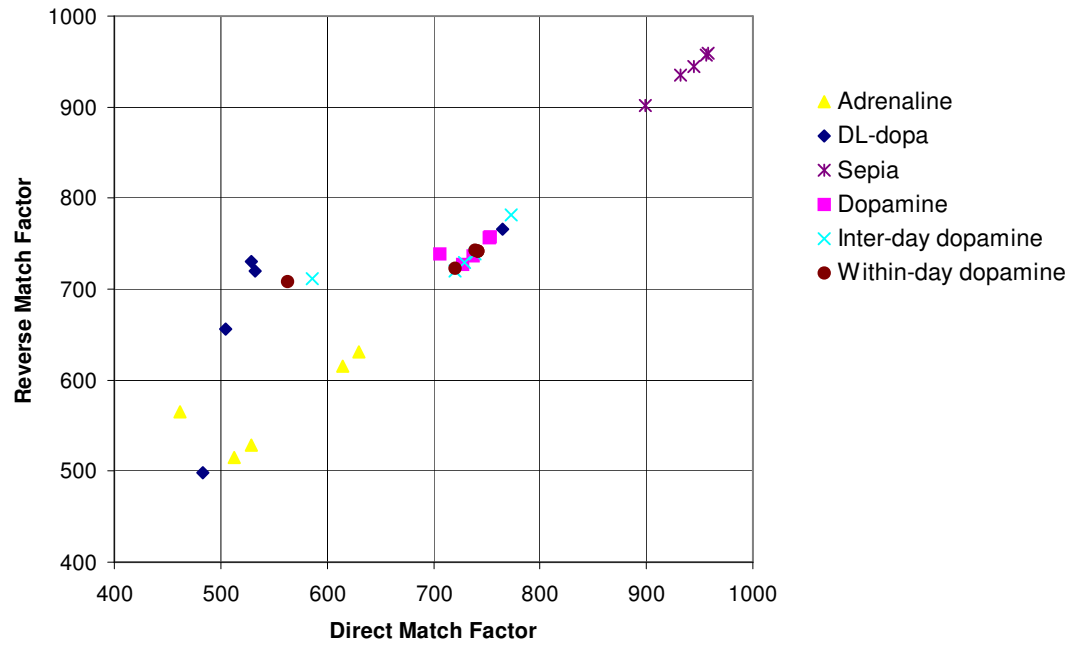


**Figure 3-8:** Plot of the direct and reverse match factors from the comparison of all individual pseudo-mass spectra to the average pseudo-mass spectrum of sepia.

**Table 3-4: A) Table of means for the direct matching factors from the comparison of all individual pseudo-mass spectra to the average pseudo-mass spectrum of dopamine melanin.**

Melanin	Mean (n=5)	Std. Dev.	Std. Error	RSD
Adrenaline	577	70	31	3.9
DL-dopa	545	132	59	12.1
Sepia	717	28	13	4.4
Dopamine	913	12	5	24.2
Inter-day dopamine	867	38	17	1.3
Within-day dopamine	831	82	37	9.9

ANOVA: DF=5 & 24, F-Value=22.8, P-Value < .0001

**B) Table of means for the reverse matching factors from the comparison of all individual pseudo-mass spectra to the average pseudo-mass spectrum of dopamine melanin.**

Melanin	Mean (n=5)	Std. Dev.	Std. Error	RSD
Adrenaline	606	45	20	4.4
DL-dopa	669	102	46	7.4
Sepia	725	32	14	4.9
Dopamine	921	8	4	15.2
Inter-day dopamine	878	43	19	0.9
Within-day dopamine	873	36	16	4.1

ANOVA: DF=5 & 24, F-Value=30.3, P-Value < .0001

**C) Probability that the mean match factors are the same. Lines in bold compare the mean match factors of dopamine to the mean match factors of other melanins. Lines in italics compare the mean match factors of dopamine to the mean match factors of melanins made with the same precursor. D = direct match factor, R = reverse match factor.**

Adrenaline	D					
	R					
DL-dopa	D	0.5				
	R	0.07				
Sepia	D	0.006	0.001			
	R	0.0015	0.1			
Dopamine	D	<b>&lt;0.0001</b>	<b>&lt;0.0001</b>	<b>0.0003</b>		
	R	<b>&lt;0.0001</b>	<b>&lt;0.0001</b>	<b>&lt;0.0001</b>		
Inter-day dopamine	D	<0.0001	<0.0001	0.003	<b>0.3</b>	
	R	<0.0001	<0.0001	0.0001	<b>0.2</b>	
Within-day dopamine	D	<0.0001	<0.0001	0.02	<b>0.084</b>	0.4
	R	0.0015	<0.0001	0.0002	<b>0.16</b>	0.9
		Adrenaline	DL-dopa	Sepia	<b>Dopamine</b>	Inter-day Dopamine
						Within-day dopamine

### Dopamine: Direct versus Reverse Match Factors

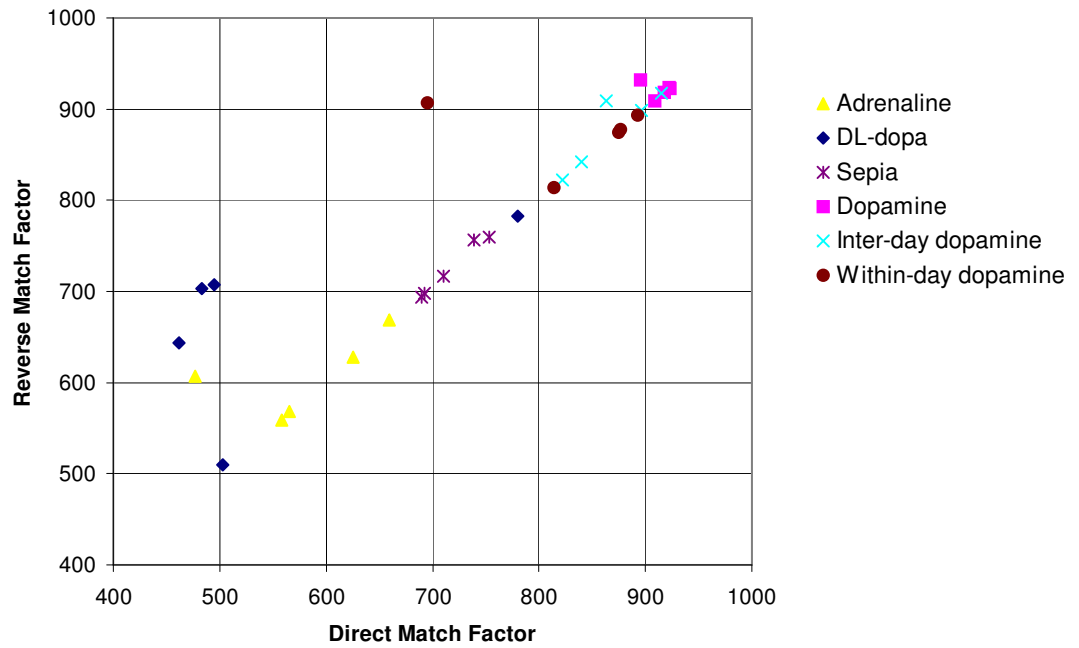


**Figure 3-9:** Plot of the direct and reverse match factors from the comparison of all individual pseudo-mass spectra to the average pseudo-mass spectrum of dopamine.

**Table 3-5: A) Table of means for the direct matching factors from the comparison of all individual pseudo-mass spectra to the average pseudo-mass spectrum of inter-day dopamine melanin.**

Melanin	Mean (n=5)	Std. Dev.	Std. Error	RSD
Adrenaline	615	65	29	4.6
DL-dopa	607	118	53	10.6
Sepia	716	33	15	2.7
Dopamine	893	23	10	19.4
Inter-day dopamine	885	24	11	2.6
Within-day dopamine	843	70	31	8.3

ANOVA: DF=5 & 24, F-Value=20.5, P-Value < .0001

**B) Table of means for the reverse matching factors from the comparison of all individual pseudo-mass spectra to the average pseudo-mass spectrum of inter-day dopamine melanin.**

Melanin	Mean (n=5)	Std. Dev.	Std. Error	RSD
Adrenaline	639	46	21	4.8
DL-dopa	708	87	39	7.2
Sepia	726	35	16	3.0
Dopamine	901	27	12	12.3
Inter-day dopamine	896	27	12	3.0
Within-day dopamine	876	30	13	3.4

ANOVA: DF=5 & 24, F-Value=29.1, P-Value < .0001

**C) Probability that the mean match factors are the same. Lines in bold compare the mean match factors of inter-day dopamine to the mean match factors of other melanins. Lines in italics compare the mean match factors of inter-day dopamine to the mean match factors of melanins made with the same precursor. D = direct match factor, R = reverse match factor.**

Adrenaline	D					
	R					
DL-dopa	D	0.9				
	R	0.03				
Sepia	D	0.02	0.01			
	R	0.08	0.6			
Dopamine	D	<0.0001	<0.0001	0.0002		
	R	<0.0001	<0.0001	<0.0001		
<b>Interday dopamine</b>	D	<b>&lt;0.0001</b>	<b>&lt;0.0001</b>	<b>0.0004</b>	<b>0.9</b>	
	R	<b>&lt;0.0001</b>	<b>&lt;0.0001</b>	<b>&lt;0.0001</b>	<b>0.9</b>	
Within-day dopamine	D	<0.0001	<0.0001	0.005	0.2	<b>0.3</b>
	R	<0.0001	<0.0001	<.0001	0.4	<b>0.5</b>
		Adrenaline	DL-dopa	Sepia	Dopamine	<b>Inter-day Dopamine</b>
						Within-day dopamine

### Inter-day Dopamine: Direct versus Reverse Match Factors

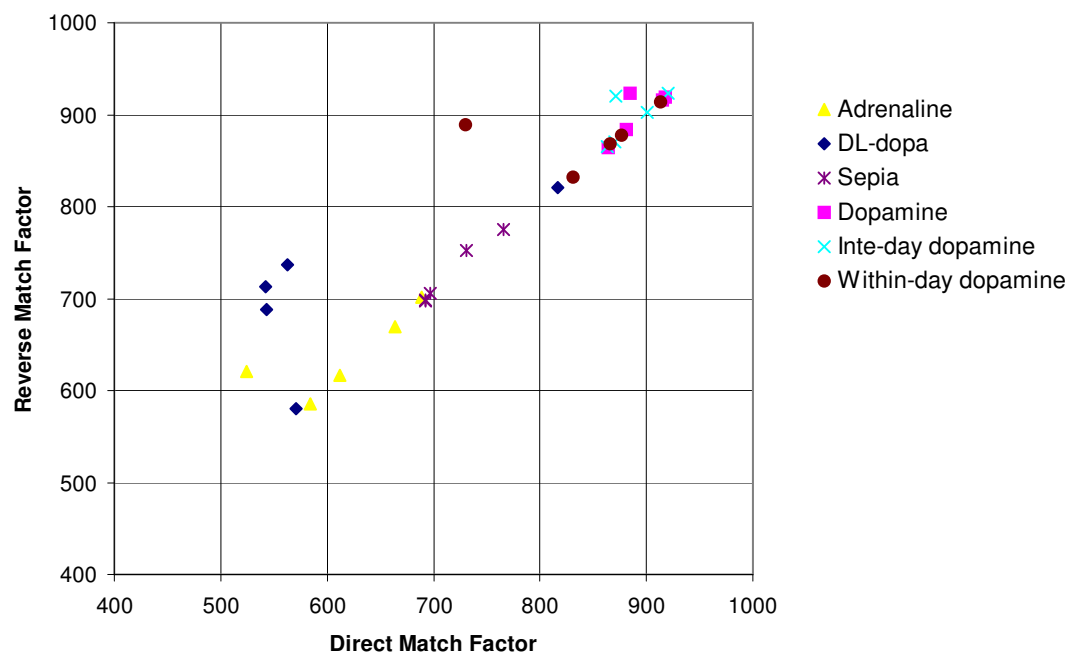


**Figure 3-10:** Plot of the direct and reverse match factors from the comparison of all individual pseudo-mass spectra to the average pseudo-mass spectrum of inter-day dopamine.

**Table 3-6: A) Table of means for the direct matching factors from the comparison of all individual pseudo-mass spectra to the average pseudo-mass spectrum of within-day dopamine melanin.**

Melanin	Mean (n=5)	Std. Dev.	Std. Error	RSD
Adrenaline	630	70	31	4.9
DL-dopa	653	88	39	11.1
Sepia	750	37	17	4.4
Dopamine	879	16	7	13.5
Inter-day dopamine	856	38	17	1.8
Within-day dopamine	889	65	29	7.3

ANOVA: DF=5 & 24, F-Value=20.35, P-Value < .0001

**B) Table of means for the reverse matching factors from the comparison of all individual pseudo-mass spectra to the average pseudo-mass spectrum of within-day dopamine melanin.**

Melanin	Mean (n=5)	Std. Dev.	Std. Error	RSD
Adrenaline	652	46	21	5.0
DL-dopa	747	71	32	7.1
Sepia	762	38	17	2.2
Dopamine	890	16	7	9.5
Inter-day dopamine	873	19	8	1.8
Within-day dopamine	919	16	7	1.7

ANOVA: DF=5 & 24, F-Value=33.6, P-Value < .0001

**C) Probability that the mean match factors are the same. Lines in bold compare the mean match factors of within-day dopamine to the mean match factors of other melanins. Lines in italics compare the mean match factors of within-day dopamine to the mean match factors of melanins made with the same precursor. D = direct match factor, R = reverse match factor.**

Adrenaline	D					
	R					
DL-dopa	D	0.5				
	R	0.0009				
Sepia	D	0.003	0.01			
	R	0.0002	0.5			
Dopamine	D	<0.0001	<0.0001	0.002		
	R	<0.0001	<0.0001	<0.0001		
Inter-day dopamine	D	<0.0001	<0.0001	0.008	0.5	
	R	<0.0001	<0.0001	0.0002	0.5	
Within-day dopamine	D	<b>&lt;0.0001</b>	<b>&lt;0.0001</b>	<b>0.0009</b>	<b>0.8</b>	<b>0.4</b>
	R	<b>&lt;0.0001</b>	<b>&lt;0.0001</b>	<b>&lt;0.0001</b>	<b>0.3</b>	<b>0.08</b>
		Adrenaline	DL-dopa	Sepia	Dopamine	Inter-day Dopamine
						<b>Within-day dopamine</b>

### Within-day Dopamine: Direct versus Reverse Match Factors

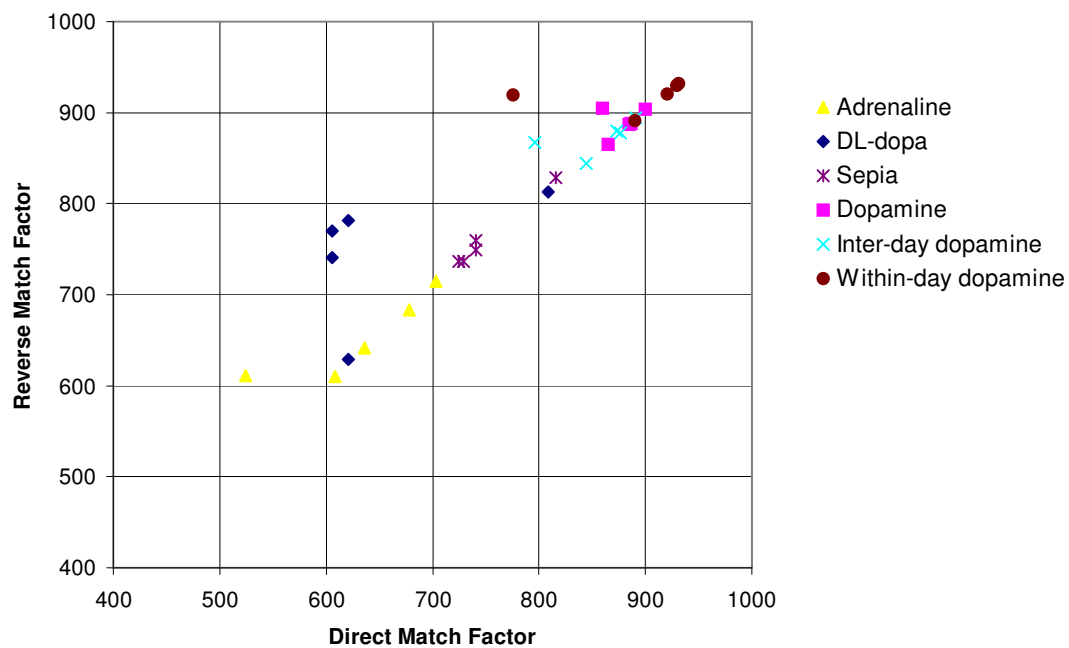


**Figure 3-11:** Plot of the direct and reverse match factors from the comparison of all individual pseudo-mass spectra to the average pseudo-mass spectrum of within-day dopamine.

**Table 3-7: Summary of the statistical comparisons (Tables 3-1 to Table 3-5; lines in bold). The probability that the mean (n=5) direct and reverse match factors, from the comparison of each different type of melanin with an average pseudo-mass spectrum (melanin<sub>av</sub>; n=5), are the same. D = direct match factor, R = reverse match factor.**

		DL-Dopa <sub>av</sub>	Dopamine <sub>av</sub>	Adrenaline <sub>av</sub>	Sepia <sub>av</sub>
DL-Dopa	D		<0.0001	<0.0001	<0.0001
	R		<0.0001	<0.0001	<0.0001
Dopamine	D	<0.0001		<0.0001	0.0001
	R	<0.0001		0.018	<0.0001
Adrenaline	D	<0.0001	<0.0001		<0.0001
	R	<0.0001	<0.0001		<0.0001
Sepia	D	<0.0001	0.0003	<0.0001	
	R	<0.0001	<0.0001	<0.0001	

Fisher's PLSD

**Table 3-8: Summary of the statistical comparisons (Tables 3-1 to Table 3-5; lines in italics). The probability that the mean (n=5) direct and reverse match factors, from the comparison of melanins synthesised from the same precursor (Dopamine) as the average pseudo-mass spectrum (melanin<sub>av</sub>; n=5), to which it was compared, are different. D = direct match factor, R = reverse match factor.**

		Dopamine <sub>av</sub>	Inter-day dopamine <sub>av</sub>	Within-day dopamine <sub>av</sub>
Dopamine	D		0.85	0.79
	R		0.87	0.26
Inter-day dopamine	D	0.32		0.37
	R	0.20		0.08
Within-day dopamine	D	0.08	0.32	
	R	0.16	0.51	

Fisher's PLSD

No significant differences all  $p > 0.05$

## Discussion

### Apparatus

A furnace-type pyrolyser was used in this study, as it was the only pyrolyser available. The principal disadvantage with this pyrolyser was the method of injection of melanin into the pyrolysis chamber. Irrespective of the injection technique used, small fragments of silicone rubber septum were deposited into the pyrolysis chamber during injection. Under normal GC/MS conditions, the occasional TIC peak/s arising from septum fragments elute at

higher temperatures. In the present pyrolysis configuration, however, small fragments of septum entering the pyrolysis chamber were pyrolysed into many compounds that were eluted over a wide range of column temperatures, resulting in many large artefact TIC peaks. These artefact peaks were the largest single source of variability in the study.

Many types of syringes, septa and methods of application were examined to reduce the number and size of these artefact TIC peaks. While some techniques were more successful than others, no technique eliminated the artefact TIC peaks or reduced them to an acceptable level. The only possible way to eliminate the artefact TIC peaks would be to remove the septum altogether. While septumless injection ports are commercially available, the expense of these systems was prohibitive.

Ideally, the method of application on to the pyrolyser would have been consistent for all melanin types studied. However, due to the different solubilities and particle sizes of the various melanins different application methods for the deposition of melanin into the pyrolyser were required.

The first method of application was by the direct injection of a melanin in methanol suspension into the pyrolyser. Injections were made with a plunger-in-needle syringe. As the needle of the plunger-in-needle syringe had a smaller diameter than the needle of the solids injector, the plunger-in-needle syringe had the advantage of coring the pyrolyser septum less than the solids injector. The use of the plunger-in-needle syringe led to fewer silicon artefact TIC peaks in pyrograms and gave more visually reproducible

results. This method was less time consuming than using the solids injector. A disadvantage with the plunger-in-needle technique was that melanin was injected into the pyrolyser with the solvent. In theory, the solvent could react with the melanin at pyrolysis temperatures leading to a different set of pyrolysis products. Furthermore, the plunger-in-needle syringe could not be used for melanins with particle sizes that were greater than the internal diameter of the needle.

The second method of application used the solids injector. The needle from the solids injector caused significantly more coring of the pyrolyser septum than the plunger-in-needle syringe. While loading the spiral needle was more time consuming, it could be used for melanins that did not suspend well in methanol or whose particle size did not allow for the use of the plunger-in-needle syringe.

Other workers such as Charman *et al* [84] used a filament pyrolysis unit in which a known amount of melanin solution was deposited on a crucible that was placed in the pyrolysis chamber. The pyrolysis chamber was flushed with carrier gas and heated to remove the solvent prior to pyrolysis. This arrangement had the advantage that there was no need to pierce a septum within the pyrolysis unit. Therefore, there would be no artefact TIC peaks arising from septum, the amount of melanin pyrolysed could be more accurately controlled and the method of application would be less affected by particle size.

Most papers dealing with PY/GC of melanins used relatively polar columns, due to the polar nature of the pyrolysis products [70, 78, 84, 92, 93].

Injections of polar compounds, 2,6-dimethyl phenol and 2,4-dimethyl aniline onto a non-polar BP-1 column gave sharp peaks. These polar compounds chromatographed well, indicating that a non-polar column could be used for the PY/GC of melanins. The principal advantage of non-polar columns, over polar columns, was the higher temperatures at which they could be operated ( $\approx 300\text{ }^{\circ}\text{C}$ ). Column temperatures could be ramped to  $300\text{ }^{\circ}\text{C}$ , removing many higher boiling point compounds from the column, extending the useful life of the column without the need for the special cleaning procedures used by other workers [84].

#### *Interpretation of data*

The custom comparison software developed for the comparison of pseudo-mass spectra could be modified in a number of ways depending on need.

The software was set up to record the peak area instead of peak height as peak area can more accurately determine the relative sizes of poorly resolved peaks. If necessary, it would be possible to modify the software to measure and record peak height.

During the development of this software it was noted that wide time windows for the identification of target ion peaks (>10 - 20 minutes) could be used without a significant increase in the mis-identification of TIC peaks.

The time windows could be easily modified for each TIC peak within the array blocks located at the start of the software.

When the comparison software detected a target ion peak within a pyrogram the software searched for all confirmation ion peaks within a time window of  $\pm 0.2$  minutes of the apex of the target ion peak. In order for the software to identify any peak it must detect the start and end of a peak. For wide or tailing confirmation ion peaks it was possible that the start and/or end-time of the ion peak would fall outside this time window. In such cases the software would not identify a confirmation ion peak and a mis-identification could be made. This problem could be overcome by increasing the duration of the time window. However, if the time window was increased, the total time taken to process a pyrogram was increased proportionately.

If two ions originated from the same compound, the apices of the ion peaks would be expected to occur at almost exactly the same time. However, if the apex of one ion peak occurred at the time of signal sampling it would be possible that the apex of the other ion peak lay within a different sampling time frame. An allowance of  $\pm 0.02$  minutes was made for this possibility. The extent of the allowance depends on the sampling frequency of the instrument. The higher the sampling frequency the smaller the time allowance required and vice versa.

The integration parameters used in the software were predominantly the default settings of the HP mass spectral software. The comparison software used the integration parameters that are set in the HP integration module at

the time the software is run. Therefore, changing parameters within data acquisition module changes the parameters in the custom comparison software.

With extensive modification, the software could be adapted to require more than two confirmation ions in set ratios before a TIC peak identification was made. In this study one target ion and one confirmation ion proved sufficient to correctly identify a TIC peak in the majority of cases. When a TIC peak was mis-identified, this usually occurred because the mis-identified TIC peak had an identical mass spectrum to the TIC peak the software was searching for indicating that the mis-identified TIC peak was a chiral isomer of the correct TIC peak. As chiral isomers have identical mass spectra, adding extra confirmation ions to the selection criteria would not overcome this problem.

For the MSD used in this study the ratios between the target ion peak and the confirmation ion peak varied due to the inherent variability of quadrupole instruments. To accommodate for this, a tolerance of  $\pm 30\%$  of the target/confirmation ratio was arbitrarily allowed for by the software when identifying peaks.

This software was written in such a way that mis-identified peaks could be easily identified with the use of the data checking ASCII files. However, very little modification to the pseudo-mass spectra files was done. Relatively few peaks were mis-identified and of those peaks that were mis-identified, few were major components of the TIC.

### Reproducibility of melanin pyrolysis

The reproducibility of the pyrolysis technique was good, with the majority of RSD values, of match factors from melanins synthesised from the same precursor, being under 10 %. This indicated that the match factors from batches of melanins synthesised from the same precursor were similar to each other. Low P values ( $<0.05$ ) from Fisher's PLSD demonstrated that melanins synthesised from different precursors were not similar.

Match factors generated by the method used in this study only gave an indication of the degree of similarity between the two spectra being compared. The NIST mass spectral search program generates match factors from the comparison of a single (unknown) mass spectrum to the mass spectra within a library of mass spectra. The technique used in this study, which relied on the NIST software, compared the degree of similarity between an average pseudo-mass spectrum (unknown) and individual pseudo-mass spectra (library). Therefore, this technique could not be used to compare the degree of similarity between individual pseudo-mass spectra (i.e. spectra within the library). However, as match factors from melanins of the same type were similar this method could be used to compare, with Fisher's PLSD, mean match factors from melanin samples of the same type to the mean match factors of the melanin samples used to create the average pseudo-mass spectrum. As the technique could not be used to compare the mean match factors of the individual melanin types, separate

comparisons between all the individual pseudo-mass spectra and each of the average pseudo-mass spectra had to be performed.

Visual interpretation of the graphs on Figures 3-6 to Figures 3-9 indicated that the analytical technique used could clearly differentiate between melanins synthesised from different precursors. Furthermore, Table 3-7 shows that these visual differences were statistically significant. Visual interpretation of the graphs on Figures 3-9 to Figure 3-10 indicated that the analytical technique used gave similar results for melanins synthesised from the same precursor. Table 3-8 shows that any visual differences in plots of match factors of melanins synthesised from the same precursor are not statistically significant.

#### *Comparison with other workers*

Statistical and pattern recognition techniques have been used by other workers to differentiate between melanins of different types. Dworzanski [92] took four TIC pyrogram peaks and expressed their peak heights as a percentage of 25 selected peaks. With this data, he calculated two discriminant functions for each type of melanin that were plotted on the same graph. Visual examination of the plot showed a good separation of the various melanins. When plotted, distances between discriminant functions from samples of different melanins were very large in comparison with the variation of discriminant functions among melanins of the same type.

A very similar method was adopted by Stepien *et al* [78]. Pyrograms were converted into a data vector by normalising the peak heights of 25 selected peaks, to a constant sum of all selected peaks. Differentiation of melanin samples was based on the evaluation of distances corresponding to the two largest eigenvalues of the matrix covariance of the 25 data vectors in the 25-dimensional space. A plot, in which the distances between samples of the different melanins were very large in comparison with the variation among melanins of the same type, was obtained.

Charman *et al* [84] used both principal component analysis and non-linear mapping to differentiate between melanins. Again plots were constructed for each technique, the distances between samples of the different melanins were very large in comparison with the variation among melanins of the same type.

While these techniques are quite useful in differentiating between melanins the statistical methods they employ are often difficult to use and interpret. The analytical method used in this study did require experience in computer programming to initially set-up. However, once set-up the custom comparison software could be used by most operators who have had some experience with mass spectra work with little training. Furthermore, the NIST mass spectral search program is readily available in many laboratories, its results are widely accepted and easily understandable.

### *Further investigations & other uses*

This study predominantly dealt with examining the differences that could be detected between melanins produced from different precursors. Future studies could examine the differences between melanins synthesised from the same precursors but under different conditions.

The use of the NIST program for the comparison of chromatograms need not be limited to pyrolysis. Other applications requiring numerical comparisons of complex mixtures would find this technique useful especially in the field of forensic science.

### *Conclusion*

This study demonstrates that the method outlined could differentiate between melanins produced from different precursors on the basis of statistically significant differences in their pyrograms. Conversely, no statistically significant differences between pyrograms of different batches of melanins produced under the same conditions from the same precursors could be detected.

Since the method was not used to examine differences between melanins produced from the same precursor, but under different conditions, it can not be used as the sole indicator that the batches of melanins synthesised, as discussed in Chapter 2, were synthesised in a reproducible manner.

However, it could be used in combination with other modes of analysis to

assess the reproducibility of melanin synthesis. It could also form the basis of other studies to ensure the differences between melanins synthesised under differing conditions from the same precursor.

# CHAPTER 4: *IN VITRO* EVALUATION OF SUN PROTECTION FACTORS OF SUNSCREEN AGENTS

## BACKGROUND

The harmful effects of solar radiation are caused predominantly by the UV region of the electromagnetic spectrum (200 – 400 nm), which can be divided into three sections (1) UVA radiation between 320 and 400 nm (2) UVB radiation from 290 - 320 nm and (3) UVC radiation from 200 –290 nm.

The energy of electromagnetic radiation is inversely proportional to the wavelength. The ability of UV radiation to penetrate the skin and underlying tissue is inversely related to the energy of the UV radiation [52, 58]. The ability of UV radiation to penetrate skin in part determines the nature and site of damage.

UVC is the most biologically potent range of UV radiation. It is highly carcinogenic and bactericidal. UVC radiation has shortest wavelength and the highest energy and does not penetrate deeply into the skin. Therefore, its primary effect is on the epidermis. UVC is completely filtered by the ozone layer in the upper atmosphere [14, 57, 106].

UVB radiation is also carcinogenic and produces acute sunburn. UVB radiation is partially filtered by the ozone layer. As all of the UVC radiation is filtered in the upper atmosphere, the oncogenic effect of ultraviolet

radiation in mammalian skin is believed to be primarily due to UVB radiation [5, 107, 108].

UVA radiation penetrates the deeper dermal layers. UVA radiation induces a number of changes in human skin and is a major contributing factor in photoaging. Changes in skin due to UVA irradiation include; elastic fibre damage, hypertrophy of deep dermal tissues, changes in the amounts and ratios of the various types of collagen and visible histological changes in skin consistent with photoaging [37, 38, 109-111].

While UVB radiation has been widely accepted for many decades as a prominent factor in the development of skin cancer, there has been less certainty about the role of UVA radiation [5, 112]. However, UVA radiation does suppress some immunological functions and is carcinogenic, although at much higher doses than UVB. UVA can also act to enhance the carcinogenic potential of UVB radiation [10, 112]. Furthermore, this may have serious implications on the safety of UVA sunbeds used to obtain a tan for cosmetic reasons [113, 114].

Sun Protection Factors (SPF) were developed as a means of quantitatively assessing the degree of protection a sunscreen offered against solar radiation. While SPF values are primarily a measure of the degree of protection against UVB radiation there is some controversy about the significance of SPF values in decreasing skin cancer mortality [10, 115]. However, SPF values are still widely accepted. SPF values can be determined by *in vivo* or *in vitro* methods.

## Theory

### *In vivo* determination of SPF values

Under a light source of constant UV intensity, the SPF of a product determined *in vivo* under specified conditions is given by the relationship:

$$SPF = \frac{\text{Exposure duration for minimum erythema in protected skin}}{\text{Exposure duration for minimum erythema in unprotected skin}}$$

**Equation 4–1: *In vivo* determination of sun protection factors [116].**

The exposure duration of the minimum erythemal dose (MED) to UV radiation has to be determined empirically over many days so as not to cause excessive burning to the skin of subjects. The average of the SPF values, determined in at least 10 subjects, is taken as the SPF value for the sunscreen tested [36, 116].

As sunscreens are intended to be used to protect human skin from the deleterious effects of sunlight, it would seem logical to use sunlight as the UV testing light source. However, sunlight is too variable and unpredictable to be used routinely for testing large numbers of sunscreen products. The intensity and spectral distribution of solar radiation vary greatly depending on latitude, altitude, time of day, season, cloud cover and stratospheric ozone concentration [116, 117]. Environmental and physiological conditions such as skin heating, sweating and evaporation caused by wind also make the use of sunlight unreliable for the determination of SPF values [117].

Many different types of light sources have been used as solar simulators. However, it is generally accepted that xenon arc lamps, with appropriate filters, have the closest spectrum to solar radiation reaching the surface of the earth [116, 118, 119] and these are the preferred testing light source.

*In vivo* sunscreen testing in the laboratory using an artificial light source has become the accepted standard for the SPF determination of sunscreens in human subjects [119]. However, *in vivo* SPF determination is time consuming and expensive.

Another disadvantage with *in vivo* methodology is that the monitored end-point is erythema. As erythema is principally due to the UVB portion of solar radiation, such methods do not take into consideration the effects of UVA radiation. In recent years there has been an increasing awareness and concern about the effects of UVA in causing skin damage and its role in skin cancer [9, 10, 116, 120-124]. There is no widely accepted technique for measuring the effectiveness of sunscreens against UVA, though many *in vitro* and *in vivo* techniques have been proposed, from spectroscopic techniques to measuring UVA induced erythema with the use of appropriate sensitising agents [115, 125-130].

#### *In vitro* determination of SPF values

Because of the time consuming and expensive nature of *in vivo* testing and the limited information concerning the protection from UVA radiation, many *in vitro* techniques have been developed to meet such shortcomings.

*In vitro* methods involve measuring the transmission spectrum of a sunscreen formulation applied to a suitable substrate and comparing it with the transmission spectrum of the substrate alone.

The *in vitro* SPF calculation differs from that of the *in vivo* SPF calculation because compensation has to be made for the energy distribution of solar UV radiation and its ability to cause erythema as a function of wavelength (see Equation 4–2) [131].

$$SPF = \frac{\sum_{290}^{400} E(\lambda)\epsilon(\lambda)}{\sum_{290}^{400} E(\lambda)\epsilon(\lambda)/MPF(\lambda)}$$

**Equation 4–2: Determination of *in vitro* SPF values, where  $E(\lambda)$  = solar simulator/sunlight intensity spectrum,  $\epsilon(\lambda)$  = Erythema action spectrum and  $MPF(\lambda)$  = is the monochromatic protection factor at wavelength  $\lambda$ nm. The MPF is determined by the transmittance of the blank substrate divided by the transmission through the substrate with the applied sunscreen.**

In Equation 4–2 the numerator  $\sum_{290}^{400} E(\lambda)\epsilon(\lambda)$  describes the ability of sunlight to

produce erythema in unprotected skin while the denominator

$\sum_{290}^{400} E(\lambda)\epsilon(\lambda)/MPF(\lambda)$  describes the ability of sunlight to produce erythema in

sunscreen protected skin.

*In vitro* techniques that have been used include; determining the transmission characteristics of sunscreen agents based on spectrophotometric analysis of sunscreens in solution, transmission data derived from film sandwiches of ingredients/products between quartz plates or films on quartz plates alone or with substrates such as wax paper or onionskin copying paper. Most of these types of *in vitro* evaluations correlate poorly

with *in vivo* evaluations [132-134]. Failure of these *in vitro* techniques to match *in vivo* results has largely been attributed to the absence of skin topography and sunscreen-skin interactions when artificial substrates are used [135, 136]. *In vitro* studies using epidermal skin from hairless mice [137] or cadaver skin [136] demonstrate better correlations with *in vivo* results.

An *in vitro* method using a substrate of transparent silicone rubber impressions from the surface of human skin has been developed. The SPF values obtained from this *in vitro* technique, while not quantified, showed some correlation with *in vivo* results. However, the preparation of the silicone impressions is time consuming [125]. Diffey and Robson [131] have obtained a good correlation between *in vivo* and *in vitro* results using Transpore™ tape for sunscreens with SPF values below 25.

The need for *in vitro* techniques to measure SPF values greater than 30

In 1985, the Australian government started major national education campaigns to encourage early detection and prevention of skin cancer and the use of sunscreens [1]. These campaigns are ongoing. In response to public demand, manufacturers have begun emphasising protective rather than tanning properties of their products. At the time this study was carried out there were few sunscreens that were labelled less than the maximum 15<sup>+</sup> allowed by the 1993 Australian and New Zealand standard for the evaluation and classification of sunscreen products [116]. With the introduction in 1997

of a new standard [36] that increases the maximum allowable SPF labelling from 15<sup>+</sup> to 30<sup>+</sup>, manufacturers may be prompted into producing a higher proportion of sunscreens with SPF values greater than 30.

Most *in vitro* SPF studies have evaluated sunscreens with SPF values of less than 30 [12, 119, 131-133, 137-139]. *In vitro* techniques need to be developed that can determine SPF values that are higher than 30 to accommodate the growing trend of producing sunscreens with high SPF values.

While *in vitro* methods may not altogether remove the need for *in vivo* testing, they may significantly reduce much of the preliminary work required for *in vivo* methods.

The present study is based on previous methods described by Diffey and Robson [131] and Pearce and Edwards [119]. However, the present study uses a standard spectrophotometer to measure the transmission characteristics of sunscreen formulations. Furthermore, the effective linear detector range of the spectrophotometer has been increased with the use of custom software to enable measurement of the transmission characteristics of very high SPF (>70) sunscreens more accurately.

### ***IN VITRO* SPF DETERMINATION PROCEDURE**

The technique described determines the relative amount of UV light, at 5 nm intervals from 290 – 400 nm, that is transmitted through an applied layer of sunscreen. From the data the *in vitro* SPF is calculated as outlined in Equation 4–2.

## Aim

The aim of this work was to develop an improved *in vitro* technique for the determination of high SPF values (>30) of sunscreens that are currently difficult to measure accurately with standard *in vitro* techniques.

## Materials and methods

### *The optical system*

A Cary<sup>®</sup> 1E double beam spectrophotometer (Varian Instruments, Melbourne) was modified for the determination of SPF values.

Two holders were constructed to support quartz plates (45 mm x 12 mm x 2 mm). The quartz plates were ground on each side with a 400 mesh abrasive until an evenly diffusing surface was created. A full discussion on the use of diffusers to reduce errors associated with measuring the transmission through scattering specimens, such as epidermal skin is given by Bruls and van der Leun [140].

The holders were constructed to locate the quartz plate as near as possible to the detector windows of the sample compartment of the spectrophotometer. This was done so that a large fraction of the quartz plate would be irradiated with light, and as much of the direct scattered light as possible could enter the detector compartment (see Figure 4-1).

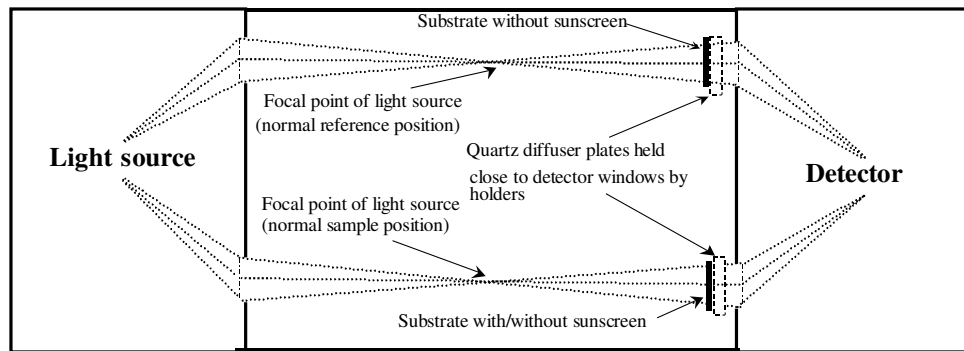


**Figure 4-1: Schematic representation of the spectrophotometer optical system for *in vitro* SPF determination.**

### Substrates

#### *Human stratum corneum*

This study protocol was approved by the Research and Ethics Committees of the Royal Hobart Hospital.

Human stratum corneum substrates were obtained using methods adapted from Marks and Dawber [141] and Pearce and Edwards [119]. The skin samples were taken in the form of skin surface biopsies (SSBs) from the flexor aspect of the forearms of volunteer subjects. Volunteers with excessive coarse hair in this area were excluded. Between three and eleven samples could be taken from each arm. Most volunteers reported that the procedure was not painful and all subjects readily volunteered for more than one SSB.

Each SSB was prepared as follows. A small amount of cyanoacrylate adhesive (Powerbond 100; Straident international, Middlesex, UK) was evenly spread over a diffusing quartz plate with a plastic pipette tip. The quartz plate was then held against the forearm skin with light pressure. The cyanoacrylate adhesive produced a complete and even film between the

quartz plate and the skin. After one minute the quartz plate was pulled away leaving an even layer of skin adhered to it.

The SSB was trimmed to the dimensions of the quartz plate along each edge using a razor blade. Wet and dry emery paper (800-grade) was rubbed lightly over the dampened surface of the SSB to remove any keratin plugs or glue spikes [119]. This step was found necessary to permit the subsequent even spread of test products. The skin substrate was rinsed in cold tap water, dried at room temperature and stored at room temperature until used [119].

Skin and cyanoacrylate was removed from the quartz plates after use by soaking in acetone.

#### *Transpore™ tape*

Transpore™ tape is a self-adhesive plastic tape with a knobbly surface. Transpore™ tape was affixed directly to the quartz plate. Edges were trimmed to the dimensions of the quartz plate with a razor blade.

#### *In vivo sunscreen standards*

Nine commercially available sunscreens were used as standards. SPF values for eight of these products had been determined by the Australian Photobiology Testing Facility (APTF) in Sydney using the Australian and New Zealand Standard *in vivo* methodology [116]. The SPF of the other sunscreen had been determined by the same methodology, but by an

unknown laboratory (this information was withheld by the manufacturer).

The labelled active ingredients of each sunscreen are shown in Table 4-1.

The actual SPF and testing location data was obtained by direct correspondence with the companies marketing each sunscreen product within Australia. To minimise a potential source of variance it was intended that only sunscreens that had been tested by the APTF were to be used in this study. However, the sunscreen with an SPF of 129 (H) was also used because it had the highest SPF value, from data supplied from all the companies, and was thought to be a good test for the *in vitro* method.

**Table 4-1: Active ingredients of each sunscreen tested**

<i>Products</i>	<b>Labelled SPF</b>	<b>Active ingredients</b>	<b>Testing Facility</b>
A	4	Octyl methoxycinnamate Butyl methoxydibenzoylmethane	APTF
B	12	Octyl methoxycinnamate Butyl methoxydibenzoylmethane	APTF
C	17 <sup>♠</sup>	Butyl methoxydibenzoylmethane Octyl methoxycinnamate Oxybenzone	APTF
D	24	Octyl methoxycinnamate Oxybenzone	APTF
E	50	Octyl methoxycinnamate Oxybenzone Padimate O Titanium Dioxide	APTF
F	77	Octyl methoxycinnamate Oxybenzone Padimate O Titanium Dioxide	APTF
G	77	Octyl methoxycinnamate Oxybenzone Padimate O Titanium Dioxide	APTF
H	129	Microfine titanium dioxide (as a complex) Oxybenzone Octyl methoxycinnamate	Unknown <sup>♠</sup>

- ♣ Alcohol/oil sunscreen formulation.
- ♣ The company in question withheld this information.

### *Increasing the effective range of the detector*

The *in vitro* SPF method described requires the measurement of the amount of light transmitted through an applied film of sunscreen product. For high SPF sunscreens the amount of light transmitted through a film of sunscreen could be very low.

In normal double beam mode the detector gain of the spectrophotometer is automatically adjusted so that the light intensity from the reference beam falls within the linear range of the detector of the instrument. Therefore, for high SPF sunscreens, where the intensity of the transmitted light through the sample position is considerably less than the transmitted light intensity through the reference position, the gain of the detector may be too low to measure the sample beam transmittance accurately, due to a poor signal to noise ratio.

While it was possible to manually alter the sensitivity of the detector in single beam mode, such measurements do not compensate for changes in detector response with time, increasing the variability of single beam mode measurements. To overcome this limitation and to measure the low levels of transmittance associated with a high SPF product, a pseudo-double beam mode of operation was developed.

In normal double beam mode operation the transmittance is calculated by Equation 4-3:

$$T = \frac{Sample_{(x)}}{Reference_{(x)}}$$

Where:

T is the transmission for the sample,

$Sample_{(x)}$  is the detector response (mA) from the sample beam at gain 'x'

$Reference_{(x)}$  is the detector response (mA) from the reference beam at gain 'x'.

**Equation 4-3: Equation for calculating the light transmission through a sample in double beam mode [142].  $Sample_{(x)}$  and  $Reference_{(x)}$  are both corrected automatically for any residual current that may be in the detector.**

When measuring the percentage transmission through a sunscreen it may be necessary to measure the sample beam intensity and the reference beam intensity at different gains in order that both fall within the linear range of the detector. However, if the reference beam and sample beam intensities are measured at different gains, it is not possible to calculate the transmittance, see Equation 4-4:

$$?_{(T)} = \frac{Sample_{(x)}}{Reference_{(y)}}$$

Where:

$?_{(T)}$  is the unknown transmission for the sample,

$Sample_{(x)}$  is the detector response (mA) from the sample beam at gain 'x' and

$Reference_{(y)}$  is the detector response (mA) from the reference beam at gain 'y'.

**Equation 4-4: It is not possible to calculate transmission through a sample if the sample and reference beam measurements are taken at different gains.  $Sample_{(x)}$  and  $Reference_{(y)}$  are both corrected automatically for any residual current that may be in the detector [142].**

The pseudo double beam mode measures detector responses (mA) taken at different gains in single beam mode. In order to compare detector responses at different gains, detector gain versus detector response curves for the

spectrophotometer were constructed (described later), so that any measurements of detector response at a particular gain setting could be converted to an equivalent value at another gain, see Equation 4–5:

$$\frac{Sample_{(x)}}{Reference_{(y)}} \xrightarrow{\text{via detector gain versus detector response curves}} \frac{Sample_{(z)}}{Reference_{(z)}} \Rightarrow T$$

Where:

$T$  is the transmission for the sample,

$Sample_{(x)}$  is the detector response (mA) from the sample beam at gain ‘x’,

$Reference_{(y)}$  is the detector response (mA) from the reference beam at gain ‘y’.

$Sample_{(x)}$  &  $Reference_{(y)}$  are the calculated sample and reference detector responses at gain ‘z’.

**Equation 4–5: Equation for calculating the light transmission through a sample in pseudo double beam method.  $Sample_{(x)}$  and  $Reference_{(y)}$  are both corrected automatically for any residual current that may be in the detector [142].**

The pseudo double beam mode can also compensate for changes in detector response with time by comparing each measurement of transmittance from the sample position, taken at any gain, to a measurement taken from the reference position at a fixed gain (discussed in more detail later).

#### *Detector gain versus detector response curve*

The relationship between detector response and gain was established by measuring the detector responses at different gain settings.

To approximate the optical conditions during *in vitro* SPF testing all light was passed through the quartz diffusing plates, during the determination of the gain response curves.

The gain versus response curve was created as follows:

1. In single beam mode scans through the reference position were performed from 290 – 400 nm at 1 nm intervals. The gain was adjusted until all detector responses were between 0.03 – 2.1 mA. The gain at which all responses were between 0.03 – 2.1 mA was then used as the reference gain in the following steps.

It was found during the development of the detector gain versus detector response curve that detector responses outside the range of 0.03 – 2.1 mA did not have the same response relationship between gains as those within the range.

2. In single beam mode scans through the sample were performed from 290 – 400 nm at 1 nm intervals position at gains 110 and 120. An aperture, consisting of a piece of thin metal plate placed over the source and/or the detector window, was manually adjusted so that all detector responses from 290 – 400 nm at gains 110 and 120 were between 0.03 – 2.1 mA.
3. Using custom software written in the Applications Development Language (ADL) of the Cary<sup>®</sup> instrument (Appendix 1-8) scans from 290 – 400 nm at 1 nm intervals at a gain of 110 were carried out by continual

beam interchanges<sup>‡</sup> between the sample and reference positions. The reference gain determined in step 1 and the aperture setting in step 2 were fixed. At 290 nm the detector response from the sample position was recorded. A beam interchange was performed and the detector response from the reference position was recorded. This process was continued for all wavelengths within the range. The same procedure was carried out at gain 120. All detector responses were stored automatically in ASCII files.

4. Using the gain determined in step 1, steps 2 and 3 were repeated for the gain sets 120 – 130, 130 – 140, 140 – 150, 150 – 160, 160 – 170, 170 – 190, 190 – 210, 210 – 230, 230 – 250.
5. All detector responses from the sample position taken at various gains, and from the reference position taken at a single gain, were exported to Microsoft Excel™ via ASCII files created in the data collection process. In Microsoft Excel™, detector responses recorded from the sample beam were adjusted for fluctuations in the detector response with time by Equation 4-6.

---

<sup>‡</sup> A beam interchange changes the light path from the sample position to the reference position and vice versa.

$$Sample_c(\lambda) = \left( \frac{reference_r(\lambda)}{reference_t(\lambda)} \right) * Sample_t(\lambda)$$

Where:

$Sample_c(\lambda)$  is the corrected detector intensity for  $\lambda$  nm,

$reference_r(\lambda)$  is the detector response from the reference beam for  $\lambda$  nm, that all other detector responses from the reference beam for  $\lambda$  nm, taken at a different time 't' are compared against,

$reference_t(\lambda)$  is the detector response from the reference beam at 't' for  $\lambda$  nm and

$Sample_t(\lambda)$  is the detector response from the sample beam at time 't' for  $\lambda$  nm.

**Equation 4-6: Equation for correcting fluctuations in the detector response with time.**

6. The equations of the lines of best fit and the correlation coefficients ( $R^2$ ) were calculated for the change in detector response (corrected) with increasing gain for the gain sets listed in step 4. The detector response from the lower gain was used as the x axis.
7. The detector response at gain 110, for each wavelength, was substituted for x in the line of best fit relating the detector responses from gain 110 to 120. The result was then substituted for x in the line of best fit relating the detector responses from gain 120 to 130. This was repeated for all the gain sets listed in step 4. Using the equations of the lines of best fit, theoretical detector response from gains 120 to 250 were calculated.
8. Plots of the detector response at gain 110 versus the calculated values (step 7) for the detector responses for gains 120 to 250 were constructed. Plots were constructed with the detector response at gain 110 along the x-axis and the calculated detector responses up to gain 250 along the y-axis. The regression equation and  $R^2$  were determined for every increase in gain.

### *Pseudo double beam mode*

In normal double beam mode the transmittance is calculated by dividing the detector response from the sample position by the detector response from the reference position (baseline), see Equation 4-3. In pseudo double beam mode two scans are needed. The detector responses from the sample position of the second scan are divided by the detector responses from the sample position of the first scan (baseline). The detector responses from the reference position of both scans are used to correct fluctuations in detector response with time, see Equation 4-6.

Scans in pseudo double beam mode, described below, were carried out between 290 – 400 nm at 5 nm intervals with quartz diffusing plates in the sample and reference positions to approximate the optical conditions during *in vitro* SPF testing. Pseudo double beam mode operations were carried out with custom software written in the Applications Development Language (ADL) of the Cary<sup>®</sup> instrument (Appendix 1-8).

The pseudo double beam mode was performed as follows; steps 1 & 2 determine the initial gain settings required for the pseudo double beam mode:

1. In single beam mode scans were performed in the reference position from 290 – 400 nm at 5 nm intervals through a quartz diffusing plate. The gain was adjusted until all readings were between 0.03 – 2.1 mA. The gain at which all readings were

between 0.03 – 2.1 mA was then used as the reference gain in the following steps.

2. In single beam mode scans were performed in the sample position from 290 – 400 nm at 5 nm intervals. The gain was adjusted until all readings were between 0.03 – 2.1 mA. The gain was adjusted to one of the gain values used to create the detector gain versus detector response curves.
3. A baseline scan was performed by measuring the sample beam intensity at 290 nm through a quartz diffusing plate. A beam interchange was performed and the reference beam intensity for the same wavelength was recorded. This process was repeated for each wavelength at 5 nm intervals from 290 – 300 nm. The gain in the reference position was that determined in step 1, the gain in the sample position was that determined in step 2.
4. To measure the transmission through a sample attached to the quartz diffusing plate in the sample position the same process as in step 3 was followed. However, if the detector response from the sample compartment was outside the 0.03 – 2.1 mA range, the gain was increased or decreased in the range 110 – 250 units, to keep the signal strength within the linear range of the detector. Where possible, the gain was increased in steps of 20 gain units, to reduce the number of jumps between gain sets for each scan. The sample beam intensity had to lie within the range 0.03 – 2.1 mA before a

beam interchange was performed to measure the reference beam intensity. From the detector gain versus detector response relationship a theoretical intensity of the sample beam was calculated as if it had been measured at a gain of 110, and hence, as if the signal strength lay within the linear range of the detector.

The theoretical intensity of the sample beam was calculated by using the linear regression equations from the detector gain versus detector responses, by dividing by the slope of the linear regression equation relating the detector response from the gain at which the sample was measured (y-axis) to the theoretical detector response at gain 110 (x-axis). As the y intercept value was less than 0.5 % for the lowest value of y (when  $x = 0.03$ ) the intercept was ignored.

5. All detector responses were exported to Microsoft Excel™ via ASCII files created in the data collection process. In Microsoft Excel™, detector responses recorded from the sample beam were adjusted for fluctuations in the detector response with time by Equation 4-6
6. To determine the transmission of the sample the corrected detector responses from the sample position of the sample scan (step 4) were divided by the corrected detector responses from the sample position of the baseline scan (step 3).

### Application of sunscreens onto substrates

A latex rubber fingerstall was tared on an electronic balance. A 1 mL insulin syringe with a 26 G needle was used to deposit enough sunscreen on the fingerstall to give an application area density of  $2 \text{ mg/cm}^2 \pm 10\%$ § after application. As some sunscreen would remain on the finger cot after application, the weight of sunscreen that needed to be applied initially was based on trial and error. The fingerstall was then placed on a finger and the sunscreen spread over the substrate. After application of sunscreen, the fingerstall was re-weighed and the amount of sunscreen which had been deposited on the substrate was calculated.

To minimise variation that may affect the predicted SPF values during the application of a sunscreen onto a substrate, the following protocol was followed;

- The percentage transmission of the substrate was initially measured (see Collection of SPF data).
- One minute 30 seconds was allowed for the application of sunscreen onto the fingerstall.
- Thirty seconds was allowed for placing the fingerstall onto a finger.

---

§ While the Australian and New Zealand Standard *in vivo* methodology has a tolerance of  $\pm 5\%$  this proved impractical due to the nature and availability of the substrates [116].

- The sunscreen was gently rubbed into the substrate with the fingerstall in a forwards and backwards motion over the period of a minute. During that time approximately 30 passes in each direction were made over the substrate surface.
- Fifteen minutes after the sunscreen had been applied the percentage transmission of the substrate and skin were measured.

The alcohol/oil base sunscreen was applied to the substrate in a different manner due to the rapid evaporation of solvent after application and the liquid nature of the solvent. Instead of applying the sunscreen to the finger cot, the density of the sunscreen formulation was measured and an appropriate volume of sunscreen was applied to the substrate directly, and then rubbed in with a fingerstall.

#### *Collection of SPF data*

The collection of SPF data from the spectrophotometer was carried out automatically by custom software. Each of the sunscreens was tested five times using both the Transpore™ tape and the SSB substrates. The collection of SPF data involved the measurement of UV light transmittance through the substrate without applied sunscreen and then with applied sunscreen

Prior to measuring the initial transmittance through the stratum corneum substrate, without applied sunscreen, 5–10 µL of arachis oil was evenly spread over the surface of the SSB to decrease the forward light scattering on the substrate (see Discussion). The substrate was then lightly blotted with

tissue paper to remove any excess oil. No arachis oil was added to the Transpore™ tape.

A substrate with no sunscreen applied was placed in the sample and reference position of the sample compartment of the spectrophotometer.

A baseline transmission through the substrate in the sample position was measured in the pseudo-double beam mode described above. The scan range was 290 – 400 nm measured at 5 nm intervals with a signal bandwidth set at a maximum of 4 nm. Due to small, observable shifts in baseline measurements which occurred when the light source changed from the deuterium to the halogen lamp, all readings were carried out under the halogen lamp.

Once the UV transmission of the blank substrate was complete, sunscreen was applied to the substrate as described above.

Fifteen minutes after the sunscreen was applied the transmission through the substrate and sunscreen was measured in pseudo-double beam mode described above. The signal bandwidth was adjusted to 0.2 nm to minimise the amount of light reaching the detector when measurements were not being made. The scan range was 290 – 400 nm measured at 5 nm intervals. Another ASCII export file, of the wavelength, gain, detector response of the sample beam, theoretical detector response of the sample beam at gain 110, and the detector response of the reference beam at a set gain, was created.

### Mathematical interpretation of data

The ASCII files created during the collection of SPF data were exported to Microsoft Excel™ and corrected for changes in detector response (see Equation 4-6). *In vitro* SPF values were calculated as outlined by Equation 4-2. The solar simulator intensity spectrum and the erythema action spectrum were those used by Diffey [131, 143] (see Appendix 2-2).

### Within-day variability of the detector gain versus detector response

A thin piece of metal plate was placed partially over the source and/or the detector window. The aperture created was adjusted until all light source readings were between 0.03 – 2.1 mA for the gains 150 and 170 in single beam mode. The changes in the detector response with increasing gain from 150 to 170 were recorded intermittently over an eight-hour period by the same method used to create the detector gain versus detector response curves described earlier. By plotting the change in the detector response with increasing gain, the regression equation and  $R^2$  was obtained. In the determination of the regression equation the x-axis was used for the lower gain and the y-axis for the higher gain (see Figure 4-4, under Results). By substituting the value of y for 100 in the equation of the line of best fit a numerical result was obtained. The numerical results obtained were used to calculate the degree of variability (RSD) between the equations.

During the course of this experiment the aperture was not adjusted. All readings were carried in pseudo–double beam mode.

*Inter-day variability of the detector gain versus detector response*

The changes in the detector response with increasing gain from 150 to 170 gain units were recorded daily over five days. The procedure for determining the inter-day variability of the gain response curve was otherwise the same as that for measuring the within-day variability for the detector gain versus detector response.

*Within-day variability of the % transmission through skin*

The change in the percentage transmission with time of a SSB, with arachis oil applied (10 µL, excess removed with tissue paper) and without arachis oil applied was measured. The percentage transmission was measured in double beam mode for the wavelength range 390 – 400 nm at 1 nm intervals. The percentage transmission was recorded at 0, 2, 5, 10, 15, 30, 60 and 120 minutes.

*In vitro versus in vivo SPF factors-Statistical analysis*

*In vitro* SPF results obtained with the Transpore™ tape and the SSB substrates were compared to the given *in vivo* SPF results using the non-parametric Spearman Rank Correlation test and the parametric Pearson correlation test.

## Results

A representative detector gain versus detector response curve is shown in Figure 4-4. The regression equations from the detector gain versus detector response curves are shown in Table 4-2. The within-day RSD for the detector gain versus detector response from 150 to 170 was 2.02 %. The inter-day RSD for the detector gain versus detector response from 150 to 170 was 3.12 %.

Changes in the percentage transmission with time for a SSB with arachis oil applied (10  $\mu$ L, excess removed with tissue paper) are shown in Figure 4-2.

Changes in the percentage transmission with time for a freshly prepared SSB are shown in Figure 4-3.

**Change in % transmission with time: freshly prepared Skin Surface Biopsy with arachis oil applied**

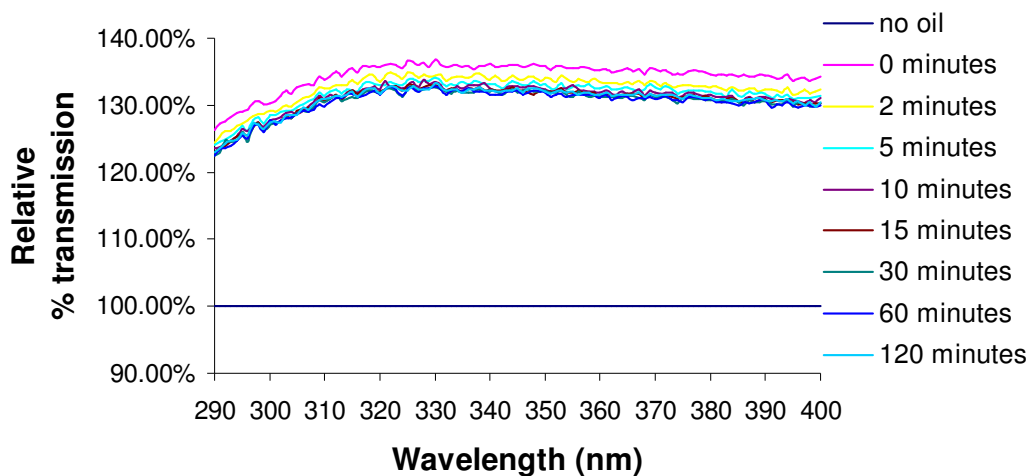


**Figure 4-2:** Change in percentage transmission with time of a freshly prepared SSB with arachis oil applied (10  $\mu$ L, excess removed with tissue paper). The baseline was the percentage transmission of the SSB with no arachis oil applied.

**Change in % transmission with time: freshly prepared Skin Surface Biopsy**

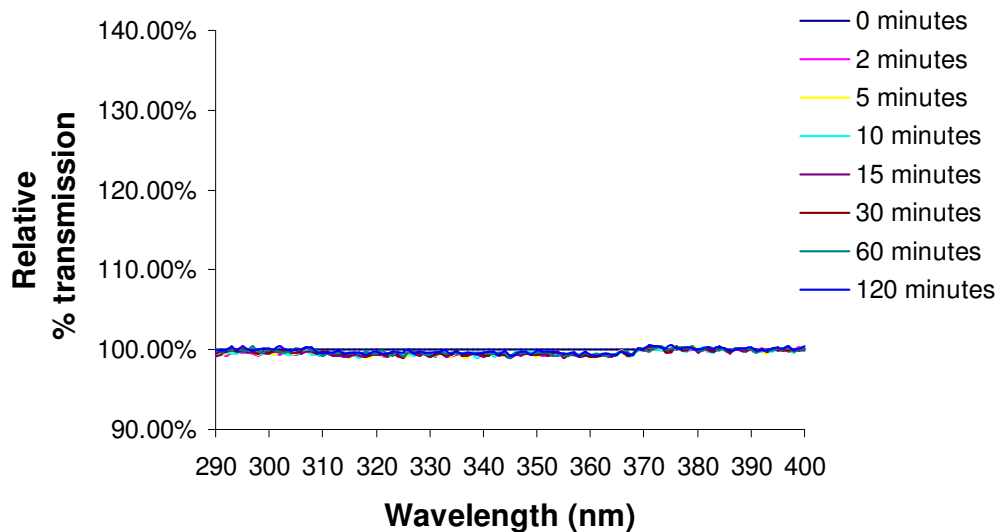


**Figure 4-3:** Change in percentage transmission with time of a freshly prepared SSB. The baseline was the percentage transmission of the SSB at time zero.

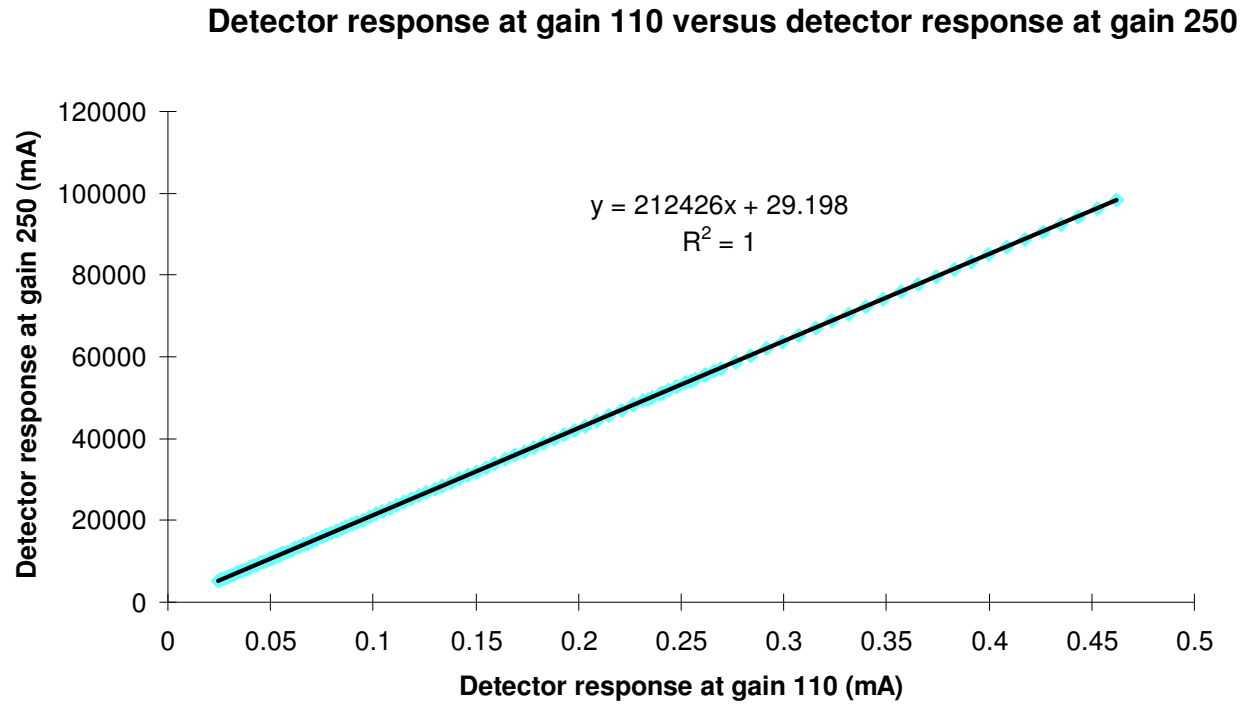


**Figure 4-4:** A representative detector gain versus detector response curve. The detector response at a detector gain of 110 versus the theoretical detector response if the detector gain is changed to 250 (see Table 4-2).

**Table 4-2: Regression equations relating the theoretical detector response (y (mA)) at a specified gain and the detector response (x (mA)) at a gain of 110.**

<u>Detector gain</u>	<u>Regression Equation</u>	<u>R<sup>2</sup></u>
120	$y = 2.3259x - 0.00005$	1
130	$y = 5.204x + 0.0002$	1
140	$y = 11.44x + 0.0009$	1
150	$y = 25.019x + 0.0029$	1
160	$y = 54.566x + 0.007$	1
170	$y = 123.11x + 0.0165$	1
190	$y = 681.83x + 0.0935$	1
210	$y = 4382.3x + 0.602$	1
230	$y = 33603x + 4.6182$	1
250	$y = 212426x + 29.198^{\wedge}$	1

<sup>^</sup>Shown in Figure 4-4

### Statistical analysis of *in vitro* SPF results

*In vitro* analysis of sunscreen H (which according to the manufacturer had an SPF of 129) with the SSB substrate gave an SPF of 12.3 (n=5, interquartile range=7.7) and with Transpore™ tape an SPF of 22.4 (n=5, interquartile range=2.7). A sample of the sunscreen was then sent to the APTF for an independent *in vitro* analysis with an Optometrics SPF Analyser™\*\* using Transpore™ tape as a substrate. This gave a mean SPF of 30 with standard deviation of 11.1 (n = 7). The company which manufactured the sunscreen was then contacted again to confirm that the original SPF information they

---

\*\* Uses same method described by Diffey and Robson [131].

supplied was correct. The company said that the original information they had given should not have been made available for the study and they would not confirm any SPF value given. However, they would confirm that the sunscreen product reportedly had an SPF greater than 60, as a brochure had been made available to dermatologists and other allied health professionals stating that the SPF of the product was greater than 60.

Another sample of the product was then sent to the APTF for a pilot *in vivo* evaluation using 4 subjects. The *in vivo* SPF results were 12.8, >16, 20 and 16. As the *in vivo* evaluation was not done on 10 subjects it could not be used to calculate an SPF value for the sunscreen by Australian methodology [36, 116]. However, agreement of this method with the independent re-evaluation by the APTF (both *in vitro* and *in vivo*) suggests that the true SPF of the product is unlikely to be close to 129. Due to the large discrepancy between the pilot *in vivo* evaluation and the original SPF data supplied by the manufacturer, the results from sunscreen H were not included in any statistical comparisons.

The *in vitro* SPF results obtained in the present study for the SSB and Transpore™ tape substrates are given in Table 2-1.

**Table 4-3: Comparison between *in vitro* methods and *in vivo* method.**

Sunscreen	<i>In vitro</i> SPF methods		<i>In vivo</i> SPF* method
	SSB Median (n=5) (interquartile range)	Tape Median (n=5) (interquartile range)	Australian Method [116]
A	5.2 (2.3)	15.5(9.9)	4
B	13.0 (2.3)	29.7(4.15)	12
C	15.7 (6.8)	27.9(4.8)	17
D	23.2 (0.6)	19.4(6.3)	24
E	63.1 (14.2)	71.2(21.9)	50
F	71.4 (7.5)	54.3(21.4)	77
G	44.4 (7.7)	50.1(24.3)	77
H	12.3 (7.7)	22.4(2.7)	129**

\*Manufactures' claims

\*\*When independently tested by the APTF this sunscreen had an SPF ranging from 12.8 – 20 (n=4).

*Parametric Pearson correlation test*

The SSB *in vitro* SPF results versus *in vivo* SPF results were:  $R^2 = 0.793$ ,  
 $p = 0.072$ ,  $n = 7$  (see Figure 4-5).

The Transpore™ tape *in vitro* SPF results versus *in vivo* SPF results were:  
 $R^2 = 0.611$ ,  $p = 0.0378$ ,  $n = 7$  (see Figure 4-6).

*Non-parametric Spearman correlation test*

The SSB *in vitro* SPF results versus *in vivo* SPF results were: Rho corrected  
for ties = 0.937, Z corrected for ties = 2.295,  $p = 0.0217$ ,  $n = 7$ .

The Transpore™ tape *in vitro* SPF results versus *in vivo* SPF results were:  
Rho corrected for ties = 0.739, Z corrected for ties = 1.81,  $p = 0.0704$ ,  $n = 7$ .

***In vivo* SPF results versus *in vitro* SPF results obtained with a SSB substrate**

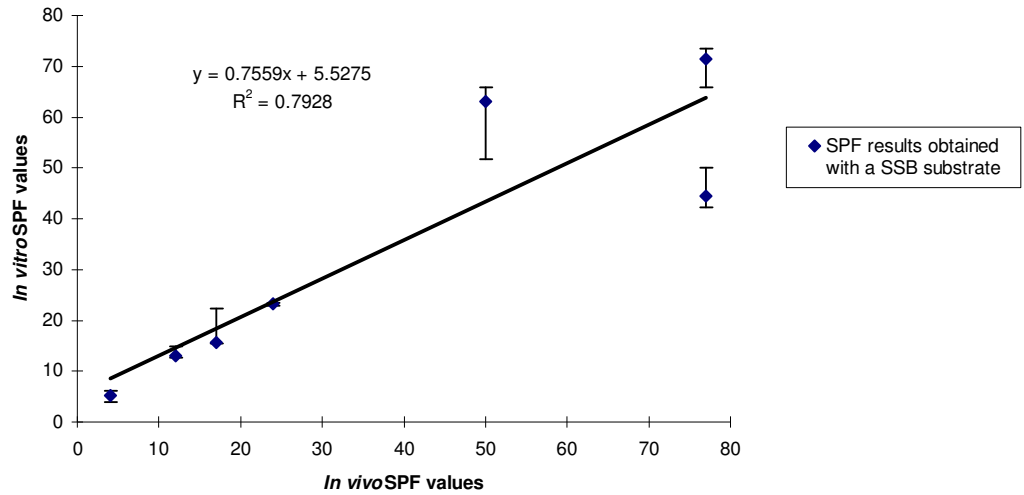


**Figure 4-5:** *In vitro* versus *in vivo* SPF for the SSB substrate, with linear regression lines. Data points are median values, error bars represent upper and lower quartile range.

***In vivo* SPF results versus *in vitro* SPF results obtained with Transpore™ tape substrate**

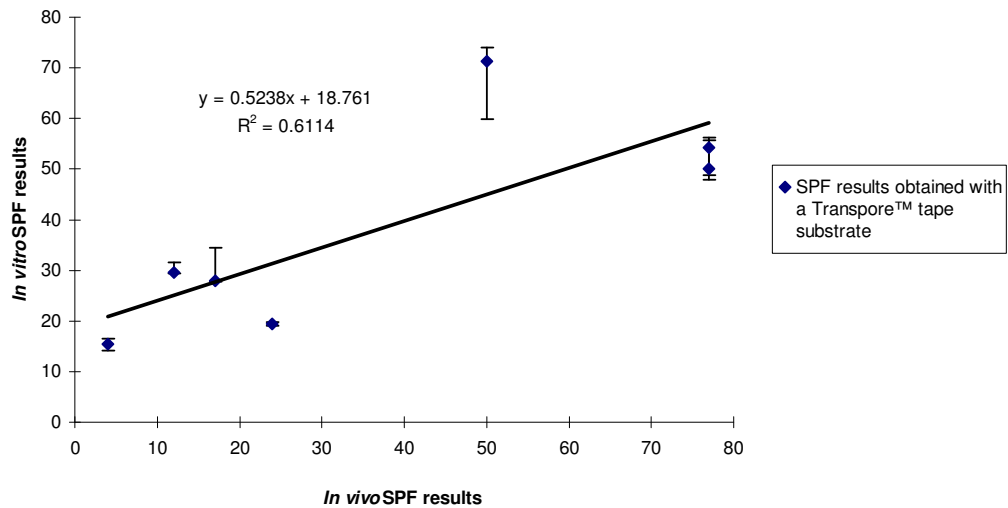


**Figure 4-6:** *In vitro* versus *in vivo* SPF for the Transpore™ tape substrate, with linear regression lines. Data points are median values, error bars represent upper and lower quartile range.

## Discussion

*In vivo* SPF data was obtained directly from the manufacturing companies as all sunscreens within Australia have to be tested by one of a small number of approved testing laboratories before they can be sold to the general public. These laboratories must meet the requirements of the current sunscreen evaluation standard [36].

There was a large discrepancy between the SPF value supplied by the manufacturer for sunscreen H and the *in vitro* results obtained with the SSB and Transpore™ tape substrate. The *in vivo* pilot carried out by an independent laboratory (n=4) study gave an SPF range 12.8 - 20 which was in good agreement with the *in vitro* results obtained with the methods outlined in this thesis. The laboratory at which sunscreen H had been originally tested for the manufacturer was not known. Therefore, it was not possible to ascertain if the difference between the *in vivo* and *in vitro* results was due to differences in the laboratory testing procedures or a fault of the product such as decomposition. If the differences in SPF values were due to a fault in the product, the *in vitro* method would be a useful quality assurance procedure after a sunscreen had been manufactured.

The results obtained with the SSB substrate correlated well with *in vivo* results and were very similar to those obtained by Pearce and Edwards [119] in both the slope of the linear regression and the Spearman's correlation

coefficient. The results obtained with the Transpore tape correlated less well with *in vivo* results.

Diffey and Robson [131] and Pearse and Edwards [119] applied sunscreen to the Transpore™ tape by “spotting” sunscreen at several sites over the application area and then rubbing the sunscreen in with a latex-gloved finger until a uniform thickness was obtained. In this study, a small trial using this method of application did not appear to alter the predicted SPF values obtained. It was noted by Diffey and Robson [131] that Transpore™ tape is not suitable for testing oil or alcohol vehicles due to absorption of these products into the tape. The *in vitro* evaluation of the alcohol/oil formulation (sunscreen C) in this study appeared to not correlate as well with the *in vivo* data as the other sunscreens tested.

Initial *in vitro* SPF evaluations on SSBs without pre-treatment of the substrate with arachis oil gave SPF values that were substantially lower than the manufacturers’ SPF values obtained with *in vivo* testing. It was noted that the surface of a SSB substrate was rougher than the surface of normal skin, possibly due to connective tissue remaining on the SSB substrate after preparation. It is possible that the application of sunscreen was decreasing the light scattering properties of the SSB more than it would for normal skin *in-situ*, thereby increasing the amount of light transmitted through the substrate and decreasing the predicted SPF of the product. In one study [144] monitoring the effects of emollients on UV-induced erythema in normal skin, the application of arachis oil, corn oil, mineral oil, Vaseline™ and other

emollients decreased the observed erythematous response 24 hours after UV exposure. Similar results were obtained in another study [145] where the application of mineral oil, or an emollient cream or liquid to normal skin either increased or had no effect on the MED. However, treatment of a SSB substrate with arachis oil significantly increased the UV transmission through the substrate (see Figure 4-2). If this effect occurred in normal skin it would be expected that the erythematous response from UV exposure would increase and the MED would decrease. To overcome the problem the SSB was pre-treated with arachis oil, prior to measuring the transmission through the blank substrate, so that the later addition of sunscreen formulation would not result in a further increase in UV transmission through the substrate.

Initial SPF determination was carried out in double beam mode with the instrument controlled by custom written software (see Appendix 1-7). This program had a number of advantages over the pseudo-double beam method, which was developed and used later in this study. The double beam mode software was very fast, scans could be done in approximately 5 seconds. By manually entering the solar intensity spectrum and the UV action spectrum for human skin into the Cary<sup>®</sup> filing system<sup>++</sup> the *in vitro* SPF value was calculated automatically by the custom software. The major disadvantage with the double beam mode method was that it could not measure SPF values of sunscreens with high SPF values (> 30) without going outside the linear range of the detector.

The pseudo-double beam mode method could measure very high SPF values (> 70) without going outside the linear range of the detector. In theory, SPF values greater than > 1000 could be measured by this method. There were, however, disadvantages with the method. The scan time for the pseudo-double beam mode method was much longer, taking approximately 4 minutes, due to a beam interchange between each wavelength reading. The detector gain versus detector response curves had to be checked periodically for changes, and raw data gathered by this method had to be exported to Microsoft Excel™ in order to calculate an SPF value.

The between day-variability of the relationship between detector gain and detector response was evaluated over a period of five days. Factors that are likely to effect the relationship between gain and detector response fall into two main categories; those factors that affect the gain of the detector and those factors that affect detector response to light. The gain of the Cary 1E is altered by changing the voltage across the detector using an array of resistors that act as voltage dividers. Physical deterioration or large fluctuations in temperatures would alter the resistance through the resistors. Similarly, physical deterioration or large fluctuations in temperatures may also alter the detector response to light. The relationship between detector gain and detector response was tested periodically during the course of the study by assessing the reproducibility of a single point on the detector gain versus detector response curve.

---

†† imported via software written in ADL (see Appendix 1-8).

The pseudo-double beam mode method increases the effective linear range of the detector by comparing detector responses at different gains using a previously determined detector gain versus detector response curve. The same effect can be achieved by using an adjustable aperture for the reference beam and altering the detector response inversely with the size of the aperture. Such devices are commercially available and can be completely automated by software. With such a device there would be no need for detector gain versus detector response curves for the comparison of detector responses taken at different gains, and the SPF data could be calculated automatically by the software. This device was not used in this study as its cost was prohibitive.

From visual examination of the *in vivo* versus *in vitro* correlation it is appears that the correlation is stronger in the below 30 SPF range than the above 30 SPF range. Unfortunately, at the time these correlations were performed there were not many sunscreens in the above 30 SPF range where the identity of the *in vivo* testing facility was known, leading to a lack of data points in this range. While it has been postulated that poor correlations between *in vivo* and *in vitro* results can be attributed to errors associated with measuring transmission through scattering substances [132, 140, 146] the author believes, in this study, this to is unlikely to be a cause of any lack of correlation. In this study, diffusers were used to reduce errors associated with measuring the transmission through scattering specimens (a full discussion is given by Bruls and van der Leun [140]). Variations in the measurement of high SPF values are more probably due to varying film

thicknesses and minor differences between sunscreen formulations in their actual content of ingredients. Minor changes in the film thickness and formulations will have a greater impact on the SPF values of sunscreens with high SPF values as opposed to sunscreens with low SPF values. For example, in a sunscreen with an SPF of 100 and equal absorbance across the UV spectrum, 99% of the light would not pass through the sunscreen film. Changing the amount of light not transmitted through the film to 98% or 100% would change the calculated SPF of that sunscreen to 50 and infinity respectively. On the other hand, for a similar sunscreen with an SPF of 10 (90% of the light would not pass through the sunscreen film) changing the amount of light not transmitted through the film to 89% or 91% would alter the SPF of that sunscreen to 9.1 and 11.1 respectively.

The method was fast, simple and the substrate easily obtained. It appeared to correctly identify a sunscreen that had a labelled SPF value that was significantly higher than its true SPF. Furthermore, as this method can measure the transmission from 290 – 400 nm through a sunscreen it could be used to evaluate the photo-protection offered against UVA irradiation. The *in vitro* method described also was capable of evaluating high SPF sunscreens (>70) and used standard laboratory equipment.

# CHAPTER 5: THE CHARACTERISATION OF SKIN COLOUR BY DIFFUSE REFLECTANCE

## BACKGROUND

### **The need for colour measurement**

Colour is a matter of perception and subjective interpretation, so that in spite of the ability of our eyes to differentiate between colours, we are unable to precisely quantify changes in colour. Instruments are therefore required to perform this task objectively [147, 148].

The perception of colour is influenced by a number of factors such as the spectral distribution of the illuminant, the spectral reflectance of the specimen, the relative sensitivity of the light receptors in the eyes, the size of the object being viewed, background differences and the direction of viewing [149, 150]. With the use of instruments the effects of these influences can be eliminated or minimised.

A variety of portable devices and standards have been developed to objectively measure colour. These devices and standards are used in the quality control of manufactured items such as clothing, carpets, paints, pigments, dyes and in the printing industry. In the area of dermatology and medicine, these devices and standards have many uses; for time-correlation studies of ultraviolet B induced erythema [151], for the measurement of the colour parameters of psoriatic plaques [152], measuring the vascular

response of skin to local anaesthetics, corticosteroids and anti histamines [153-155], non-invasive measurement of haemoglobin saturation in brain and muscle vasculature after circulatory arrest and the quantitation of cutaneous haemoglobin and melanin [30, 156-158].

Spectrophotometers are used in many laboratories, irrespective of discipline, and have most of the features required for the measurement of diffuse reflectance. They usually consist of a polychromatic light source, a monochromator, a detector and the electronic hardware required to control these devices. Most modern spectrophotometers also have computerised software packages to display and manipulate collected data. However, in terms of the requirements for measuring diffuse reflectance of the skin, they lack a means of irradiating a sample outside the usual sample compartment and of measuring the light reflected from the sample. These functions can be achieved by the use of fibre optic light guides and a measuring probe similar to those used by other workers in their custom-built spectrometers [29-31, 159].

## **Theory of Colour Perception**

### Colour

The perception of colour can be objectively described in terms of three variables; value, chroma and hue which are explained with the use of a 3D colour mapping system (see Figure 5-1).

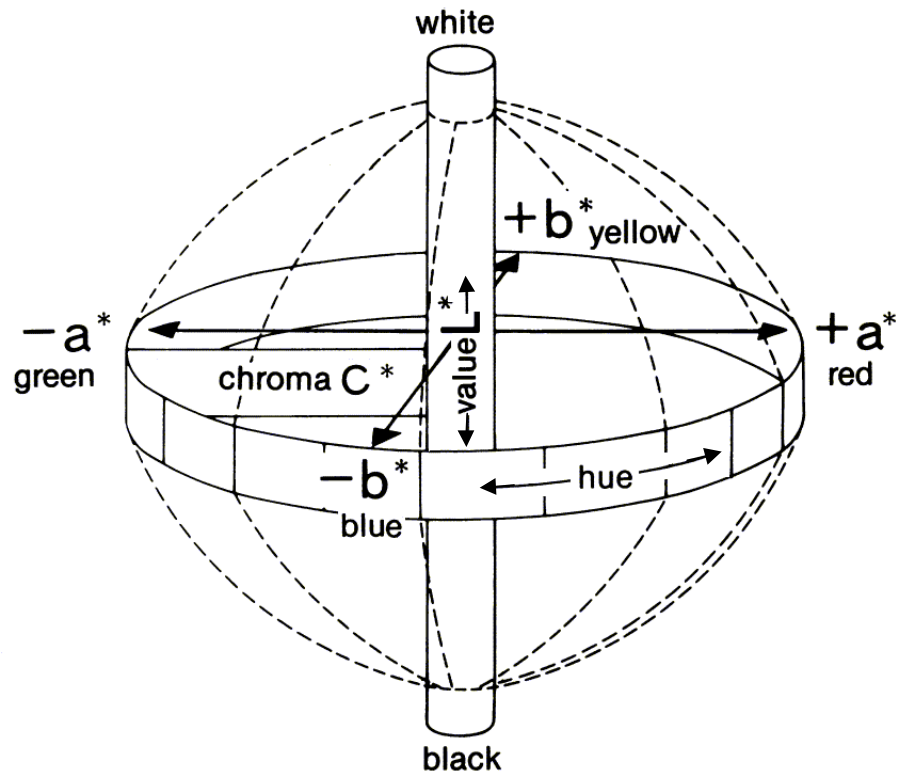


Figure 5-1: The CIE  $L^*a^*b^*$  solid 3D colour mapping system (adapted from [150])

A 3D colour mapping system can be represented as a sphere with three axes  $L^*$ ,  $a^*$ ,  $b^*$  (see Figure 5-1). The value or lightness ( $L^*$ ) of an object is a measure of the percentage of the amount of light reflected from the surface of an object<sup>††</sup>.  $L^*$  is a number between 0 – 100. An object with an  $L^*$  of 0 appears black and absorbs all light in the visible range. An object with  $L^*$  of 100 appears white and reflects all light in the visible range.

Chroma ( $C^*$ ), also known as saturation or vividness, is a measure of the intensity of colour an object has. On the three-dimensional (3D) colour mapping chart, chroma is represented as the distance away from the centre

of the chart along the  $a^*$ ,  $b^*$  plane. Chroma ( $C^*$ ) can be calculated by Equation 5-1 (see Figure 5-2).

$$C^* = \sqrt{a^{*2} + b^{*2}}$$

**Equation 5-1: The calculation of chroma ( $C^*$ ) from the colour mapping co-ordinates  $a^*$ ,  $b^*$ .**

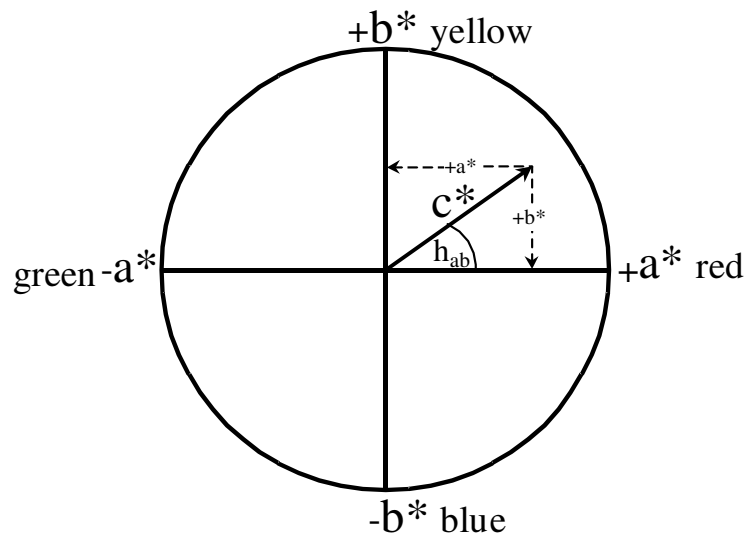


**Figure 5-2: Cross-sectional view of the CIE  $L^*a^*b^*$  solid 3D colour mapping system.**

The influence that chroma has on the perception of colour is analogous to that seen by adjusting the colour control on a colour television. By altering the chroma of an object the intensity of colour and not the hue of colour changes.

Hue is also known as the tint or colour of an object. On the 3D colour mapping chart hue can be represented as the angle  $\tan^{-1}(a^*/b^*)$  having a value of 0 - 360. This is called the hue angle, represented as  $h_{ab}$ . By

---

‡‡ In the calculation of  $L^*$  the percentage reflection at each wavelength has a different weighting, therefore  $L^*$  is not a true representation of the percentage reflection across the whole visible range.

convention, objects with positive  $b^*$  values contain yellow, those with negative  $b^*$  values contain blue, those with positive  $a^*$  values contain red and those with negative  $a^*$  values contain green. Unlike chroma, changing the hue does not change the intensity of colour.

A colour space is a method for expressing the colour of an object or a light source using some quantitative notation. The notation can be used as the co-ordinates which designate the position of a colour within a colour mapping system such as the one shown in Figure 5-1. A uniform colour space is one in which equal distances on the co-ordinates in the colour diagram correspond to equal visually perceived colour differences [150].

It is estimated that as many as 20 different colour space formulas are being used in various parts of the world [160]. From the 3D-colour mapping system shown in Figure 5-1 it is possible to plot the values for the  $L^*a^*b^*$  and  $L^*C^*h_{ab}$  uniform colour spaces.

$L^*a^*b^*$ ,  $L^*C^*h_{ab}$ , Hunter Lab, and other colour spaces are calculated from XYZ tristimulus values. The concept of XYZ tristimulus values is based on the three-component theory of colour vision, which states that the eye possesses receptors for three primary colours (red, green and blue). The XYZ tristimulus values are calculated by the CIE colour matching functions. The

CIE in 1931 defined the Standard Observer<sup>§§</sup> to have the colour matching functions  $\bar{x}$ ,  $\bar{y}$  and  $\bar{z}$  shown in Figure 5-3 [150, 161].

The colour matching functions  $\bar{x}$ ,  $\bar{y}$  and  $\bar{z}$  represent the amount of each of the primary colours required to match the colours produced at each wavelength of the visible spectrum by an observer under specified conditions. The relative sensitivities of the colour receptors in the eye and the viewing angle of the observer influence the amount of each primary colour required [149].

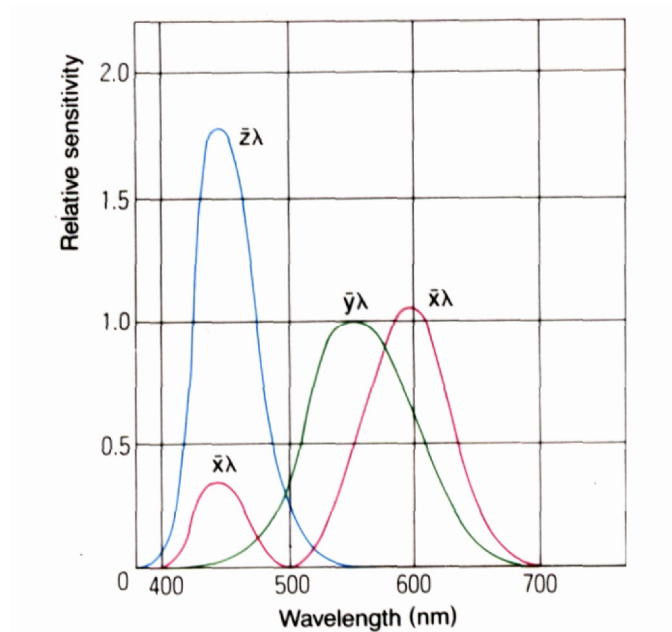


**Figure 5-3: Spectral sensitivity corresponding to the human eye (Colour-matching functions of the CIE 1931 Standard Observer) [150].**

The XYZ tristimulus functions in their calculation take into consideration the light source by which an object is viewed, the spectral reflectance of the object and the colour matching functions. The method for calculating the XYZ tristimulus functions and the  $L^*a^*b^*$ ,  $L^*C^*h_{ab}$  values is described in the

---

<sup>§§</sup> Standard Observer is an ideal observer defined in terms of colour matching functions.

American Society for Testing and Materials (ASTM) standards on colour and appearance measurement [161].

### **The optics of human skin**

“From the optical point of view, skin is a very complicated system because of its inhomogeneous, multilayered structure, and the anisotropy of its physical properties [162]”. Many models have been used in an attempt to describe the optical properties of skin [29, 162, 163].

The colour of skin is largely determined by the amount and distribution of various pigments within it. These pigments include the carotenoids (yellow), oxy-haemoglobin (red), reduced haemoglobin (blue) and melanin (eumelanin; brown/black, pheomelanin; yellow/red) [18, 45]. Differences in the distribution, type and amount of melanin in keratinocytes determines skin type and hair pigmentation [18].

The skin consists of three main layers, the stratum corneum, the epidermis and the dermis (see Figure 5-4). The stratum corneum of both white and black skin reflects between 4 and 7% of incident light over the entire spectrum from 250 – 3000 nm [163]. In the epidermis, melanin scatters impinging radiation and absorbs energy in the UV and visible ranges, dissipating it as heat [52]. Dermal collagen reflects all wavelengths almost linearly and, therefore, incident light is reflected back through the epidermis to the skin surface, thus passing through the haemoglobin and melanin containing layers twice [163].

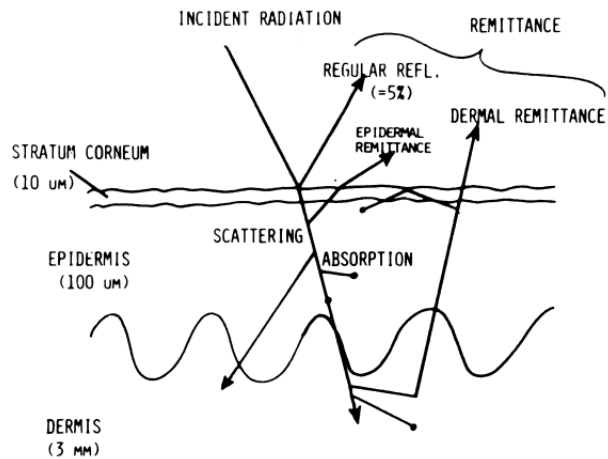


**Figure 5-4:** Diagram of the optical pathways in skin [163].

### Logarithm of the inverse reflectance

The logarithm of the inverse reflectance (LIR) is analogous to absorbance and changes in this parameter have been adopted by other workers as an index of colour change [17, 30, 31, 54, 159]. Absorbance is the logarithm (to base ten) of the inverse transmittance when light is passed through a solution [45] and the LIR is the logarithm (to base ten) of the inverse reflectance of light reflected off an object.

Dawson et al., 1980 proposed a skin pigmentation index based on the LIR from skin [29]. A straight line was drawn through the average LIR at 650 nm and at 700 nm and the slope of this line was assumed to be correlated to the concentration of melanin in the skin [29, 31].

LIR values determined between 650 – 700 nm were chosen as the best range of the spectrum over which to quantify melanin pigmentation because light absorption due to other chromophores is minimal in this region [31].

However, results from the present work and from that of Dwyer et al [164]

indicate that estimates of skin colour and melanin are better correlated by values taken between 400 - 420 nm.

### **Other instrumentation for the determination of diffuse reflectance**

Several non-commercial devices for the determination of haemoglobin or melanin in skin have been described in recent literature. These include;

- a portable reflectance instrument using light emitting diodes to illuminate the skin and a silicone photodiode to detect diffusely reflected light [156],
- a modified video-microscope [165]
- a number of purpose-built reflectance spectrophotometers incorporating a polychromatic light source, one or two variable monochromators, fibre optic light guides, a measuring probe, a detector and the necessary electrical hardware (including amplifiers for the reference and incident light sources and stepper drives for the monochromators) and an analogue to digital converter for collected data to be manipulated by custom software on a computer [29-31, 159].

## EXPERIMENTAL PROCEDURE: DETERMINATION OF DIFFUSE REFLECTANCE

### Aims

To modify a commercially available spectrophotometer to objectively characterise changes in skin colour by the determination of the diffuse reflectance of the skin and to compare the results obtained with results from a commercial colour-measuring device.

### Materials and Methods

#### *The optical systems*

##### *The adapted spectrophotometer*

A Cary<sup>®</sup> 1E double beam spectrophotometer (Varian Instruments, Melbourne) was modified to allow the measurement of diffuse reflectance external to the normal sample compartment. All modifications to the spectrophotometer were readily reversible, external additions.

A glass fibre optic bundle (92 cm in length with a 3.2 mm active light-carrying diameter) was mounted in the sample compartment in a position such that light which would normally pass through the sample position, was conducted by the optical fibre to an external measuring probe (see Figure 5-5). The fibre optic bundle entered the top of the probe perpendicular to the surface being measured. A second fibre optic bundle, 92 cm in length with a 6.9 mm light carrying diameter, was used to transmit

light reflected from the surface being measured to the detector of the spectrophotometer. This light collecting fibre was mounted in the probe head at an angle of  $45^\circ$  to the perpendicular. The probe was similar to that described by Feather *et al*[30] and consisted of a Perspex block with a hemispherical cavity (25 mm diameter) machined into the bottom surface. The interior surface of the hemisphere was painted matt black to minimise internal reflection and to absorb light reflected specularly at the surface being measured.

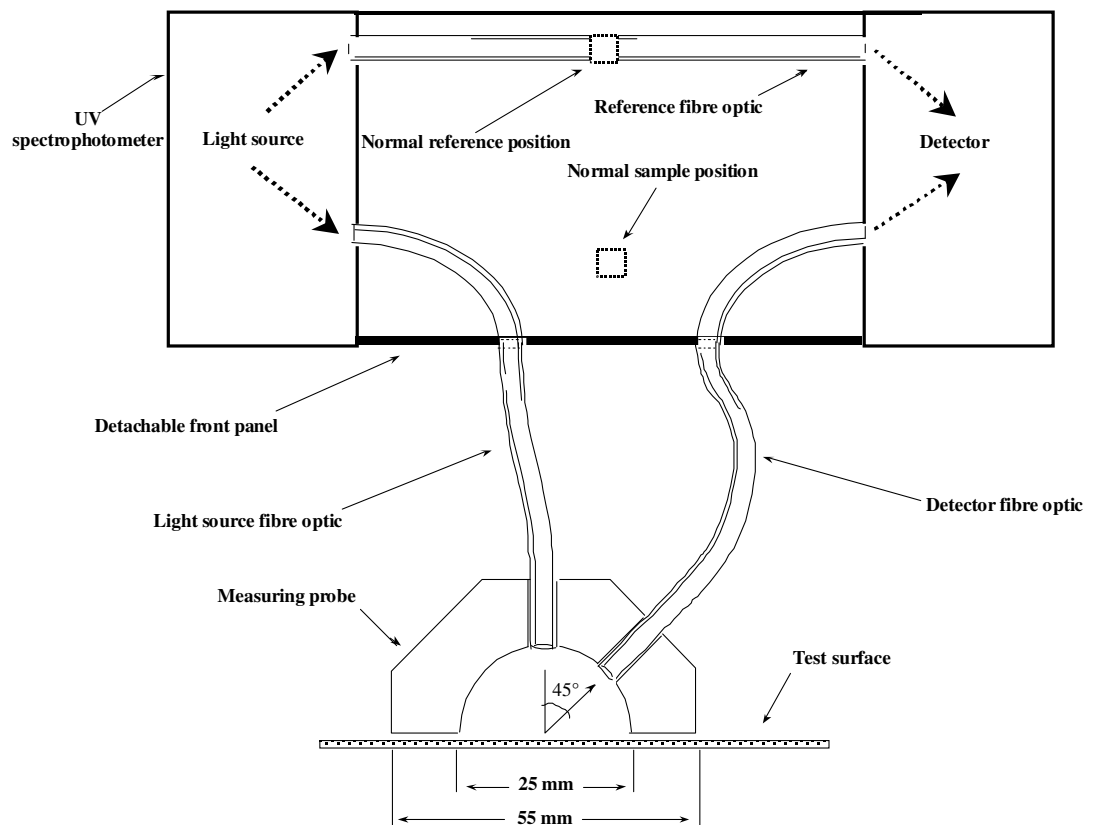


**Figure 5-5: Schematic representation of the spectrophotometer optical system used to measure diffuse reflectance.**

A third fibre optic bundle, 92 cm in length with a 1.9 mm light carrying diameter, was mounted in the sample compartment of the spectrophotometer to conduct the reference beam of the spectrophotometer

directly to the detector. In double beam mode the attenuation of the instrument was automatically regulated by the amount of light detected by the reference beam. By placing a piece of opaque black tape partially over one end of the reference optical fibre the amount of light reaching the detector from the reference beam, and therefore the gain of the instrument, could be altered if necessary.

#### *Minolta CM-508d portable spectrophotometer*

Some of the results obtained using the adapted spectrophotometer were compared against those obtained using a commercially available Minolta CM-508d portable spectrophotometer.

#### *Reflectance standards*

A 5 cm cube of Spectrolon<sup>®</sup> (Labsphere, U.K.) was used as a 100 % diffuse reflectance standard. Spectrolon<sup>®</sup> is a material with the highest diffuse reflectance of any known material, or coating, over the ultra-violet/visible/near infrared region of the spectrum [166]. Reflectance is generally >99 % over the range 400 to 1500 nm and >95 % between 250 and 2500 nm. The matt black internal surface of the sample compartment of the spectrophotometer was used as a black reference standard, representing a zero percent diffuse reflectance baseline.

### Reflectance standards

The instrument was operated in double beam mode. Scans of both the white and black reference standards were carried out between 400 and 700 nm and the light intensities at 1 nm intervals over this wavelength range were stored for subsequent calculations. The white reference surface was used as a 100% diffuse reflectance baseline to compensate for any loss of light intensity through the system while the black reference surface was used as a 0% diffuse reflectance baseline to compensate for any internal reflections in the probe. The intensity of the reference beam (carried through the third fibre optic bundle) was monitored to compensate for any changes in the intensity of the light emitted from the source during the course of a scan. Pre-spectral averaging (n = 5) was used in these scans to provide a stable reference baseline upon which it was possible to base subsequent calculations.

### Mathematical interpretation of data

#### *Logarithm of the inverse reflectance*

The LIR has been used in previous studies as a parameter analogous to absorbance [29, 156]. The LIR at 1 nm intervals over the scan range of 400 – 700 nm was calculated using Equation 5–2.

$$\text{LIR} = \text{Log} \left( \frac{\left( \frac{I_W}{I_{RW}} - \frac{I_B}{I_{RB}} \right)}{\left( \frac{I_T}{I_{RT}} - \frac{I_B}{I_{RB}} \right)} \right)$$

Where:

$I_W$	=	reflected intensity, white standard
$I_{RW}$	=	reference intensity, white standard
$I_T$	=	reflected intensity, test surface
$I_{RT}$	=	reference intensity, test surface
$I_B$	=	reflected intensity, black standard
$I_{RB}$	=	reference intensity, black standard

**Equation 5-2: Equation for the calculation of LIR values. A detailed derivation of this relationship is given by Feather *et al* [30].**

These calculations were performed by software written in the Applications Development Language (ADL) of the Cary<sup>®</sup> instrument software (see Appendices 1-2 to 1-6).

$$L^*, a^*, b^*, C^*, h_{ab}$$

The colour space co-ordinates  $L^*, a^*, b^*, C^*, h_{ab}$  were calculated for the CIE illuminant D65, 1964 Standard Observer at 20 nm. The methods for calculating the colour space co-ordinates  $L^*, a^*, b^*, C^*, h_{ab}$  are described in ASTM standards on colour and appearance measurement [161].

### *In vitro evaluations*

The reproducibility of LIR determination using the modified instrument was assessed by carrying out replicate scans of an arbitrarily selected test surface consisting of a vertical stack of ten sheets of green paper. For each LIR spectrum the black and white reference surfaces were separately scanned between 400 and 700 nm at 1 nm intervals, followed immediately by a scan of the green test surface. The probe was lifted from each scanned surface and replaced on the surface before any subsequent scan. The resulting LIR was calculated and the process was repeated to give five within-day and five between-day replicates.

Prespectral averaging was not used in this *in vitro* work, since it significantly increased the time required to scan over the necessary wavelength range. Since subjects in the *in vivo* section of the study would be required to hold their breath during the scan to minimise movement, pre-spectral averaging would not be feasible when conducting *in vivo* studies with the instrument.

### *In vivo evaluations*

Ten volunteer subjects with skin colour types subjectively assessed by eye as ranging from lightly to heavily pigmented were independently ranked in order of perceived skin colour (from lightest to darkest) by a panel of ten volunteer evaluators. These evaluators were tested for colour blindness with Ishihara plates [167] prior to the commencement of the evaluation process. Each evaluator had also previously ranked eleven cardboard tiles painted with a mixture of varying amounts of brown pigment (9C8, Tas Paints; Australia) in a matt white paint, designed to resemble the colour range of skin. The amount of pigment in each tile increased in 10% increments from 0% to 100%.

After the ranking of the volunteer subjects had been completed, an LIR value was obtained from a scan of the skin of each subject. Subjects lay on their stomach for ten minutes in a darkened room maintained at  $20 \pm 2^\circ\text{C}$ . The lower back was left exposed for this period to equilibrate with room temperature. The measuring probe was held on the skin by a partially counterweighted arm such that the weight of the counterweighted arm plus probe was approximately 0.3 kg on the skin surface (see Figure 5-6). This weight was distributed over an area of  $1.88 \times 10^{-3} \text{ m}^2$  resulting in a pressure of 1.56 kPa. For each volunteer, five scans (400 – 700 nm) were taken with no prespectral averaging. The five scans were later averaged to produce a single mean scan from which all calculations were later performed.

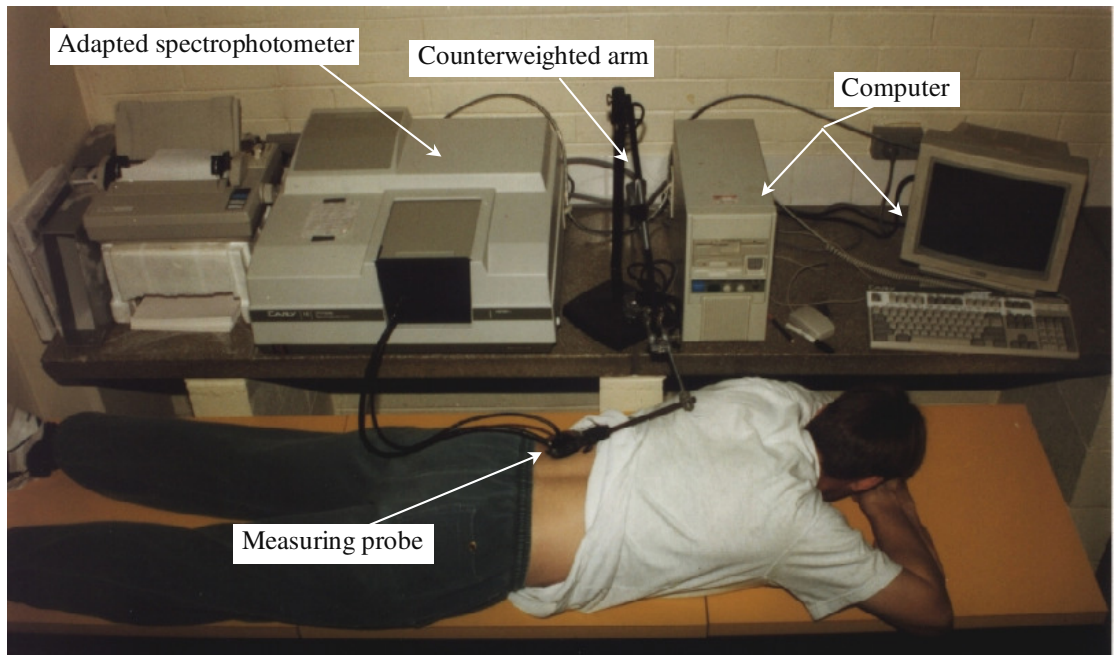


**Figure 5-6:** *In vivo* evaluation of skin colour using the adapted spectrophotometer.

Scans of the painted tiles were carried out with prespectral averaging (n=5).

The LIR values from the scans of the tiles and subjects were later used to calculate the CIE values for  $L^*$ ,  $a^*$ ,  $b^*$ ,  $C^*$  and  $h_{ab}$  for the CIE illuminant D65, 1964 Standard Observer at 20 nm intervals. This data was correlated with the ranking of the subjects by the evaluators.

All *in vivo* evaluations were carried out on the same day in order to minimise changes in skin colour that may have occurred with time.

### Monitoring changes in the inflammatory response

The ability of the device to measure changes in skin colour was evaluated. A volunteer subject with dermatographia<sup>†</sup> lightly scratched her back with her fingernails to produce an inflammatory response. Repeated scanning of the same area of the subject's skin followed the time course of the response.

### Comparisons with Minolta CM-508d

All scans for the *in vivo* evaluations were repeated using a Minolta CM-508d portable spectrophotometer using prespectral averaging (n=5). As the Minolta CM-508d used a diode array detector, five scans could be done in a few seconds. The percentage transmission data at 20 nm intervals and the CIE L\*, a\*, b\* calculated with the CIE illuminant D65, 1964 Standard Observer at 20 nm intervals were exported to an ASCII file for later use. The value of chroma C\* and the Hue angle, h<sub>ab</sub>, were later calculated from a\* and b\*.

Results obtained from the evaluators, for the ranking of the coloured tiles and skin colour, were correlated with the L\*, a\*, b\*, C\*, h<sub>ab</sub> and percentage reflectance (at 400 nm) data obtained from the adapted spectrophotometer and the Minolta CM-508d on the same surfaces.

---

<sup>†</sup> A condition in which moderate stroking of the skin produces a pale, raised welt or wheal with a red flare on either side.

## Results

### *In vitro evaluations*

Figure 5-7 shows a composite LIR spectrum obtained from the average of the five inter-day scans of a green test surface. The mean LIR (n=5) at each 1 nm interval between 400 and 700 nm was plotted. The spectrum shows a minimum LIR (ie. a maximum reflectance) at a wavelength of  $\approx 520$  nm which falls in the wavelength range of green light. The standard deviation of each set of five LIR values at each wavelength was also plotted on the same axes (mean SD = 0.003, range 0.001 - 0.01, n=300).

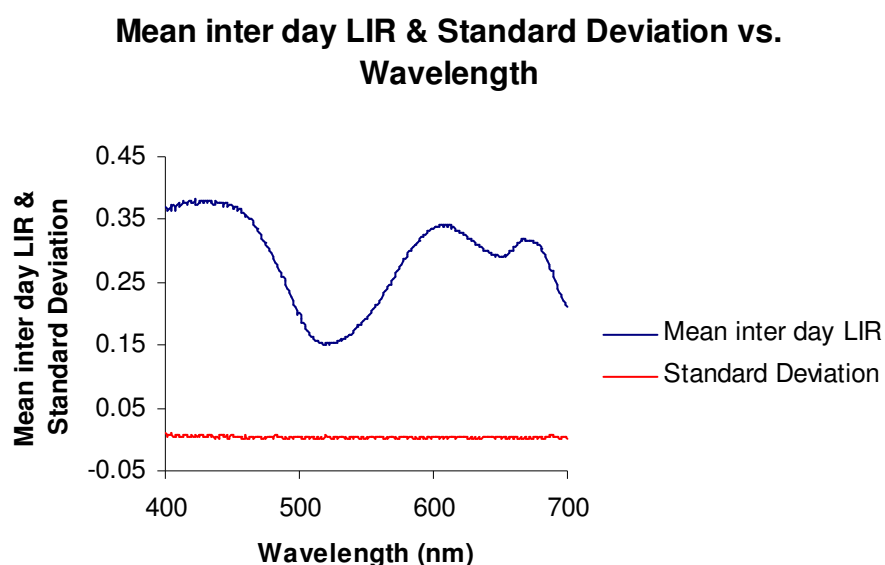


**Figure 5-7:** A mean LIR spectrum obtained from the average of five inter-day scans of a green test surface. The standard deviation of each set of five LIR values at each wavelength was plotted on the same axes.

The variability in the within and inter-day data for the different scans from which the overall LIR values were calculated is summarised in Figure 5-7.

**Table 5-1: Within-day inter-day RSD (n=300) values for the white reference, black reference, green reference and the calculated LIR of the green reference.**

Parameter	Relative Standard Deviation % of five replicate scans, at 1 nm intervals from 400 – 700 nm (Mean (range),(n = 300))	
	Within-day	Between Day
<b>Reflected intensity (I<sub>w</sub>) White standard</b>	0.42 (0.44 - 1.91)	0.75 (0.20 - 2.45)
<b>Reflected intensity (I<sub>B</sub>) Black reference</b>	2.04 (0.46 - 7.56)	6.51 (2.65 - 14.1)
<b>Reflected intensity (I<sub>G</sub>) Green test surface</b>	0.60 (0.10 - 2.54)	0.70 (0.16 - 2.38)
<b>Calculated LIR of Green test surface</b>	0.93 (0.12 - 3.27)	1.25 (0.20 – 3.92)

*In vivo evaluations*

The results from the ranking of the coloured tiles by the ten evaluators are shown in Table 5-2. With one exception evaluators, ordered the tiles correctly from lowest to highest pigment content. Table 5-3 shows the ranking of the subjects from lightly to heavily pigmented by the same evaluators. Most of the evaluators commented that subject TW was difficult to rank as this subject appeared flushed and red. The ranking of TW showed the greatest variability. Table 5-4 shows the ranking of the coloured tiles by both the adapted spectrophotometer and the Minolta CM-508d Table 5-5 shows the ranking of the subjects by both the adapted spectrophotometer and the Minolta CM-508d. At the time the subjects were ranked with the spectrophotometers subject TW appeared to be visibly less flushed.

**Table 5-2: Ranking of the tiles by the evaluators from lowest to highest pigment content.**

	<u><i>Evaluators</i></u>										
	MN	AP	KB	RB	RR	SM	KM	JJ	SA	WF	Sum/11
<b>0</b>	1	1	1	1	1	1	1	1	1	1	1
<b>10</b>	2	2	2	2	2	2	2	2	2	2	2
<b>20</b>	3	3	3	3	3	3	3	3	3	3	3
<b>30</b>	4	4	4	4	4	4	4	4	4	4	4
<b>40</b>	5	5	5	5	5	5	5	5	5	5	5
<b>50</b>	6	6	6	6	6	6	6	6	6	6	6
<b>60</b>	7	7	7	7	7	7	7	7	7	7	7
<b>70</b>	8	8	8	8	8	8	8	8	8	8	8
<b>80</b>	9	9	9	9	9	9	9	10	9	9	9.1
<b>90</b>	10	10	10	10	10	10	10	9	10	10	9.9
<b>100</b>	11	11	11	11	11	11	11	11	11	11	11

**Table 5-3: Ranking of the subjects by the evaluators from lightly to heavily pigmented.**

	<u>Evaluators</u>										Sum/10	Range
	MN	AP	KB	RB	RR	SM	KM	JJ	SA	WF		
<b>CB</b>	1	2	3	2	2	1	2	1	2	1	1.7	1-3
<b>SJ</b>	2	1	1	3	3	2	1	2	1	2	1.8	1-3
<b>LS</b>	3	4	2	4	1	3	3	3	4	4	3.1	1-4
<b>MA</b>	6	3	6	5	5	4	4	5	5	5	4.8	3-6
<b>GP</b>	4	5	5	7	4	6	5	4	6	3	4.9	3-7
<b>TW***</b>	5	7	4	1	6	8	7	6	3	6	5.3	1-8
<b>GH</b>	8	6	7	6	8	5	6	7	7	7	6.7	5-8
<b>TA</b>	7	8	8	8	7	7	8	8	8	8	7.7	7-8
<b>OH</b>	9	9	9	9	9	9	9	9	9	10	9.1	9-10
<b>AR</b>	10	10	10	10	10	10	10	10	10	9	9.9	9-10

*Subjects*

\*\*\* Most of the evaluators commented that subject TW was difficult to rank as this subject appeared flushed and red.

**Table 5-4: Colorimetric values of coloured tiles by the adapted spectrophotometer and the Minolta CM-508d.**

	<i>Adapted Spectrophotometer</i>						<i>Minolta CM-508d</i>					
	<b>LIR at 400 nm</b>	<b>L*</b>	<b>a*</b>	<b>b*</b>	<b>C*</b>	<b>h<sub>ab</sub></b>	<b>LIR at 400 nm</b>	<b>L*</b>	<b>a*</b>	<b>b*</b>	<b>C*</b>	<b>h<sub>ab</sub></b>
<b>0%</b>	0.38	98.11	-0.83	1.16	1.43	-35.52	0.38	95.77	-0.31	2.02	2.04	-8.72
<b>10%</b>	0.49	85.80	11.21	18.99	22.05	30.56	0.47	84.20	10.73	17.51	20.54	31.50
<b>20%</b>	0.59	80.93	15.08	23.55	27.97	32.63	0.55	80.03	14.28	21.39	25.72	33.73
<b>30%</b>	0.65	77.90	17.19	25.87	31.06	33.61	(0.64	74.95	17.80	24.64	30.40	35.84) <sup>†††</sup>
<b>40%</b>	0.69	75.36	18.41	27.10	32.77	34.19	0.65	74.77	17.63	24.66	30.31	35.56
<b>50%</b>	0.74	73.45	20.75	28.86	35.54	35.72	0.69	72.86	19.17	25.93	32.25	36.48
<b>60%</b>	0.78	71.53	21.21	29.56	36.39	35.67	0.72	71.13	19.78	26.39	32.98	36.85
<b>70%</b>	0.82	69.67	21.96	30.59	37.66	35.67	0.75	69.62	20.65	27.12	34.09	37.29
<b>80%</b>	0.85	68.52	22.83	31.02	38.52	36.35	0.78	68.30	21.28	27.52	34.79	37.71
<b>90%</b>	0.89	67.38	23.15	31.86	39.38	36.00	0.80	67.31	21.50	27.78	35.13	37.74
<b>100%</b>	0.93	65.73	24.03	32.40	40.34	36.56	0.83	66.17	22.36	28.46	36.19	38.16

*%Pigment in matt white paint*

†††These readings from the Minolta CM-508d were probably taken from the 40% pigment tile, in error, and have not been used in subsequent calculations.

**Table 5-5: Colorimetric values of subjects by the adapted spectrophotometer and the Minolta CM-508d. Subjects are arranged from lightly to heavily pigmented as determined by the evaluators.**

	<i>Adapted Spectrophotometer</i>							<i>Minolta CM-508d</i>					
	<b>LIR at 400 nm</b>	<b>Mean RSD (Range; n = 300)</b>	<b>L*</b>	<b>a*</b>	<b>b*</b>	<b>C*</b>	<b>h<sub>ab</sub></b>	<b>LIR<sup>†††</sup> at 400 nm</b>	<b>L*</b>	<b>a*</b>	<b>b*</b>	<b>C*</b>	<b>h<sub>ab</sub></b>
<b>CB</b>	0.42	4.49 (1.47 - 7.34)	75.37	4.69	4.26	6.33	47.77	0.55	71.97	6.03	12.68	14.04	25.43
<b>SJ</b>	0.46	3.05 (0.62 - 6.03)	76.87	4.56	8.34	9.50	28.68	0.64	71.29	5.57	15.82	16.77	19.40
<b>LS</b>	0.48	4.16 (2.37 - 6.89)	75.03	4.19	8.23	9.23	26.97	0.62	69.81	7.80	14.51	16.47	28.26
<b>MA</b>	0.55	4.29 (2.18 - 6.87)	73.43	3.96	11.60	12.26	18.87	0.71	68.43	6.84	17.37	18.67	21.49
<b>GP</b>	0.56	4.36 (1.43 - 7.81)	74.18	4.48	13.83	14.54	17.95	0.67	70.05	7.18	18.08	19.45	21.66
<b>TW</b>	0.66	4.93 (0.36 - 2.58)	68.39	9.48	11.64	15.02	39.16	0.78	63.40	9.18	16.02	18.46	29.81
<b>GH</b>	0.63	2.48 (1.00 - 5.27)	70.54	6.00	12.64	13.99	25.40	0.75	65.35	9.87	17.09	19.74	30.01
<b>TA</b>	0.72	4.81 (3.17 - 7.35)	68.08	7.86	16.20	18.01	25.87	0.82	63.46	8.81	18.37	20.37	25.62
<b>OH</b>	0.78	1.67 (0.58 - 3.62)	66.18	9.03	19.09	21.12	25.32	0.99	57.47	12.14	20.92	24.19	30.13
<b>AR</b>	1.03	1.73 (0.23 - 3.01)	57.56	9.52	22.32	24.27	23.11	1.02	54.18	10.59	19.81	22.46	28.13

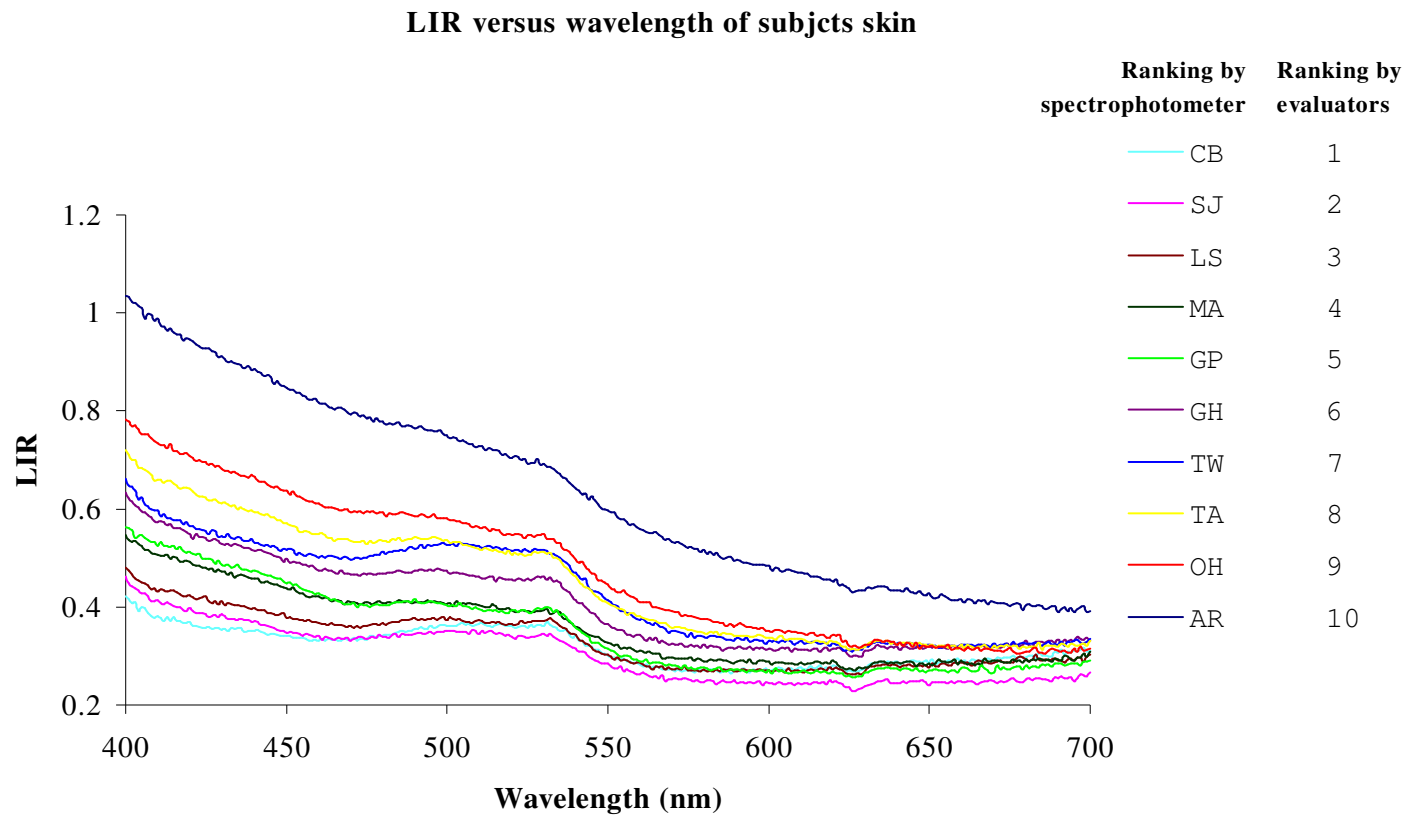
††† The RSD was not calculated as the Minolta CM-508d recorded the mean spectra of subjects.

Figure 5-8 shows the LIR values of the skin of subjects versus wavelength, there is a significant overlap of the LIR spectra in the region of 600 – 700 nm. This region of the spectrum would have poor correlation between perceived skin colour and the LIR values because of the overlap of LIR values in this area.

### *Monitoring changes in the inflammatory response*

Scratching the skin on the lower back of the subject with dermatographia produced an immediate inflammatory fare and wheal response visible as distinct red lines and swelling in the area of stimulation. The time course of the response to changes in the LIR values with time (see Figure 5-9). The LIR spectrum of the skin involved is shown in Figure 5-9. The double peak between 510 and 600 nm is from oxyhaemoglobin and is a distinctive feature of the LIR of skin [29]. This double peak indicated an increase in blood flow to the area, which made the skin appear redder.

The oxyhaemoglobin double peak was almost back to baseline levels after 34 minutes. The decrease in magnitude of the double peak of oxyhaemoglobin corresponded with a visibly observed lessening of redness in skin involved and probably a decrease in blood flow to the area.



**Figure 5-8:** LIR versus wavelength for each subject. Measurements were performed with the adapted spectrophotometer. Ranking was from lightest (1) to darkest (10). Spectrophotometer ranking was by the LIR at 400 nm.

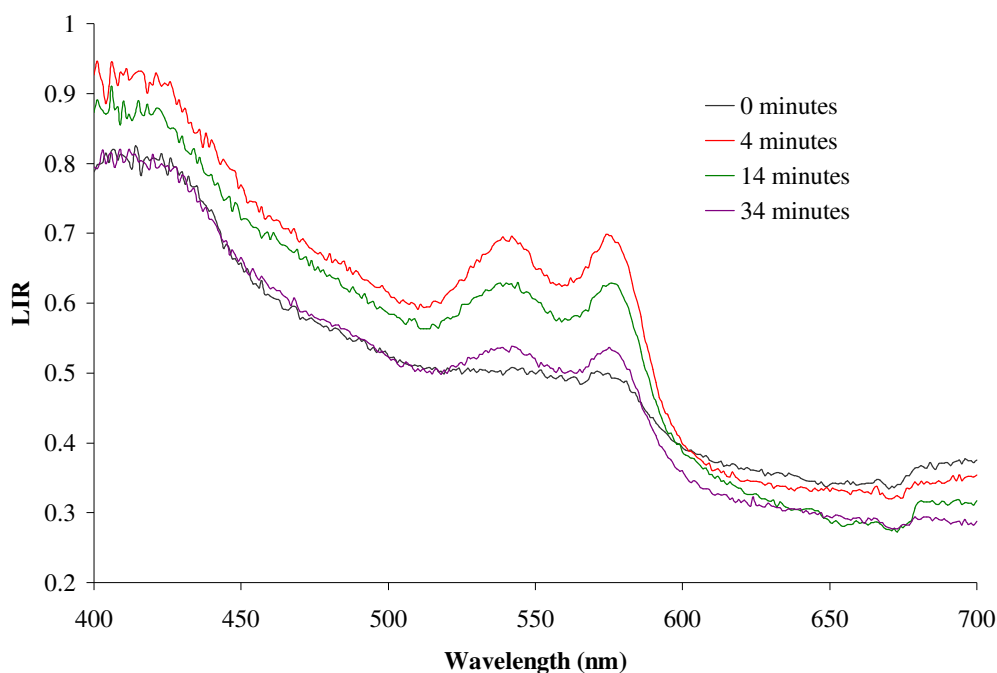


**Figure 5-9: Colorimetric time course of inflammation and wheal response of a subject with dermatographia after being scratched.**

*Comparisons with Minolta CM-508d*

The  $L^*$ ,  $a^*$ ,  $b^*$ ,  $C^*$ ,  $h_{ab}$  values and the LIR at 400 nm obtained using the Minolta CM-508d and the adapted spectrophotometer for the coloured tiles are shown in Table 5-4. The  $L^*$ ,  $a^*$ ,  $b^*$ ,  $C^*$ ,  $h_{ab}$  values and the LIR at 400 nm obtained using the Minolta CM-508d and the adapted spectrophotometer for the ranking of the subjects are shown in Table 5-5.

Figure 5-10 shows the correlations between  $L^*$ ,  $a^*$ ,  $b^*$ ,  $C^*$ ,  $h_{ab}$  colorimetric values and the LIR at 400 nm versus the ranking of the subjects skin colour by the evaluators for the adapted spectrophotometer. Figure 5-11 shows the correlations between  $L^*$ ,  $a^*$ ,  $b^*$ ,  $C^*$ ,  $h_{ab}$  colorimetric values and the LIR at

400 nm versus the ranking of the subjects skin colour by the evaluators for the Minolta CM-508d.

All colorimetric values, with the exception of  $h_{ab}$ , correlated well with the average ranking of the subjects colour skin from lightest to darkest by the evaluators. The colorimetric value  $h_{ab}$  would not be expected to correlate with perceived lightness or darkness as it is a measure of the tint of colour (ie yellow, blue, green) and not a measure of the amount of colour or the amount of light reflected.

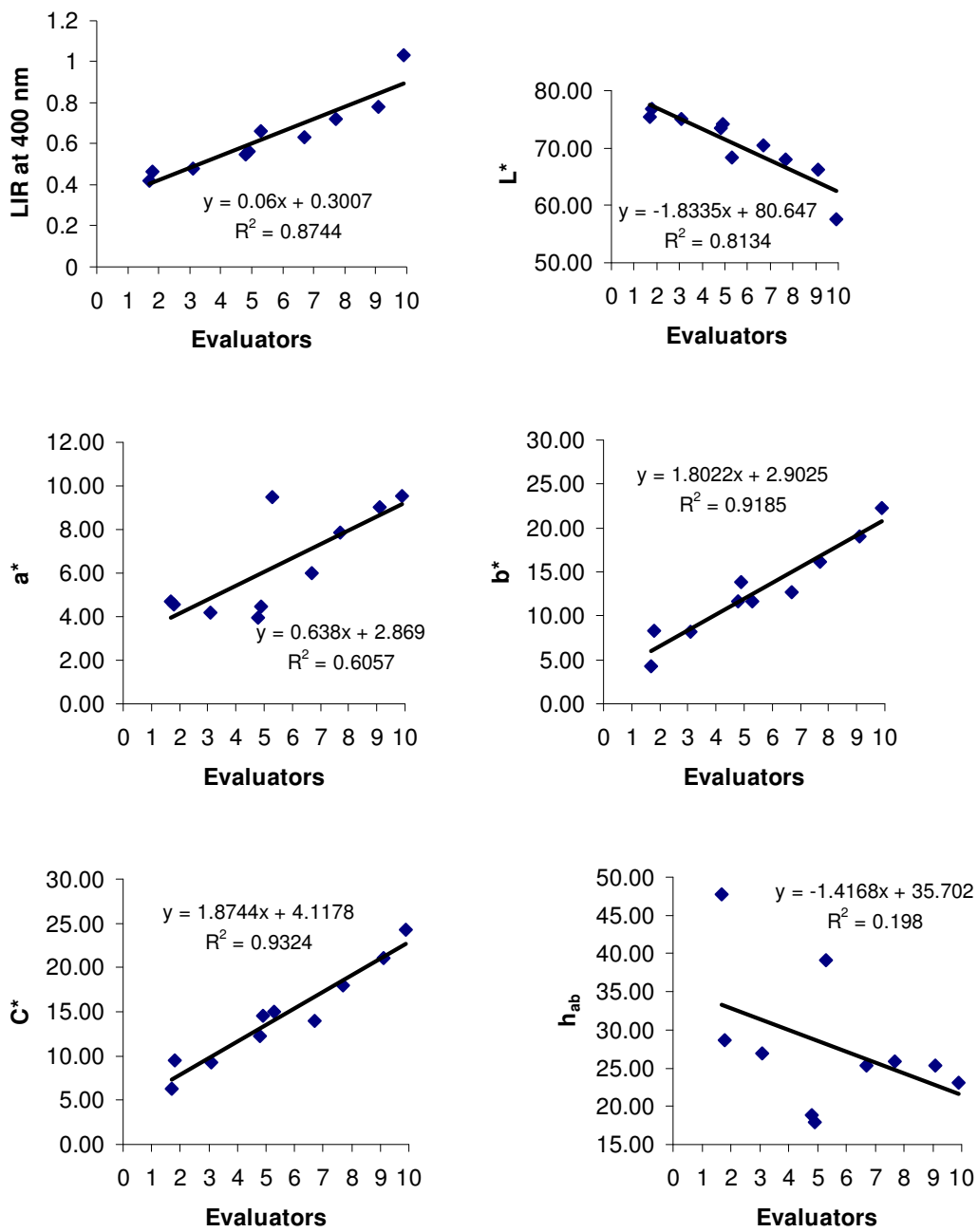
Figure 5-12 shows the correlations between the colorimetric values  $L^*$ ,  $a^*$ ,  $b^*$ ,  $C^*$ ,  $h_{ab}$  and the LIR at 400 nm of subjects skin, measured with the Minolta CM-508d, versus the results obtained by the adapted spectrophotometer. The results from the Minolta CM-508d, versus the results obtained by the adapted spectrophotometer for  $L^*$ ,  $a^*$  and the LIR at 400 nm of subjects skin, correlated well. The slopes of these correlations ranged from 0.9 – 1.1, with  $R^2 \approx 0.9$  for the LIR at 400 nm and  $L^*$ . The  $R^2$  for  $a^*$  was 0.65. While the correlation between  $b^*$  for the two devices was good ( $R^2 = 0.89$ ) the slope of the linear regression was 2.08. As positive  $b^*$  values indicate yellow the Minolta CM-508d was measuring approximately twice as much yellow for each reading than the adapted spectrophotometer.  $C^*$  is calculated from  $a^*$  and  $b^*$  (see Equation 5-1), therefore, the slope of this regression is similarly affected.

Figure 5-13 shows the correlations between the colorimetric values  $L^*$ ,  $a^*$ ,  $b^*$ ,  $C^*$ ,  $h_{ab}$  and the LIR at 400 nm of the coloured tiles, measured with the Minolta CM-508d, versus the results obtained by the adapted spectrophotometer. As

$h_{ab}$  is a measure of tint, value  $h_{ab}$  for the tile that contained no brown pigment was not included in the graph comparing  $h_{ab}$  values as it disproportionately distorted the results. The correlations between the two devices were good, with all  $R^2$  values being greater than 0.98 and the all slopes within the range of 0.9 – 1.2.

The Hue angle,  $h_{ab}$ , is also calculated from  $a^*$  and  $b^*$ . As skin tint does not alter significantly between subjects (i.e. no purple, green or blue tints) the  $h_{ab}$  values of human skin were clustered. Therefore, minor variations in the measured  $h_{ab}$  values between the two instruments resulted in a poor correlation for this colorimetric value.

The intensity of light source from the Minolta CM-508d was noticeably brighter than that from the adapted spectrophotometer. It is possible that the Minolta CM-508d was measuring the diffuse reflectance of the yellowish fat layer below the dermis that the adapted spectrophotometer was unable to measure due to insufficient light intensity.



**Figure 5-10:** Correlations between the colorimetric values; LIR at 400 nm, L\*, a\*, b\*, C\* and h<sub>ab</sub> of subjects' skin, measured with the adapted spectrophotometer, versus the average ranking from lightest (1) to darkest (10) by a panel of ten evaluators.

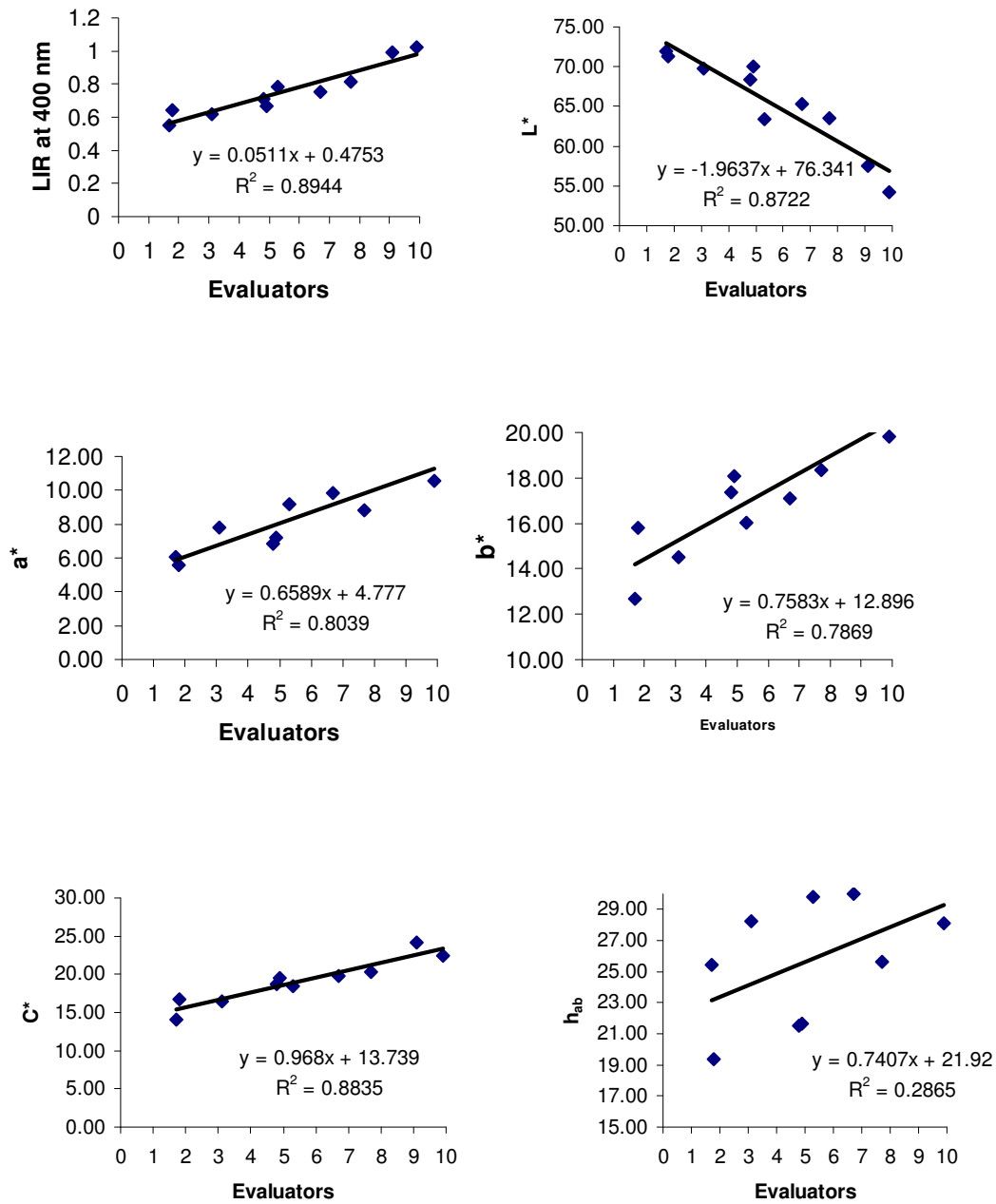


**Figure 5-11: Correlations between the colorimetric values; LIR at 400 nm, L\*, a\*, b\*, C\* and h<sub>ab</sub> of subjects' skin, measured with the Minolta CM-508d, versus the average ranking from lightest (1) to darkest (10) by a panel of ten evaluators.**

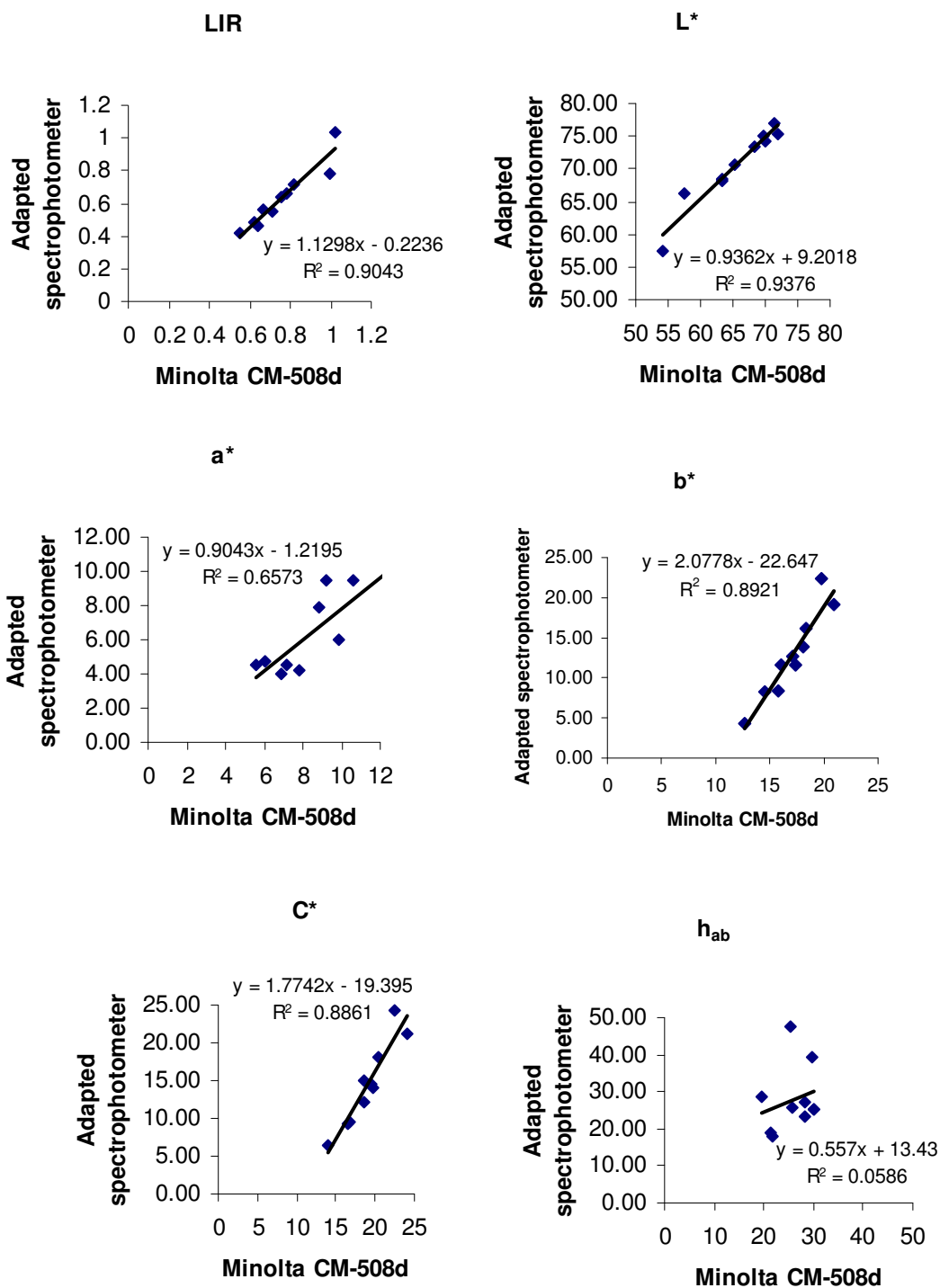


Figure 5-12: Correlations between the colorimetric values LIR at 400 nm, L\*, a\*, b\*, C\* and h<sub>ab</sub> of the subjects' skin, measured with the Minolta CM-508d, versus the results obtained by the adapted spectrophotometer. As h<sub>ab</sub> is a measure of tint, the tile that contained no pigment was removed from the graph comparing h<sub>ab</sub> values as it disproportionately distorted the results.

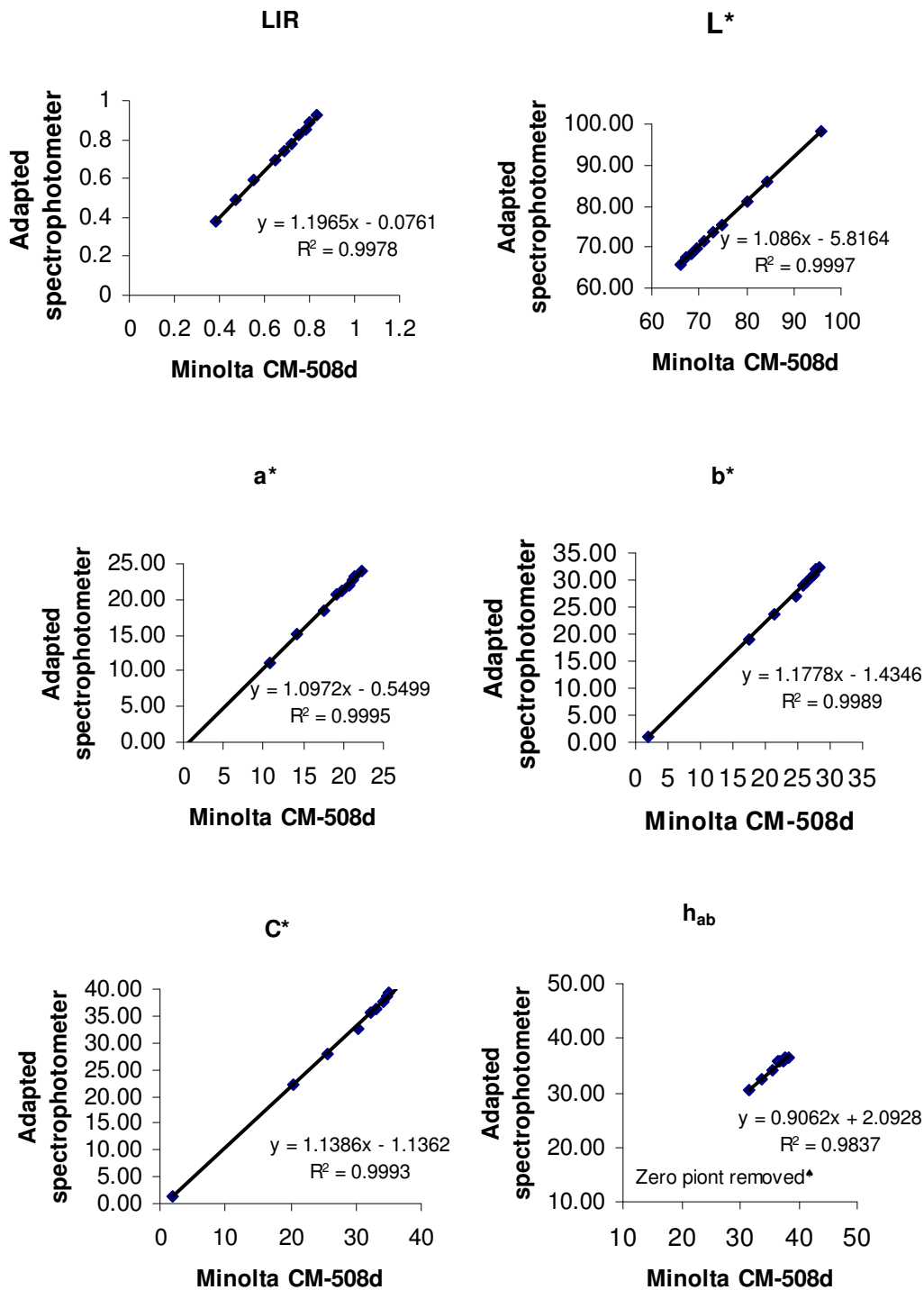


Figure 5-13: Correlations between the colorimetric values; LIR at 400 nm L\*, a\*, b\*, C\* and h<sub>ab</sub> of the coloured tiles, measured with the Minolta CM-508d, versus the results obtained by the adapted spectrophotometer.

## Discussion

### *Apparatus design*

The modifications to the spectrophotometer described yielded a device that was easily adaptable to most spectrophotometers, relatively inexpensive, reliable, and which could accurately quantify changes in the colour of human skin.

There are a number of alterations to the basic design of this instrument that could alter the sensitivity, resolution and range of the device.

The sensitivity of the device could be improved by increasing the amount of light reaching the test surface. This could be achieved by:

- increasing the diameter of the optical fibre bundle to the probe,
- increasing the spectral bandwidth (SBW) of each wavelength reading. This proportionally increases the amount of incident light entering the probe and impinging on the test surface (eg increasing the SBW from 0.2 nm to 1 nm increases the amount of light five fold). However, this is achieved at the expense of a decrease in resolution. The spectral bandwidth of each wavelength can be altered easily in the method file of the spectrophotometer,
- adjusting the focal point of the spectrophotometer light beam from the centre of the sample position to the entrance of the light source fibre. An attempt was made to alter the focal point of the apparatus

(as shown in Figure 5-14) to increase the bandwidth of the apparatus down to 200 nm. Although changing the focal point of the apparatus did increase the amount of light reaching the detector, because of the poor transmission below 400 nm it did not increase the spectral range of the apparatus. A spectral range from 290 to 900 nm could have been achieved with the use of quartz fibres that can transmit light over these frequencies. Quartz optical fibre bundles were not available for use in this study.

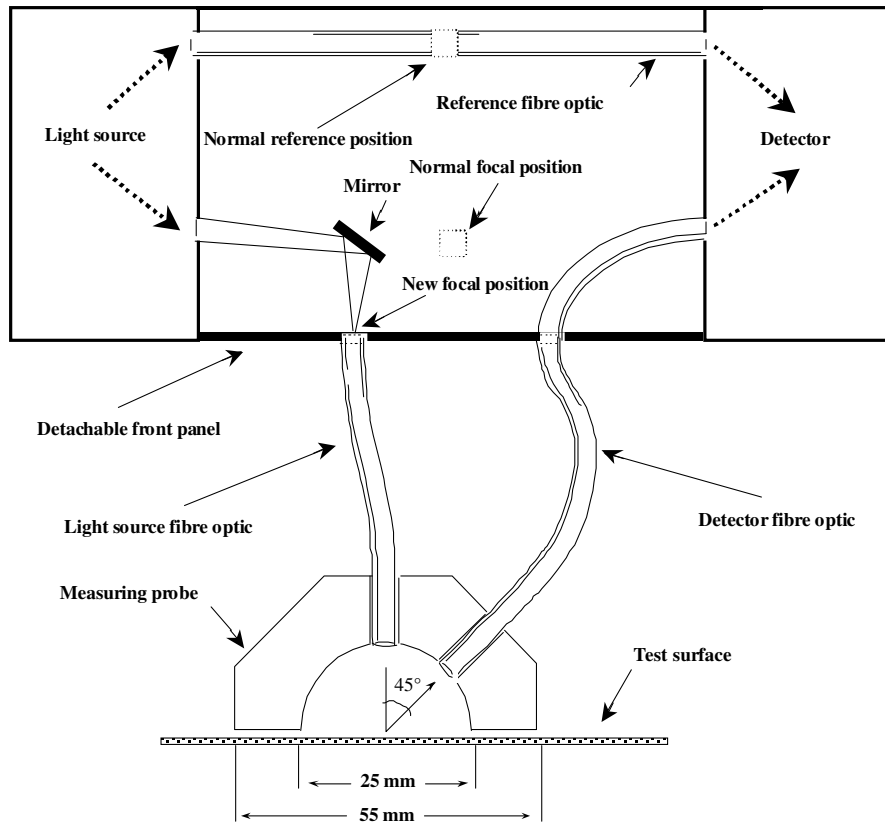


**Figure 5-14: Diagrammatic representation of the adapted spectrophotometer with an altered focal position.**

- Instrument sensitivity could also be enhanced by increasing the sensitivity of the detector, which could be achieved by operating the instrument in single beam mode. In this case the operator, using

the black and white reference scans as external standards, can manually set the sensitivity of the instrument. If the instrument is operated in double beam mode the Cary® software changes the sensitivity of the detector according to the amount of light transmitted through the reference fibre. Adjusting the size of the aperture at either end of the fibre could be used to adjust the amount of light entering the reference fibre. Comparisons of the single and double beam modes gave very similar numerical results, for both the raw data and calculated LIR values, regardless of the sensitivity. The double beam mode had less variance, as determined by lower RSD values, because it could compensate for any changes in intensity of the light source.

The choice of probe design in this study was arbitrary and was largely determined by the availability of materials within the laboratory. The design of the measuring probe was adapted from Feather *et al* [30]. The principle advantage of this design was the ease of construction and the availability of the optical fibre. Disadvantages of this design were the need to compensate for internal reflections within the measuring probe and the reduction in light intensity through absorption by the matt black interior of the measuring probe.

The integrating sphere<sup>§§§</sup> measuring probe used by Bjerring and Andersen [148] is more difficult to construct but has the advantage of less light absorption by the white interior of the integrating sphere than the probe design used in this study. Measuring reflectance with an integrating sphere probe is subject to error, because replacing the test sample with a white standard changes the average reflectance of the walls of the sphere, even if the sample aperture is relatively small area of the sphere wall [149]. The ASTM recommends that the window area of an integrating sphere should be less than 3% of the total area of the sphere wall [161].

Kollias and Baqer [159] used a bifurcating optical fibre such that the ends of the afferent and efferent fibres were flush with each other and the ends of the fibres were held in contact with the surface being measured (see Figure 5-15). Bifurcating optical fibres minimise the problem of internal reflections within the measuring probe. Kollias found it necessary to have the bifurcating optical fibre in contact with the skin to reduce the unacceptable errors associated with specular reflection of the surface of the stratum corneum.

---

§§§ An integrating sphere is a hollow sphere which has its interior coated with a nearly perfectly diffuse substance and which has extremely high reflectance [168].

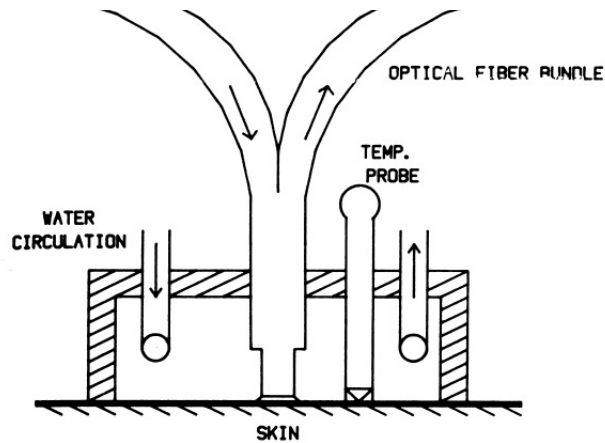


**Figure 5-15:** Bifurcating optical fibre probe used by Kollias and Baqer [159]. The outer part of the probe is made of polyethylene and the inner part aluminium. Water is circulated through the block to maintain the temperature at 31 °C. A thermocouple probe is in contact with the skin to maintain temperature monitoring throughout the measurements.

Zeng *et al* [169] used a probe design that allows the angle of the light source and detector fibres to be moved to any angular position in three-dimensional space. This allows the measurement of the complete angular distribution of the diffuse reflectance.

### Reducing variability

There were a number of steps taken to reduce the variability of colour measurements of the skin of subjects. The variables that were controlled included room temperature, the amount of external light, the pressure of the measuring probe, changes in blood flow from the movement of the subject and the movement from breathing. The breathing of the subject resulted in movement of the skin and this resulted in increased RSD values. Having the subjects hold their breath for the duration of the scan reduced this variable.

The temperature of the probe on the skin was another possible source of variation of skin colour measurement. This problem was addressed by

Kollias and Baqer [159] who described the use of a water jacket in the probe to maintain the probe at 31 °C. Due to the increased complexity of design for the probe the temperature of the probe was not thermostatically adjusted.

However, reproducible results have been obtained from studies that use measuring probes with no temperature control [30, 148].

Prespectral averaging could also be used to decrease the variability of the instrument. Initial work showed that the within-day LIR of the green reference could be reduced to 0.2 % with prespectral averaging (n=5).

However, prespectral averaging proportionally increased the duration of a scan. A scan that averaged five readings at each wavelength had a scan time of 55 seconds. This was an unacceptable time to require subjects to hold their breaths while skin colour was measured. Instead post-spectral averaging, in which five separate scans across the wavelength range were averaged, was used. This required a scan time of only 11 seconds.

### *Interpretation of results*

The reproducibility of the instrument was good with the average RSD for the inter-day variation of the calculated LIR being 1.25 % (range 0.20 – 3.92, n = 300).

The adapted spectrophotometer was able to objectively follow the time course of an inflammatory response and correlated well with the visually observed skin changes. While this study did not correlate changes in blood flow during the inflammatory response with changes in the LIR values in the subject with

dermatographia, other studies have found correlations between haemoglobin content and diffuse reflectance measurements [158, 170].

The correlation between the ranking of the subjects by the evaluators and the colorimetric values were good for all the colorimetric values that would be expected to correlate. These correlations were very similar to those obtained by the Minolta CM-508d.

The correlations between the colorimetric values obtained by the adapted spectrophotometer and the Minolta CM-508d for the coloured tiles were good with high  $R^2$  values ( $> 0.99$ ) and a slope of the linear regression approximately 1.1. However, from the correlations between the colorimetric values obtained by the adapted spectrophotometer it appeared that the Minolta CM-508d detected significantly more yellow in the skin than the adapted spectrophotometer. This is most probably due to the higher intensity of the light source from the Minolta CM-508d being able to penetrate and reflect enough light from the yellowish fatty tissue below the dermis to be measured by this device. If this is the case then the intensity of the light source or the sensitivity of the detector could be significant sources of variance between colorimetric values of skin measurements obtained by different instruments.

As can be clearly seen from Figure 5-8, LIR values from 650 –700 nm from the subjects skin colour flatten out in this region with substantial overlap of spectra. For this reason, this region of the spectrum was not used to correlate LIR values with perceived skin colour. Other workers have found that the

400 – 420 region of the spectrum correlates better with melanin pigment content in skin [164].

### Conclusion

This device compares favourably with similar devices described in the literature in terms of reproducibility and has the advantages of shorter scan times and a higher resolution [17, 29-31]. It is also simpler to construct and at about A\$600 is approximately one tenth the cost of commercial devices.

## CHAPTER 6: GENERAL CONCLUSION

The work described in this thesis investigated new procedures that could be used to synthesise melanin in a reproducible fashion and to test the effectiveness of sunscreens containing melanin or other sunscreen agents and characterise skin colour by diffuse reflectance.

### **Synthesis of melanins**

Despite a large number of studies incorporating synthetic melanins, relatively few studies have examined melanin synthesis techniques as a means of synthesising melanin reproducibly.

With the method of melanin synthesis outlined in this study melanins were synthesised in batches. As melanins were synthesised in batches synthesis variables, such as reaction temperature, condenser water temperature, room temperature and ambient light, between the batches were minimised.

The synthesis procedure outlined was simple and inexpensive and the variables were easily monitored and controlled. The method also allowed for the synthesis of multiple batches of melanin simultaneously in a reproducible fashion.

### **Characterisation of melanins**

The complex, heterogeneous, polymeric structure of melanin makes it difficult to characterise by many standard analytical techniques.

Conversion of the melanin pyrograms to “pseudo-mass spectra” allowed the objective comparison of melanin batches using software commercially available for the comparison of mass spectra.

From the results of this study, melanins produced from different precursors could be differentiated the basis of statistically significant differences in their pyrograms. Conversely, statistically significant differences between pyrograms of different batches of melanins produced under the same conditions from the same precursors could not be demonstrated. The analytical technique in this study could be used in combination with other analytical techniques to determine if the melanins synthesised by the methods outlined in this thesis were reproducible or as the basis of future studies examining differences between melanins synthesised from the same precursor but under different conditions.

### **Characterisation of skin colour by diffuse reflectance**

This section of work was undertaken to provide a method for assessing the ability of sunscreen formulations to adhere to the skin. As a melanin containing sunscreen is likely to be brown, the ability of a formulation to adhere to skin could be monitored by objectively measuring changes in the skin colour as the product was washed or worn off the skin.

A spectrophotometer was modified to measure diffuse reflectance outside of the sample compartment. The modifications to the spectrophotometer described yielded a device that was easily adaptable to most

spectrophotometers, relatively inexpensive, reliable, and which could accurately quantify changes in the colour of human skin

This device developed compares favourably with similar devices described in the literature in terms of reproducibility and has the advantages of shorter scan times and a higher resolution. It was simple to construct and at about A\$600 was approximately one tenth the cost of similar commercial devices.

### ***In vitro* evaluations of Sun Protective Factors of sunscreen agent**

*In vivo* methods are the accepted method for the determination of SPF values of sunscreens. However, *in vivo* methods for determination of the SPF values of sunscreens formulations are time consuming and expensive. *In vitro* methods have the potential to give rapid results at a fraction of the cost of *in vivo* methods. Unfortunately, *in vitro* methods often correlate poorly with *in vivo* results and are generally unable to determine high SPF values accurately due to limitations in the ability of *in vitro* methods to measure a wide range of light levels.

The *in vitro* study presented here used human stratum corneum and Transpore™ surgical tape as substrates, which were easily obtained. The *in vitro* method was fast, simple and capable of measuring high SPF sunscreens (>70). Although more data in the high SPF range (>30) would be required to confirm results in this range. The value of this technique was demonstrated when it correctly measured the SPF value of a commercially available sunscreen that had been assigned an incorrect SPF value from earlier

*in vivo* testing. The corrected value was subsequently confirmed by independent *in vivo* testing.

Few naturally occurring pigments command more widespread interest than melanins [22]. As the development of novel pharmaceutical products containing melanin increases, methods for the synthesis and characterisation of melanin containing products will become increasingly important.

Furthermore, there is currently a high consumer demand for sunscreen products that offer better protection from sun damage, due in part to public education campaigns and the increased understanding of the mechanisms and long term effects of sun exposure. The development of fast, inexpensive and reliable techniques for ascertaining the efficacy of sunscreens will hasten the development of better sunscreen products.

# APPENDICES

## Appendix 1: Computer software

### Melanin analysis software

#### Appendix 1-1 : Software for identifying peaks within TIC melanin pyrograms software

##### Appendix 1-1

```
NAME Py5

LOCAL Array_Index, S_Time, E_Time, Targ_Ion, Unique_Ident, Num_of_TPeaks
LOCAL Targ_Int, Conf_Ion, Conf_Int, LoopA, LoopB, Log, Peak_Thresh, Peak_Count,
LOCAL Targ_Ret_Time, Targ_Conf_Ratio, Conf_Ret_Time, Ret_Times_Match , Alternat_peaks
LOCAL LoopAb, Tp_S_Time, Tp_E_Time, Tp_Targ_Ion, Tp_Conf_Ion, Tp_Ratio, Tp_Ion_Ratio
LOCAL Tp_UI, Tp_Targ_Int, Tp_Targ_ReTT, Tp_Conf_Int, Log_Index, LoopC, LoopD, PHV
LOCAL Num_of_CPeaks, FileName2$, FileName$, Conf_Int_Sub, Conf_ReTT_Sub
LOCAL PHV_Conf, LoopBb, Ion_Ratio, Found_a_Peak, Found_X_Peaks, TEMP, TEMP2, TEMP3
LOCAL Tp_Conf_ReTT, LoopE, Targ_ReTT, Array_Count
!Declare local variables

Array_Index = 25
Log_Index = 3000
!Set array length for all array variables

Dim S_Time, Array_Index
Dim E_Time, Array_Index
Dim Targ_Ion, Array_Index
Dim Targ_Int, Array_Index
Dim Conf_Ion, Array_Index
Dim Unique_Ident, Array_Index
Dim Targ_Conf_Ratio, Array_Index
Dim Tp_S_Time, Log_Index
Dim Tp_E_Time, Log_Index
Dim Tp_Targ_Ion, Log_Index
Dim Tp_Conf_Ion, Log_Index
Dim Tp_Ratio, Log_Index
Dim Tp_Ion_Ratio, Log_Index
Dim Tp_UI, Log_Index
Dim Tp_Targ_Int, Log_Index
Dim Tp_Targ_ReTT, Log_Index
Dim Tp_Conf_Int, Log_Index
Dim Targ_Int_Sub, Log_Index
Dim Targ_ReTT_Sub, Log_Index
Dim Conf_Int_Sub, Log_Index
Dim Conf_ReTT_Sub, Log_Index
Dim Tp_Conf_ReTT, Log_Index
Dim Targ_ReTT, Log_Index
!Declare all arrays and their lengths

Array_Count = 1

S_Time[Array_Count] = 0 !1.81
E_Time[Array_Count] = 3.81
Targ_Ion[Array_Count] = 78
Conf_Ion[Array_Count] = 51
Targ_Conf_Ratio[Array_Count] = 4.68
Unique_Ident[Array_Count] = 100 + Array_Count
Array_Count = Array_Count + 1
```

- 
- - 
  - 
  -

Most of the array blocks above have been removed to conserve space and improve readability.

The information that was contained in these array blocks can be found in Appendix 2-1.

- - 
  - 
  -
-

```

S_Time[Array_Count] = 0.39 ! 2.39
E_Time[Array_Count] = 4.39
Targ_Ion[Array_Count] = 79
Conf_Ion[Array_Count] = 52
Targ_Conf_Ratio[Array_Count] = 1.37
Unique_Ident[Array_Count] = 100 + Array_Count
Array_Count = Array_Count + 1

LoopA = 0
Log = 0
Peak_Thresh = 0
Peak_Count = 0

WHILE LoopA < Array_Index
  LoopA = LoopA + 1
  Alternat_peaks = 0 !Changing this value to 0 (from 1) will result in all ions found in
the !correct time frame and ratio to be printed in the alternate an ASCII file with extention
".LOG"

  !Clears altanate_peaks variable for next target ion

  CHR S_Time[LoopA]:E_Time[LoopA], Targ_Ion[LoopA] !selects target ion
  !uses the chr command to plot a particular ion in a specified time frame.
  RTEINT !Integrate that part of the chromatogram
  R0=X
  Num_of_TPeaks = Npeaks !Finds number of Target Ion Peaks in Time frame

  IF Conf_Ion[LoopA] = 0 AND Num_of_TPeaks > 0 THEN !find largest peak & logs all peaks
found

  !for Target ions without confirmation ions
  LoopAb = 0
  WHILE LoopAb < Num_of_TPeaks
    LoopAb = LoopAb + 1
    PEAKNUMBER LoopAb,,R0

    Targ_Int_Sub[LoopAb] = Peak_Area !Find the peak area of the sub targ ion
    Targ_ReTT_Sub[LoopAb] = Ret_Time !Find retention time of sub targ ion

    Alternat_peaks = Alternat_peaks + 1

    IF Alternat_peaks > 0 THEN !Logs alternative peaks and logs all peaks if
!initial Alternat_peaks value set to 0
      Log = Log + 1

      Tp_S_Time[Log] = S_Time[LoopA]
      Tp_E_Time[Log] = E_Time[LoopA]
      Tp_Targ_Ion[Log] = Targ_Ion[LoopA]
      Tp_Conf_Ion[Log] = Conf_Ion[LoopA]
      Tp_Ratio[Log] = Targ_Conf_Ratio[LoopA]
      Tp_UI[Log] = Unique_Ident[LoopA]
      Tp_Targ_Int[Log] = Targ_Int_Sub[LoopAb]
      Tp_Targ_ReTT[Log] = Targ_ReTT_Sub[LoopAb]
    ENDIF

    IF LoopAb = 1 THEN
      Targ_Int[LoopA] = Targ_Int_Sub[LoopAb] !Assigns
!Targ_Int_Sub[LoopA] the highest value
      Targ_ReTT[LoopA] = Targ_ReTT_Sub[LoopAb]
    ENDIF

    IF Num_of_TPeaks > 1 AND LoopAb > 1 THEN

      IF Targ_Int[LoopA] < Targ_Int_Sub[LoopAb] THEN
        Targ_Int[LoopA] = Targ_Int_Sub[LoopAb] !Assigns
!Targ_Int_Sub[LoopA] the highest
value

        Targ_ReTT[LoopA] = Targ_ReTT_Sub[LoopAb]
      ENDIF
    ENDIF

    IF LoopAb = Num_of_TPeaks THEN !if peak is found & end of loop
      Peak_Count = Peak_Count + 1
    ENDIF

  ENDWHILE ! LoopAb < Num_of_TPeaks

  ENDIF

  IF Conf_Ion[LoopA] > 0 AND Num_of_TPeaks > 0 THEN
!makes sure there is a confirmation ion
!LoopB finds the number of confirmation peaks around each target ion peak
  LoopB = 0

```

```

Found_a_Peak = 0
Found_X_Peaks = 0
WHILE LoopB < Num_of_TPeaks
    LoopB = LoopB + 1

    PEAKNUMBER LoopB,,R0
    Targ_Int_Sub[LoopB] = Peak_Area !Find peak area of the sub targ ion

    Targ_ReTT_Sub[LoopB] = Ret_Time !Find retention time of the sub targ ion

    CHR Targ_ReTT_Sub[LoopB] - 0.2:Targ_ReTT_Sub[LoopB] + 0.2,
Conf_Ion[LoopA]
frame.
    !uses the chr command to plot a particular ion in a specified time
    RTEINT          !Integrate that part of the chromatogram
    R1 = X
    Num_of_CPeaks = Npeaks !number of Confirmation Ion Peaks in Time frame

    LoopBb = 0
    WHILE LoopBb < Num_of_CPeaks
    !LoopB sorts through the confirmation peaks around target ion peaks &
    !checks correct Ret time and ratio
        LoopBb = LoopBb + 1

        PEAKNUMBER LoopBb,,R1
        Conf_Int_Sub[LoopBb] = Peak_Area !Find peak area of the sub
Conf_ion
        Conf_ReTT_Sub[LoopBb] = Ret_Time !Find retention time of sub
Conf_ion

        IF Num_of_Cpeaks > 1 AND LoopBb > 1THEN
        !sorting algorithm for finding confirmation ions closest to
        !retention times
            PHV_Conf = LoopBb -1 ! PHV_Conf Previous retention time

            IF ABS(Targ_ReTT_Sub[LoopB] - Conf_ReTT_Sub[LoopBb] ) >
ABS(Targ_ReTT_Sub[LoopB] - Conf_ReTT_Sub[PHV_Conf] ) THEN
                Conf_ReTT_Sub[LoopBb] =
                Conf_ReTT_Sub[PHV_Conf]
                Conf_Int_Sub[LoopBb] = Conf_Int_Sub[PHV_Conf]
                !Assigns Conf_Int_Sub[LoopBb] the
highest value

            ENDIF
        ENDIF

        IF LoopBb = Num_of_Cpeaks THEN
        !At the end of each loop another peak is found,

            Conf_Int_Sub[LoopB] = Conf_Int_Sub[LoopBb]
            Conf_ReTT_Sub[LoopB] = Conf_ReTT_Sub[LoopBb]

        ENDIF

    ENDWHILE ! LoopBb < Num_of_CPeaks
    IF ABS(Conf_ReTT_Sub[LoopB] - Targ_ReTT_Sub[LoopB]) < 0.02 THEN
    !retention times are the same
        Ion_Ratio = Targ_Int_Sub[LoopB] / Conf_Int_Sub[LoopB]

        IF Ion_Ratio < (Targ_Conf_Ratio[LoopA] * 1.4) AND Ion_Ratio >
(Targ_Conf_Ratio[LoopA] * 0.6) THEN
        !checks confirmation ion is correct ratio to target ion
            Alternat_peaks = Alternat_peaks + 1

            IF Alternat_peaks > 0 THEN
            !Logs alternative peaks if Alternat_peaks =1/all peaks
if =0
                !logs alternative peaks/all peaks
                Log = Log + 1
                Found_a_Peak = 1
                Found_X_Peaks = Found_X_Peaks + 1

                Tp_S_Time[Log] = S_Time[LoopA]
                Tp_E_Time[Log] = E_Time[LoopA]
                Tp_Targ_Ion[Log] = Targ_Ion[LoopA]
                Tp_Conf_Ion[Log] = Conf_Ion[LoopA]
                Tp_Ratio[Log] = Targ_Conf_Ratio[LoopA]
                Tp_Ion_Ratio[Log] = Ion_Ratio
                Tp_UI[Log] = Unique_Ident[LoopA]
                Tp_Targ_Int[Log] = Targ_Int_Sub[LoopB]
                Tp_Targ_ReTT[Log] = Targ_ReTT_Sub[LoopB]
                Tp_Conf_Int[Log] = Conf_Int_Sub[LoopB]
                Tp_Conf_ReTT[Log] = Conf_ReTT_Sub[LoopB]
                Temp = Tp_UI[Log]
                Temp2 =Tp_Targ_Ion[Log]
            ENDIF
        ENDIF
    ENDIF

```

```

IF Found_X_Peaks > 1 THEN
!only logs selected peaks
    IF Targ_Int[LoopA] < Tp_Targ_Int[Log] THEN
        Targ_Int[LoopA] = Tp_Targ_Int[Log]
        !Assigns Targ_Int_Sub[LoopA] the
highest value
        Targ_ReTT[LoopA] = Tp_Targ_ReTT[Log]
    ENDIF
ENDIF

IF Found_X_Peaks = 1
    Targ_Int[LoopA] = Tp_Targ_Int[Log]
    Targ_ReTT[LoopA] = Tp_Targ_ReTT[Log]
    Temp2 = Unique_Ident[LoopA]
ENDIF

ENDIF

ENDIF

ENDWHILE      ! LoopB <= Num_of_TPeaks

IF Found_a_Peak = 1 THEN !records when a peak is found
    Peak_Count = Peak_Count + 1
    Found_a_Peak = 0
ENDIF

ENDIF      endif for if conf_ion > 0

ENDWHILE      ! LoopA <= Array_Index

FileName$ = _DataPath$ + _DataFile$ + "\" + _DataFile${1:INSTR(_DataFile$, ".")-1} + ".MSP"
PRINT "Exporting points ... "
OPEN FileName$ FOR OUTPUT AS #1
!file #1 is data to be exported to NIST MS library
PRINT USING #1, "% ", "NAME "
PRINT #1, _Dataname$
PRINT #1, "MISC. : ", _Miscinfo$
PRINT #1, "COMMENT : Acquired on " + _DateAcquired$ + " by " + _Operator$ + " using " +
_OrgMethFile$
PRINT #1, "MW : "
PRINT #1, "CAS : "
POINTS
PRINT #1, "Num Peaks : ", Peak_Count
LoopC = 1

WHILE LoopC <= Array_Index
    IF Targ_Int[LoopC] > 0 THEN !peak has to exist !prints peak only if one is found
        PRINT USING #1, "#####   #####/", Unique_Ident[LoopC], Targ_Int[LoopC]
    ENDIF
    LoopC = LoopC + 1
ENDWHILE
CLOSE #1

FileName2$ = _DataPath$ + _DataFile$ + "\" + _DataFile${1:INSTR(_DataFile$, ".")-1} + ".LOG"
!file #2 logs alternative/all peaks with correct characteristics
OPEN FileName2$ FOR OUTPUT AS #2

PRINT USING #2, "% ", "NAME "
PRINT #2, _Dataname$
PRINT #2, "MISC. : ", _Miscinfo$
PRINT #2, "COMMENT : Acquired on " + _DateAcquired$ + " by " + _Operator$ + " using " +
_OrgMethFile$
PRINT #2, "Total Num Peaks : ", Log
PRINT #2, "Num of alternative Peaks : ", Log - Peak_Count
PRINT #2, "   UI Targ_Ion Targ_Int   S_Time   E_Time Targ_ReTT Conf_ReTT Conf_Ion
Conf_Int Exp_Ratio Set_Ratio"
LoopD = 1
WHILE LoopD <= Log

PRINT USING #2, "   ####   #####", Tp_UI[LoopD], Tp_Targ_Ion[LoopD]
PRINT USING #2, "   #####   ####.###", Tp_Targ_Int[LoopD], Tp_S_Time[LoopD]
PRINT USING #2, "   ####.###   ####.###", Tp_E_Time[LoopD], Tp_Targ_ReTT[LoopD]
PRINT USING #2, "   ####.###", Tp_Conf_ReTT[LoopD]
PRINT USING #2, "   #####   #####", Tp_Conf_Ion[LoopD], Tp_Conf_Int[LoopD]
PRINT USING #2, "   ####.###   ####.###/", Tp_Ion_Ratio[LoopD], Tp_Ratio[LoopD]

LoopD = LoopD + 1

ENDWHILE
CLOSE #2

FileName3$ = _DataPath$ + _DataFile$ + "\" + _DataFile${1:INSTR(_DataFile$, ".")-1} + ".TME"
OPEN FileName3$ FOR OUTPUT AS #3
!file #3 logs all peaks in file #1 with there corresponding retention times. A checking mechanism

```

```

!ie they have to increase sequentially
PRINT USING #3, "% ", "NAME "
PRINT #3, _Dataname$
PRINT #3, "MISC. : ", _Miscinfo$
PRINT #3, "COMMENT : Acquired on " + _DateAcquired$ + " by " + _Operator$ + " using " +
_OrgMethFile$
PRINT #3, "Num Peaks : ", Peak_Count
PRINT #3, "   UI   Targ_Int  Targ_RetT"

LoopE = 1

WHILE LoopE <= Array_Index
    PRINT USING #3, "#####      #####      ####.###/", Unique_Ident[LoopE], Targ_Int[LoopE],
Targ_ReTT[LoopE]
    LoopE = LoopE + 1
ENDWHILE
CLOSE #3

PRINT " ... Completed exporting points"
RETURN

```

## Appendix 1-2: Method file for the black and white diffuse reflectance standards

### Diffuse reflectance software

The black and white standards method file (see Appendix figure 1) contains the spectrophotometric parameters that are used to measure the black and white standards by the software described in Appendix 1-3.



```

1.0000      B&W Standards      23 Jun 1997      500.00
%TRANS      Gain      100      SBW      2.0
Baseline    OFF      Page      2      NM
Press F2 to EDIT      Instrument Offline
ADVANCED PARAMETERS

Factor      1.000
Calibrate Concentration      1.000      Units
Source Change (nm)      310.0
Beam Mode      DOUBLE
Gain      100
Beam Interchange      NORMAL
Cycle Time (min)      0.0
Cycle Count / Replicates      1
Peak Threshold      2.0000
Peak Type      Min/Max
Weight Correction      NO
Volume Correction      NO
Collection Mode      DEFAULT

User_result= READ(400.0)

Parameters  Display  Reports
Set-up basic instrument parameters

```

Appendix figure 1: Screen dumps of the black and white standards method file.

**Appendix 1-3: Software for measuring the diffuse reflectance of the white and black standards**

This program saves the spectrum collected under the conditions specified in the black and white method file (Appendix 1-2) and stores the data in a set slot (24) of the data filing page of the Cary® 1E software. This data is later used by the diffuse reflectance software (Appendix 1-5) for determining the LIR of an object. An ASCII file of the white spectrum is also created and stored in the next available slot of the reports filing page of the Cary® 1E software.

```

{-----}
{ ADL file : FN9.ADL }
{THIS PROGRAM WAS WRITTEN BY MARTIN BLEASEL 17/3/95 }
{THIS PROGRAM LOADS A SET METHOD, THEN COLLECTS DATA. }
{SAVES THE DATA THEN PRINTS OUT AND SAVES A REPORT }
{IN THE CORRECT FORMAT SUCH THAT THE DATA CAN BE EXPORTED}
{AND MANIPULATED BY EXCEL I.E. REPORT IN TWO COLUMNS. }
{-----}
DEFINE Martin_WHITE_BLACK
loadmethod(4) {loadmethod(3) for black standads}
post_load_method
graphics collect auto_scale archive(current#,24,"WHITE REFERENCE
SPECTROLON")

```

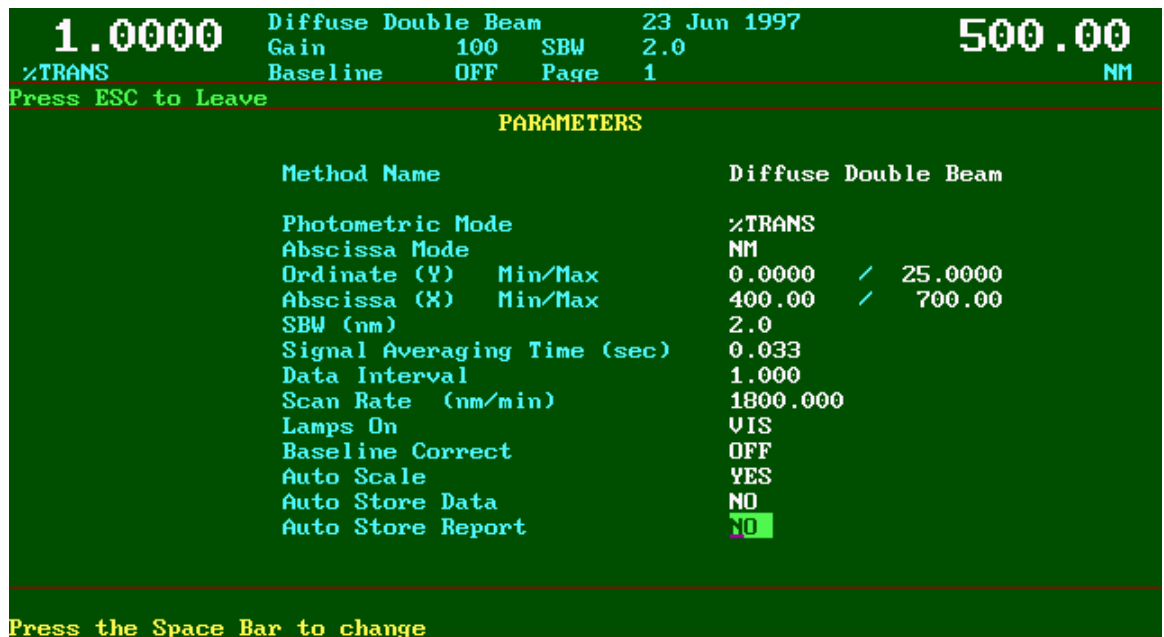
```

startprint
tablefmt("dddz", "dddz.dddddddd")
tablehdr("nm", "Result")
for i=400 to 700
j=extract(current#, i)
tabledata(i, j)
next
archive_report(999, "WHITE REFERENCE REPORT")
ENDDDEF

```

#### Appendix 1-4: Diffuse reflectance method file

The diffuse reflectance method (see Appendix figure 2) file contains the spectrophotometric parameters used to measure the diffuse reflectance of objects outside of the sample compartment of the spectrophotometer by the software described in Appendix 1-5. Advanced parameters are the same as those for the black and white method file (see Appendix 1-2).



Appendix figure 2: Screen dump of the diffuse reflectance method file used to measure the diffuse reflectance of objects outside the sample compartment.

## Appendix 1-5: Software for the measurement of diffuse reflectance

This software collects data under the conditions specified in the colour method file (see Appendix 1-4). Using the data collected from the black and white standards (see Appendix 1-3) and the current data collection it creates a LIR spectrum. This LIR spectrum is stored in the next available slot of the data filing page of the Cary<sup>®</sup> 1E software. An ASCII file of the LIR spectra is also created and stored in the next available slot of the reports filing page of the Cary<sup>®</sup> 1E software.

```
{-----}
{This program was written by Martin Bleasel          }
{This program takes the raw data from the white and black  }
{standards that are stored in slots 24 & 25 of data file and }
{then carries out the mathematical operation as follows:   }
{a#=log((RW-RB)/RT-RB)                                   }
{where: a# is the data file of the mathematical operation }
{      RW is the raw data of the white reference         }
{      RB is the raw data of the black reference         }
{      RT is the raw data of the surface being measured  }
{-----}

DEFINE MARTIN_MATHS
GRAPHICS
RETRIEVE (RW#, 24)
RETRIEVE (RB#, 25)
result#=LOG((RW#-RB#)/(CURRENT#-RB#))
AUTO_SCALE
STARTPRINT
TABLEFMT("DDDZ", "DDDZ.DDDDDDD")
TABLEHDR("nm", "Result")
FOR i=400 TO 700 STEP 1
J=EXTRACT(result#, I)
TABLEDATA(I, J)
NEXT
ARCHIVE_REPORT(999, "LIR DATA")
ARCHIVE(CURRENT#, 999, "LIR DATA")
ENDDF

DEFINE Martin_SKIN
loadmethod(3)
post_load_method
graphics collect auto_scale
martin_maths
enddef
```

## In vitro SPF determination software

### Appendix 1-6: Software for creating Cary® 1E data files

This program allowed for the manual entry of continuums (or spectrums) into the Cary® 1E filing system. This allowed for the automatic calculation of SPF values by the double beam method software (Appendix 1-7) with the use of erythral action spectrum and the solar energy distribution spectrum (Appendix 2-2) entered in the Cary® 1E filing system.

```
{-----}
{Program written by MARTIN BLEASEL SCHOOL OF PHARMACY TAS. }
{This program allows you to manually enter data into the }
{Cary spectrophotometer to create a continuum. }
{ADL file : DATA.ADL }
{-----}

DEFINE DATA_ENTRY_SOFTWARE
CURVEFITDATA(CONTINUUM#,0,0,0) {clears continuum}
STARTPRINT
PAGE=4
GOTO_PAGE
LPRINT("This program allows you to manually enter data into")
LPRINT("the Cary to create a continuum. Follow directions at")
LPRINT("the bottom of this page. ")
LPRINT(" MARTIN BLEASEL Uni. of Tas. School of Pharmacy 1995")
LPRINT("")
LPRINT("")
LPRINT("To exit program continue pressing STOP (F12) until program
is exited.")
REPEAT {makes sure max>min}
PRINT("Enter Xmin=")
X=INPUT
PRINT("Enter Xmax=")
B = INPUT
IF B<=X THEN
BEGIN
PRINT("Xmin is > or = to Xmax, press Enter to continue.")
E=INPUT
END
UNTIL X<B
PRINT ("Data interval=")
C=INPUT
REPEAT {loop to create continuum}
PRINT("X=",X," Y= ")
Y=INPUT
CURVEFITDATA (CONTINUUM#, X, Y, 1)
X=X+C
UNTIL X>B
CURVEFITDATA (CONTINUUM#, X, Y, 1) {inputs last data point}
CURVEFITDATA (CONTINUUM#, 0, 0, 2)
SET (ABS, 0)
SET (ORD, 1)
```

```

LOADHEADER (CONTINUUM#)
GRAPHICS
RESULT#=CONTINUUM#
AUTO_SCALE
PRINT ("File name= ")
FILENAME$=INPUT
ARCHIVE (CONTINUUM#,999,FILENAME$)
STARTPRINT

ENDDDEF

```

### **Appendix 1-7: Software for the *in vitro* SPF determination using double beam operation**

This software uses double beam mode to determine the transmission of light through substrates with and without sunscreen applied for the *in vitro* determination of the SPF values of sunscreens. The solar energy distribution and erythema effectiveness spectra were entered into the Varian software by the program described in Appendix 1-6.

```

{This program operates in double beam mode. }
{This program calculates the SPF of a given sunscreen. 2mg/cm^2 of }
{sunscreen to be tested is spread over skin glued to a cuvette. }
{Scans of skin/tape with and without sunscreen are done. }
{The SPF is calculated from the procedure outlined by BL Diffy. J. Soc }
{Cosmet. Chem. 40, 127-133. 1989 }

{Solar energy distribution and erythema effectiveness were entered }
{into the Varian software by a program written earlier }
{Author-Martin Bleasel, School of Pharmacy 1995 }

define SPF_determination
graphics
print("Setting up instrument for SPF determination program")
set (bline,0)
set (abs,0)
set (xmax,400)
set (xmin,290)
set (autos,1)
set (bemd,1) {program uses double beam mode}
set (intv,1)
set (lamp,0)
set (ord,1)
set (ymin,0)
set (ymax,100)
set (sat,.033)
set (srch,289)
graphics
statusstr("in vitro SPF determination program")

{preliminary scan of skin by itself}

```

```

print("Insert skin sample & then cuvette in reference position,
Press Enter")
skinref$=input
graphics collect auto_scale
c#=result#
{preliminary scan finished}

repeat
print("Insert reference skin samples, then press Enter to collect
data")
startref$=input
graphics collect auto_scale
print("Is this attenuation correct, i.e. between 100-150%: y/n?")
responce$=input
until responce$="y"

print("Performing baseline correction....")
graph_clear
do_baseline
graph_clear
collect auto_scale
print("Enter sample name ")
name$=input
Print("Insert sample, then press enter ")
A$=input
Print("")
set(ymin,0)
set(ymax,200)
graphics collect auto_scale
Print("Performing in vitro SPF calculations")
a#=current#
b#=previous#
result#=-b#/a#      {taking reference sample into consideration=
1/trans or the protection factor}

graphics auto_scale
retrieve(SED#,26) {solar energy distribution in slot 26}
retrieve(EE#,27) {erythemal effectiveness in slot 27}
low=get(xmin)
high=get(xmax)
X=0      {set values to 0}
y=0
for count = low to high step 5
    xn=extract(SED#,count)
    yn=extract(EE#,count)
    an=extract(result#,count)
    X=X+(yn*xn){sum of solar distribution*erythemal
effectiveness}
    Y=Y+((yn*xn)/an){(solar distribution*erythemal
effectiveness/Protection Factor)}
next
SPF=X/Y
statusstr("SPF result is calculated.")
print("Calculated SPF for sample ",name$," is ",SPF,". Reprt y/n? ")
y_or_n$=input
if y_or_n$="y" then
    begin

{files skin scan in reports page}

```

```

startprint
tablefmt("dddz","dddz.dddddddd") {report in exportable format
use 'parse' command in excel}
tablehdr("nm","%Trans of skin")
for i=290 to 400 step 5
j=extract(c#,i)
tabledata(i,j)
next
archive_report(999,"Skin %Trans")

{end of skin scan report}

startprint
tablefmt("dddz","dddz.dddddddd") {report in exportable format
use 'parse' command in excel}
tablehdr("nm","protection factor")
for i=290 to 400 step 5
j=extract(result#,i)
tabledata(i,j)
next
archive_report(999,name$)

end
graphics {returns graphics page back to normal}
startprint {clears report page after generating report}
enddef

```

#### **Appendix 1-8: Software for the *in vitro* SPF determination using pseudo - double beam**

This software uses pseudo-double beam mode to determine the transmission of light through substrates with and without sunscreen applied for the *in vitro* determination of the SPF values of sunscreens.

This program consists of three parts. The first part sets the parameters required for data collection. The second part collects and exports the data for the substrate without sunscreen to an ASCII file. The third part collects and exports the data for the substrate with sunscreen, to an ASCII file. By modifying the variable 'well\_do' each section of the program can be operated independently. To collect data for the detector gain versus detector responses the first and last sections of the program were run sequentially. To predict a sunscreen's SPF, the three parts were run sequentially.

```

{Author-Martin Bleasel, School of Pharmacy 1995 }

define Initial_setup

out_of_range_sample=0
out_of_range_ref=0
well_do =100 {for operating the two halves of the program
independantly or otherwise}
mart_in=0 {used for reproducibility studies}

repeat
startprint
page=4
goto_page
print("Setting up instrument for SPF determination program....")
set(blinc,0)
set(abs,0)
set(sat,1.0)
set(srch,289)
set(xmax,400)
set(xmin,290)
set(bemd,0) {program uses single beam mode; need to adjust
gain}
set(lamp,0)
set(ord,1) {%Trans}
set(ymin,0)
set(ymax,100)
set(sbw,.2) {ensures detector is not blinded by light}
set(gain,ref_gain)
statusstr("in vitro SPF determination program")

if well_do =100 then
begin

print("Insert reference sample, then press Enter to collect data")
startref$=input
print("Performing scan for SPF determination program")

startprint

tablefmt("dddz","dddz","dddz.ddddddddd","dddz.ddddddddd","dddz.dddd
dddd") {report in exportable format use 'parse' command in excel}
tablehdr("nm","gain","skin sample","skin sample at 110",
"reference 1")

set(sbw,4) {opens entry slit just prior to measurements}

for x_start= 400 to 290 step -5 {start of reference collect}

set(bein,0)
set(gain,init_gain)
skin_sample=read(x_start)
skin_sample=skin_sample/100 {converts to raw data}
set(gain,ref_gain)
set(bein,1) {reverses sample/reference beams}
set(gain,ref_gain)
ref_l=read(x_start) {ref at ref_gain}

```

```

ref_1=ref_1/100 {converts to raw data}

if (skin_sample > 2.1) or (skin_sample < .03) then
out_of_range_sample=1 {sample out of range?}
if (ref_1 >2.1) or (ref_1 <.03) then out_of_range_ref=1 {reference
out of range}

case gain_set          {adjust values for different gains}

    110:skin_samp110=skin_sample/1
    120:skin_samp110=(skin_sample)/2.3259
    130:skin_samp110=(skin_sample)/5.204
    140:skin_samp110=(skin_sample)/11.44
    150:skin_samp110=(skin_sample)/25.019
    160:skin_samp110=(skin_sample)/54.566
    170:skin_samp110=(skin_sample)/123.11
    190:skin_samp110=(skin_sample)/681.83
    210:skin_samp110=(skin_sample)/4382.3
    230:skin_samp110=(skin_sample)/33603
    250:skin_samp110=(skin_sample)/212426

    end      {case end}

tabledata(x_start,gain_set,skin_sample,skin_samp110,ref_1)
next

set(sbw,.2)

archive_report(999,"Ref data for next report")

end {*****TEMP END*****}

if (out_of_range_ref=1) or (out_of_range_sample=1) then
begin

    if out_of_range_sample=1 then
    begin
        lprint("The sample has gone out of range. Need to change
init_gain.")
        lprint("")
    end

    if out_of_range_ref=1 then
    begin
        lprint("The reference has gone out of range. Need to change
ref_gain.")
    end

    lprint("")
    lprint("Hit Enter key to exit program")
    print("Hit Enter key to exit program")
    a$=input
    well_do=101
end

```

```

if well_do = 100 then
begin

{sample to be tested}

startprint
page=4
goto_page
tablefmt("dddz", "dddz", "dddz.dddddddd", "dddz.dddddddddddddddd", "ddd
z.dddddddd") {report in exportable format use 'parse' command in
excel}
tablehdr("nm", "gain", "pre-result", "skin & crm at 110", "referance 2")

print("Enter sample name ")
name$=input
Print("Insert sample, then press enter ")
A$=input

loop_end=1000
gain_set=init_gain

set(sbw, 4)

gain_temp=gain_set

for x2_start= 400 to 290 step -5

repeat
    gain_set=gain_temp
    set(bein, 0)
    set(gain, gain_set)
    skin_samp2=read(x2_start)
    set(gain, ref_gain)
    skin_samp2=skin_samp2/100
    print("raw data sample 2 ", skin_samp2, " ", x2_start)

if (gain_set=250) and (-log(skin_samp2)>1.7) then
begin
loop_end=0
gain_notify=gain_notify-1
if gain_notify=0 then print("Out of range at ", x2_start)
end

if gain_set <250 then
begin

    if (-log(skin_samp2)>1.7) and ((gain_set=120) or (gain_set=140)
or (gain_set=160)) then gain_temp=gain_set+10
    if (-log(skin_samp2)>1.7) and ((gain_set=110) or (gain_set=130)
or (gain_set=150) or (gain_set=170) or (gain_set=190) or
(gain_set=210) or (gain_set=230)) then gain_temp=gain_set+20
    if ((gain_set=120) or (gain_set=140) or (gain_set=160)) and (-
log(skin_samp2)<-0.3) then gain_temp=gain_set-10
    if ((gain_set=130) or (gain_set=150) or (gain_set=170) or
(gain_set=190) or (gain_set=210) or (gain_set=230) or

```

```

(gain_set=250)) and (-log(skin_samp2)<-0.3) then gain_temp=gain_set-
20
    if (gain_set=110) and (-log(skin_samp2)<-0.3) then loop_end=0
else loop_end =1000

    end

until ((-log(skin_samp2)<1.7)) or (loop_end=0)

set(bein,1) {reverses sample/reference beams}
set(gain,ref_gain)
ref_2=read(x2_start) {ref at ref_gain}
ref_2=ref_2/100 {converts to raw data}
print("ref raw data ",ref_2, " ",x2_start)

case gain_set {adjust values for different gains}

    110:skin_samp=skin_samp2/1
    120:skin_samp=(skin_samp2)/2.3259
    130:skin_samp=(skin_samp2)/5.204
    140:skin_samp=(skin_samp2)/11.44
    150:skin_samp=(skin_samp2)/25.019
    160:skin_samp=(skin_samp2)/54.566
    170:skin_samp=(skin_samp2)/123.11
    190:skin_samp=(skin_samp2)/681.83
    210:skin_samp=(skin_samp2)/4382.3
    230:skin_samp=(skin_samp2)/33603
    250:skin_samp=(skin_samp2)/212426

    end {case end}

tabledata(x2_start,gain_set,skin_samp2,skin_samp,ref_2)

next {for/to/next}

archive_report(999,name$)
startprint
lprint("SPF data has been gathered")

{for i=0 to 1 step 1 minutes next, for reproducibility studies}

mart_in=mart_in-1 {for reproducibility studies}

end {if well_do = then else}
until mart_in<=0 {for reproducibility stusies}

set(sbw,0.2)

if (out_of_range_sample=0) or (out_of_range_ref=0) then
    begin
        print("Program finnished, press Enter key to exit.")
        a$=input
    end

```

```

loadmethod(7)
post_load_method {puts back the control to normal}

startprint
graphics

endif

define vari_ables
init_gain=120 {initial scan gain}
ref_gain=120 {reference gain}
gain_set=init_gain {gain is varied through the program}
initial_setup {go to define init_setup}
endif

```

## Miscellaneous

### **Appendix 1-9: Software to export Cary® data files as two column ASCII files**

This program was modified from a program described elsewhere [171]. This program was modified to convert multiple data files (as opposed to individual files) into multiple ASCII files. It was also modified to allow the user to chose between exporting the data files as raw data or converted data i.e. absorbance, transmittance  $\log(\text{absorbance})$  and the derivatives of the absorbance normally available during data collection.

```

{This program generates a simple ASCII XY table on the Reports page.}
{ This can then be stored in the Reports page. }
{ Copyright Varian Techtron 1990 }
{ Author Michelle Archard }
{ Revised 23 November, 1990 /MODIFIED BY MARTIN BLEASEL 1996 }

define adlnew3

startprint
page=4
goto_page

lprint("This program generates an ASCII XY table on the Reports page.")
lprint("Which is then stored in the Reports filing page.")
lprint("")
lprint("Files to be exported must be already tagged")
lprint("FILES ARE EXPORTED IN THE ORDER BY WHICH THEY ARE SELECTED")
lprint("NOT THE ORDER THEY APPEAR ON THE DATA PAGE")
lprint("")
lprint("If you want to transform data you have to FIRST select the ")
lprint("appropriate ordinate mode on the parameter page")

```

```

lprint("")
lprint("Files are numbered according to data file number")

repeat
print("Format data as raw or transformed data R/T? ")
rort$=input
until (rort$="r") or (rort$="t")

file_num =0

repeat

startprint
tagged=recall(tag_data,file_num)
if tagged>0 then
begin
retrieve(a#,tagged)
a_mode=header(a#,0)
set(abs,a_mode)
if header(a#,1) = 20 then

trans_form=get(ord)
if rort$="r" then trans_form = 10

CASE trans_form
0:a#=(-LOG(a#))           {ABS}
1:a#=(a# * 100)           {%T}
2:a#=(LOG(-LOG(a#)))      {LOG(ABS)}
3:a#=(-LOG(a#))           {conc}
4:a#=(DERIV1#(-LOG(a#)))  {DER 1}
5:a#=(DERIV2#(-LOG(a#)))  {DER 2}
6:a#=(DERIV3#(-LOG(a#)))  {DER 3}
7:a#=(DERIV4#(-LOG(a#)))  {DER 4}
8:a#=(DERIV5#(-LOG(a#)))  {DER 5}
9:a#=(DERIV6#(-LOG(a#)))  {DER 6}
10:a#=a#*1
END {CASE}

result#=a#
graphics auto_scale
startprint
page=4
goto_page

abs_x=get(abs)
ord_y=get(ord)

case abs_x
0:abs$="nm"
1:abs$="min"
2:abs$="deg"
3:abs$="mm"
4:abs$="SN"
end

case ord_y
0:ord$="Abs"
1:ord$="%Trans"

```

```

2:ord$="Log A"
3:ord$="Conc"
4:ord$="Deriv 1"
5:ord$="Deriv 2"
6:ord$="Deriv 3"
7:ord$="Deriv 4"
8:ord$="Deriv 5"
9:ord$="Deriv 6"
end

tablehdr(abs$,ord$)
a=get(intv)
min=get(xmin)
max=get(xmax)
b=max-min
statusstr("generating table")
tablefmt("dddz.ddd", "dddz.dddddddd")

for i= 0 to b/a
    c=i*a
    c=c+min
    d=extract(a#,c)
    tabledata(c,d)
next {for i=.....}

number$=int$(tagged)
archive_report(999,number$)

end {if tagged>0 then...}
file_num=file_num+1
print(file_num," ",tagged)
until (tagged<0) or (file_num=49)

if rort$="s" then    {r can not =s section is inactive,test purpose
only}
begin

file_num = 0

repeat
tagged=recall(tag_data,file_num)
if tagged>0 then
begin
retrieve(current#,file_num)

abs_x= get(abs)

    case abs_x
    0:abs$="nm"
    1:abs$="min"
    2:abs$="deg"
    3:abs$="mm"
    4:abs$="SN"
    end

tablehdr(abs$,"raw_data")
a=get(intv)
min=get(xmin)
max=get(xmax)

```

```

b=max-min
statusstr("generating table")
tablefmt("dddz.ddd","dddz.dddddddd")

for i= 0 to b/a
    c=i*a
    c=c+min
    d=extract(current#,c)
    tabledata(c,d)
next
number$=int$(tagged)
archive_report(999,number$)
end {if tagged>0 then....}
file_num=file_num+1
until (tagged<0) or (file_num=49)
end {if rort=r then...}

page=4
goto_page
enddef

define start
x=24
IF X=23 THEN
BEGIN
for file_num= 0 to 49
tagged=recall(tag_data,file_num)
lprint("tagged= ",tagged," tag_data=",tag_data,"
file_num=",file_num)
next
a$=input
END
if x=24 then adlnew3
enddef

```

## Appendix 2: Tables

Appendix 2-1: Parameter values used by the Software for identifying peaks within TIC melanin pyrograms

Unique identifier	4 minute target ion window		Target ion (m/z)	Confirmation ion	Target / confirmation abundance ratio
	Start time	End time			
101	0	3.81	78	51	4.68
102	0.26	4.26	58	183	1
103	0.39	4.39	79	52	1.37
104	0.42	4.42	69	70	1.7
105	0.6	4.6	67	41	1.89
106	0.85	4.85	91	92	1.94
107	1.52	5.52	93	66	1.97
108	1.82	5.82	80	81	1.37
109	2.5	6.5	91	106	2.6
110	2.8	6.8	104	78	1.29
111	4.1	8.1	103	76	2.36
112	4.54	8.54	94	66	2.55
113	4.66	8.66	118	89	2.2
114	4.67	8.67	107	106	1.67
115	5.48	9.48	115	116	1.1
116	5.65	9.65	117	90	1.91
117	5.77	9.77	108	107	1.1
118	6.59	10.6	133	63	2.18
119	7.76	11.8	188	102	9.8
120	8.3	12.3	42	140	3.9
121	8.42	12.4	147	78	1
122	8.74	12.74	83	42	1.5
123	8.81	12.8	129	102	2.72
124	9.27	13.3	117	90	1.91
125	9.5	13.5	141	142	1
126	9.84	13.8	133	104	1.9
127	10.29	14.3	130	131	1.7
128	10.79	14.8	154	153	2.4
129	11.6	15.6	152	76	5.3
130	11.7	15.7	157	156	2.2
131	11.95	16	83	42	4.3
132	12.2	16.2	153	126	4.4
133	12.5	16.5	168	139	2.1
134	13.35	17.4	166	165	1.16
135	15.6	19.6	178	76	4.7
136	15.8	19.8	83	42	4.8
137	16.4	20.4	42	67	2.5
138	18.15	22.2	191	190	3.8

**Appendix 2-2: Erythema action spectrum & Solar energy distribution spectrum tables**

$E(\lambda)$  = solar simulator / sunlight intensity spectrum,  $e(\lambda)$  = Erythema action spectrum and  $(\lambda)$  = wavelength in nm [131, 143].

$\lambda(\text{nm})$	$E(\lambda)$	$e(\lambda)$	$E * e(\lambda)$	(%) contribution to erythema	Cumulative (%) contribution
290	3.68E-06	1.00E+00	3.68E-06	0.007	0.007
295	7.97E-04	1.00E+00	7.97E-04	1.472	1.479
300	1.28E-02	6.50E-01	8.32E-03	15.371	16.850
305	6.51E-02	2.20E-01	1.43E-02	26.459	43.309
310	1.71E-01	7.40E-02	1.27E-02	23.378	66.687
315	2.95E-01	2.50E-02	7.38E-03	13.625	80.312
320	3.98E-01	8.60E-03	3.42E-03	6.323	86.636
325	5.36E-01	2.90E-03	1.55E-03	2.872	89.507
330	6.30E-01	1.40E-03	8.82E-04	1.629	91.137
335	6.50E-01	1.20E-03	7.80E-04	1.441	92.578
340	6.80E-01	9.70E-04	6.60E-04	1.219	93.796
345	6.90E-01	8.10E-04	5.59E-04	1.033	94.829
350	7.00E-01	6.80E-04	4.76E-04	0.879	95.708
355	7.10E-01	5.70E-04	4.05E-04	0.748	96.456
360	7.30E-01	4.80E-04	3.50E-04	0.647	97.103
365	7.50E-01	4.00E-04	3.00E-04	0.554	97.657
370	7.80E-01	3.40E-04	2.65E-04	0.490	98.147
375	8.00E-01	2.90E-04	2.32E-04	0.429	98.576
380	8.30E-01	2.40E-04	1.99E-04	0.368	98.944
385	8.60E-01	2.00E-04	1.72E-04	0.318	99.262
390	9.00E-01	1.70E-04	1.53E-04	0.283	99.544
395	9.30E-01	1.40E-04	1.30E-04	0.241	99.785
400	9.70E-01	1.20E-04	1.16E-04	0.215	100.000
<b>Sum=</b>			5.41E-02		

## REFERENCES

1. Marks, R (1995). Skin cancer control in Australia: The balance between primary prevention and early detection. *Arch Dermatol.* **131** 474-478.
2. Marks, R, M Staples, and GG Giles (1993). Trends in non melanocytic skin cancer treated in Australia - the 2nd national survey. *Int J Cancer.* **53** (4) 585-590.
3. Jelfs, PL, G Giles, D Shug, *et al* (1994). Cutaneous malignant melanoma in Australia 1989. *Med J Aust.* **161** 182-187.
4. Giles, GG, BK Armstrong, RC Burton, *et al* (1996). Has mortality from melanoma stopped rising in Australia? Analysis of trends between 1931 and 1994. *BMJ.* **312** 1121-1125.
5. Harper, L and D Bickers (1981). Ultraviolet Carcinogenesis, In: *Photosensitivity diseases: principles of diagnosis and treatment*, Philadelphia: W. B. Saunders Company. 246-257.
6. Fears, TR, J Scotto, and MA Schneiderman (1977). Mathematical models of age and ultraviolet effects on the incidence of skin cancer among whites in the United States. *Am J Epidemiol.* **105** 420-427.
7. McKenzie, RL and JM Elwood (1990). Intensity of solar ultraviolet radiation and its implications for skin cancer. *N Z Med J.* **103** (887) 152-154.

8. Naylor, MF and KC Farmer (1997). The case for sunscreens. A review of their use in preventing actinic damage and neoplasia. *Arch Dermatol.* **133** (9) 1146-1154.
9. Farmer, KC and MF Naylor (1996). Sun exposure, sunscreens, and skin cancer prevention: a year-round concern. *Ann Pharmacother.* **30** (6) 662-673.
10. Moan, J (1994). UVA radiation, melanoma induction, sunscreens, solarium and ozone reduction. *J Photochem Photobiology B: Biol.* **24** (3) 201-203.
11. Krien, PM and D Moyal (1994). Sunscreens with broad-spectrum absorption decrease the *trans* to *cis* photoisomerization of urocanic acid in the human *stratum corneum* after multiple UV light exposures. *Photochem Photobiol.* **60** (3) 280-287.
12. Diffey, BL (1994). A method for broad spectrum classification of sunscreens. *Int J Cosmet Sci.* **16** 47-52.
13. Ishikawa, T, K Kodama, J Matsumoto, *et al* (1984). Photoprotective role of epidermal melanin granules against ultraviolet damage and DNA repair in guinea pig skin. *Cancer Res.* **44** (11) 5195-5199.
14. Margolis, RJ, M Sherwood, DJ Maytum, *et al* (1989). Longwave ultraviolet radiation (UVA, 320-400 nm)-induced tan protects human skin against further UVA injury. *J Invest Dermatol.* **93** (6) 713-718.

15. Kaidbey, KH and AM Kligman (1978). Sunburn protection by longwave ultraviolet radiation-induced pigmentation. *Arch Dermatol.* **114** (1) 46-48.
16. Pathak, MA (1989). Photoprotective role of melanin (eumelanin) in human skin, In: *Psoralens: past, present and future of photochemoprotection and other biological activities*, TB Fitzpatrick, P Forlot, MA Pathak, et al, eds., Paris: John Libbey Eurotext. 25-33.
17. Kollias, N and AH Baqer (1988). The role of human melanin in providing photoprotection from solar mid-ultraviolet radiation (280-320 nm). *J Soc Cosmet Chem.* **39** 347-354.
18. Cripps, DJ (1981). Natural and artificial photoprotection. *J Invest Dermatol.* **77** (1) 154-157.
19. Whiteman, DC, P Valery, W McWhirter, et al (1997). Risk factors for childhood melanoma in Queensland, Australia. *Int J Cancer.* **70** (1) 26-31.
20. Swan, GA (1974). Structure, chemistry, and biosynthesis of the melanins. *Fortschr Chem Org Naturst.* **31** 521-582.
21. Butler, MJ, G Lazarovits, VJ Higgins, et al (1989). Identification of a black yeast isolated from oak bark as belonging to the genus *Phaeococcomyces* sp. Analysis of melanin produced by the yeast. *Can J Microbiol.* **35** (7) 728-734.

22. Prota, G (1988). Progress in the chemistry of melanins and related metabolites. *Med Res Rev.* **8** (4) 525-556.
23. Udo, G, J Roeding, K Stanzyl, *et al* (1993). Melanin-containing sunscreen for topical application, In: *DE 42 21 269 [Patent]*, Lancaster Group AG.
24. Agin, PP (1990). Liposome compositions, In: *EP 0 386 680 [Patent]*, Plough Inc.
25. Chung, KK and I Nardolillo (1992). Styrene-ethylene-propylene copolymer containing cosmetic compositions and their use, In: *EP 0 497 144 [Patent]*, Estee Lauder Inc.
26. Herve, A, C Didier, M Myriam, *et al* (1991). Fine dispersion of melanic pigments, its preparation and utilisation in cosmetics, In: *WO 93/05754 [Patent]*, L'Oreal.
27. Junino, A, H Andrian, R Tulpoup, *et al* (1991). Enzymatic preparation of a melanin pigment and use in cosmetics, In: *EP 0 441 689 [Patent]*, L'Oreal.
28. Leong, H, M Katz, A Delk, *et al* (1989). Synthetic melanin aggregates, In: *US 4,806,360 [Patent]*, Advanced Polymer Systems.
29. Dawson, JB, DJ Barker, DJ Ellis, *et al* (1980). A theoretical and experimental study of light absorption and scattering by *in vivo* skin. *Phys Med Biol.* **25** (4) 695-709.

30. Feather, JW, M Hajizadeh-Saffar, G Leslie, *et al* (1989). A portable scanning reflectance spectrophotometer using visible wavelengths for the rapid measurement of skin pigments. *Phys Med Biol.* **34** (7) 807-820.
31. Kollias, N and A Baqer (1986). On the assessment of melanin in human skin *in vivo*. *Photochem Photobiol.* **43** (1) 49-54.
32. Shaath, N (1990). Evolution of modern sunscreen chemicals, In: *Sunscreens: development, evaluation, and regulatory aspects*, NJ Lowe and NA Shaath, eds., New York: Marcel Dekker Inc. 3-35.
33. Shaath, N (1990). The chemistry of sunscreens, In: *Sunscreens: development, evaluation, and regulatory aspects*, NJ Lowe and NA Shaath, eds., New York: Marcel Dekker Inc. 211-233.
34. Kimbrogh, DR (1997). The photochemistry of sunscreens. *J Chem Educ.* **74** (1) 51-53.
35. Shaath, NA (1987). Encyclopedia of UV absorbers for sunscreen products. *Cosmet Toilet.* **102** 21-39.
36. AS/NZS-2604 (1997). *Sunscreen products-Evaluation and classification AS/NZS 2604:1997*: Joint Technical Committee CS/42, Australian/New Zealand Standard AS/NZS 2604.

37. Fourtanier, A, J Labat-Robert, P Kern, *et al* (1992). In vivo evaluation of photoprotection against chronic ultraviolet-A irradiation by a new sunscreen Mexoryl SX. *Photochem Photobiol.* **55** (4) 549-560.
38. Harrison, J, S Walker, S Plastow, *et al* (1991). Sunscreens with low sun protection factor inhibit ultraviolet B and A photoaging in the skin of the hairless albino mouse. *Photodermatol Photoimmunol Photomed.* **8** 12-20.
39. Thompson, SC, D Jolley, and R Marks (1993). Reduction of solar keratoses by regular sunscreen use. *NEJM.* **329** (16) 1147-1151.
40. Cohen, C, KG Dossou, A Rougier, *et al* (1994). EPISKIN: An in vitro model for the evaluation of phototoxicity and sunscreen photoprotective properties. *Toxicology in Vitro.* **8** (4) 669-671.
41. van-Praag, M, L Roza, B Boom, *et al* (1993). Determination of the photoprotective efficacy of a topical sunscreen against UVB-induced DNA damage in human epidermis. *J Photochem Photobiol.* **19** 129-134.
42. Freeman, SE, RD Ley, and KD Ley (1988). Sunscreen protection against UV-induced pyrimidine dimers in DNA of human skin *in situ*. *Photodermatology.* **5** 243-247.
43. Naylor, MF, A Boyd, DW Smith, *et al* (1995). High sun protection factor sunscreens in the suppression of actinic neoplasia. *Arch Dermatol.* **131** (2) 170-175.

44. Fitzpatrick, TB (1988). The validity and practicality of sun-reactive skin types I through VI. *Arch Dermatol.* **124** 869.
45. Bennington, JL ed. (1984). *Saunders Dictionary and Encyclopedia of Laboratory Medicine and Technology.* , Philadelphia: W.B Saunders Company. .
46. Roy, P, KK Nayak, and NK Pandey (1989). Characterization of a novel yeast synthesizing melanin-like pigment. *J Gen Microbiol.* **135** (12) 3385-3391.
47. Keinath, AP and R Loria (1990). Melanin-producing *Streptomyces* spp. respond to potato plant growth and differentially to potato cultivars. *Can J Microbiol.* **36** (4) 279-285.
48. Schraermeyer, U and H Stieve (1994). A newly discovered pathway of melanin formation in cultured retinal pigment epithelium of cattle. *Cell Tissue Res.* **276** (2) 273-279.
49. Coyne, VE and L Al-Harhi (1992). Induction of melanin biosynthesis in *Vibrio cholerae*. *Appl Environ Microbiol.* **58** (9) 2861-2865.
50. Palumbo, A, M Dischia, G Misuraca, *et al* (1994). A new dopachrome-rearranging enzyme from the ejected ink of the cuttlefish *Sepia officinalis*. *Biochem J.* **299** (1) 839-844.
51. Ito, S (1986). Reexamination of the structure of eumelanin. *Biochim Biophys Acta.* **883** (1) 155-161.

52. Nacht, S (1993). Melanin, the natural biopolymer for ultraviolet protection, In: *Biotechnol Polym*, CG Gebelein, ed., Lancaster: Technomic. 104-122.
53. Marrett, LD, WD King, SD Walter, *et al*(1992). Use of host factors to identify people at high risk for cutaneous malignant melanoma. *Can Med Assoc J.* **147** (4) 445-453.  
  
[published erratum appears in *Can Med Assoc J*1992 **147** (12): 1764]
54. Kollias, N, RM Sayre, L Zeise, *et al*(1991). Photoprotection by melanin. *J Photochem Photobiol B.* **9** (2) 135-160.
55. McFadden, AW (1961). Skin Disease in the Cuna Indians. *Arch Dermatol.* **84** 1013-1185.
56. Muir, C, J Waterhouse, T Mack, *et al* eds. ( 1987). *Cancer incidence in five continents.* Vol. 5, Lyon, France: IARC Scientific Publications.
57. Nacht, S (1991). Melanin, nature's own sunscreen polymer, In: *Cosmetic and pharmaceutical applications of polymers*, CG Gebelein, ed., New York: Plenum Press. 83-94.
58. Fitzpatrick, TB, G Szabó, and MM Wick (1983). Biochemistry and Physiology of melanin pigmentation, In: *Biochemistry and physiology of the the skin*, LA Goldsmith, ed., New York: Oxford University Press. 687-712.

59. Das, KC, MB Abramson, and R Katzman (1978). Neuronal pigments: spectroscopic characterization of human brain melanin. *J Neurochem.* **30** (3) 601-605.
60. Stepien, KB, JP Dworzanski, B Bilinska, *et al* (1989). Catecholamine melanins. Structural changes induced by copper ions. *Biochim Biophys Acta.* **997** (1-2) 49-54.
61. Crescenzi, O, M Dischia, A Napolitano, *et al* (1993). The alleged stability of dopa melanins revisited. *Gazzetta Chimica Italiana.* **123** (4) 241-242.
62. Ito, S, E Novellino, F Chioccare, *et al* (1980). Co-polymerization of dopa and cysteinyl-dopa in melanogenesis *in vitro*. *Experientia.* **36** 822-823.
63. Chirila, TV, RL Cooper, IJ Constable, *et al* (1991). "Black prosthesis" revisited: a study of epinephrine-induced pigment deposits on poly(methyl methacrylate). *Graefes Arch Clin Exp Ophthalmol.* **229** (6) 578-582.
64. Wolfram, L and I Hui (1970). The mechanism of hair bleaching. *Soc Cosmet Chem.* **21** 875-900.
65. Ito, S, K Wakamatsu, and H Ozeki (1993). Spectrophotometric assay of eumelanin in tissue samples. *Anal Biochem.* **215** (2) 273-277.

66. Duff, GA, JE Roberts, and N Foster (1988). Analysis of the structure of synthetic and natural melanins by solid-phase NMR. *Biochemistry*. **27** (18) 7112-7116.
67. Enochs, WS, MJ Nilges, and HM Swartz (1993). Purified human neuromelanin, synthetic dopamine melanin as a potential model pigment, and the normal human substantia nigra - characterization by electron paramagnetic resonance spectroscopy. *Journal Of Neurochemistry*. **61** (1) 68-79.
68. Piattelli, M and RA Nicolaus (1961). The structure of melanins and melanogenesis-I. *Tetrahedron*. **15** 66-75.
69. Vitkin, IA, J Woolsey, BC Wilson, *et al*(1994). Optical and thermal characterization of natural (*Sepia officinalis*) melanin. *Photochem Photobiol*. **59** (4) 455-462.
70. Vèkey, K, J Tamès, and A Somogyi (1992). Studies on structure characterization of tryptophan melanin: comparison between filament and curie-point pyrolysis gas chromatography/mass spectrometry. *Org Mass Spectrom*. **27** 1216-1219.
71. d'Ischia, M, A Napolitano, K Tsiakas, *et al*(1990). New intermediates in the oxidative polymerization of 5,6-dihydroxyindoles to melanin promoted by the peroxidase/H<sub>2</sub>O<sub>2</sub> system. *Tetrahedron*. **46** (16) 5789-5796.

72. d'Ischia, M, A Napolitano, and G Prota (1991). Peroxidase as an alternative to tyrosinase in the oxidative polymerization of 5,6-dihydroxyindoles to melanin(s). *Biochim Biophys Acta.* **1073** (2) 423-430.
73. Kertesz, D and R Zito (1965). Mushroom polyphenol oxidase. I. Purification and general properties. *Biochim Biophys Acta.* **96** 447-462.
74. Sigma (1997). *Sigma: Product catalogue.* Sigma (Australia). 1062.
75. Howells, L, M Godfrey, and MJ Sauer (1994). Melanin as an adsorbent for drug residues. *Analyst.* **119** (12) 2691-2693.
76. Kaliszan, R, A Kaliszan, and IW Wainer (1993). Prediction of drug binding to melanin using a melanin based high performance liquid chromatographic stationary phase and chemometric analysis of the chromatographic data. *J Chromatogr.* **615** (2) 281-288.
77. Ings, RM (1984). The melanin binding of drugs and its implications. *Drug Metab Rev.* **15** (5-6) 1183-1212.
78. Stepien, KB, JP Dworzanski, S Imielski, *et al* (1986). Study of chloroquine binding to melanins by pyrolysis-gas chromatography and electron spin resonance spectroscopy. *J Anal Appl Pyrol.* **9** 297-307.

79. Korytowski, W and T Sarna (1990). Bleaching of melanin pigments. Role of copper ions and hydrogen peroxide in autooxidation and photooxidation of synthetic dopa-melanin. *J Biol Chem.* **265** (21) 12410-12416.
80. Palumbo, A, M d'Ischia, G Misuraca, *et al* (1987). Effect of metal ions on the rearrangement of dopachrome. *Biochim Biophys Acta.* **925** 203-209.
81. Rosei, MA, L Mosca, and C De-Marco (1995). Spectroscopic features of native and bleached opio-melanins. *Biochim Biophys Acta.* **1243** (1) 71-77.
82. Krysciak, J (1985). Molecular weight determination of alkali-soluble melanin based on absorbancy of the solution. *Folia Biol.* **33** (1-2) 43-47.
83. Bilinska, B, K Stepien, and T Wilczok (1987). Infrared spectroscopy of melanins and melanoproteins. *Stud Biophys.* **122** (1-3) 47-55.
84. Charman, WN, CJ Farquhar, BC Finnin, *et al* (1987). Characterization of biopolymers by pyrolysis gas chromatography and multidimensional analysis. Application to synthetic melanins. *J Chromatogr.* **388** (2) 389-396.
85. Enochs, WS, MJ Nilges, and HM Swartz (1993). A standardized test for the identification and characterization of melanins using electron paramagnetic resonance (epr) spectroscopy. *Pigment Cell Res.* **6** (2) 91-99.

86. Caiti, E, PR Crippa, and C Viappiani (1993). Application of photoacoustic phase angle spectroscopy ( $\phi$  as) to eumelanins and pheomelanins. *Pigment Cell Res.* **6** (3) 140-144.
87. Cheng, J, SC Moss, M Eisner, *et al* (1994). X-ray characterization of melanins .1. *Pigment Cell Res.* **7** (4) 255-262.
88. Cheng, J, SC Moss, and M Eisner (1994). X-ray characterization of melanins .2. *Pigment Cell Res.* **7** (4) 263-273.
89. Seraglia, R, P Traldi, G Elli, *et al* (1993). Laser desorption ionization mass spectrometry in the study of natural and synthetic melanins .1. Tyrosine melanins. *Biol Mass Spectrom.* **22** (12) 687-697.
90. Allegri, G, M Biasiolo, G Frison, *et al* (1988). Collisional spectroscopy in structural characterization of melanins. 2- Laser desorption experiments on bio- and synthetic tryptophan melanins. *Biomed Environ Mass Spectrom.* **15** (6) 353-355.
91. Bertazzo, A, M Biasiolo, C Costa, *et al* (1994). Laser desorption ionization mass spectrometry in the study of natural and synthetic melanins II- Serotonin melanins. *Biol Mass Spectromet.* **23** (7) 391-398.
92. Dworzanski, JP (1983). Pyrolysis-gas chromatography of natural and synthetic melanins. *J Anal Appl Pyrol.* **5** 69-79.

93. Vas, G, K Vekey, G Czira, *et al* (1993). Characterization of melanins by pyrolysis gas chromatography mass spectrometry. *Rapid Communications In Mass Spectrometry*. **7** (10) 870-873.
94. Herve, M, J Hirschinger, P Granger, *et al* (1994). A C 13 solid state NMR study of the structure and autoxidation process of natural and synthetic melanins. *Biochim Biophys Acta*. **1204** (1) 19-27.
95. Poole, CF and SK Poole (1991). *Chromatography Today*, Amsterdam: Elsevier. 916-921.
96. Scientific-Glass-Engineering (1986). Pyrojector installation and operation manual, SGE: Melbourne.
97. May, RW, EF Pearson, and D Scothern (1977). *Pyrolysis-Gas Chromatography*, ed. TC Society, Cambridge England: Heffers Printers Ltd.
98. Alberts, AC (1990). Chemical properties of femoral gland secretions in the desert iguana, *Dipsosaurus dorsalis*. *J Chem Ecol*. **16** (1) 13-26.
99. Chu, AY and W Lopatin (1986). Application of pattern-recognition techniques in wavelength selection for instrumentally read reagent strips. *Clin Chem*. **32** (9) 1666-1671.
100. Kowalski, BR and CF Bender (1973). Pattern Recognition. II. Linear and nonlinear methods for displaying chemical data. *J Amer Chem Soc*. **95** (3) 686-693.

101. Lai, EPC, GR D., NL Chen, *et al*(1993). Pattern recognition for screening of crude oils using multivariate circular profiles. *Can J Chem.* **71** (7) 968-975.
102. Ghoos, YCD, B Geypens, M Hiele, *et al*(1994). Screening method for the determination of volatiles in biomedical samples by means of an off line closed loop trapping system and high resolution gas chromatography ion trap detection. *J Chromatogr A.* **665** (2) 333-345.
103. Shaw, PE, BS Buslig, and MG Moshonas (1993). Classification of commercial orange juice types by pattern recognition involving volatile constituents quantified by gas chromatography. *J Agric Food Chem.* **41** (5) 809-813.
104. Chang, WT, CW Huang, and YS Giang (1993). An improvement on pyrolysis gas chromatography for the differentiation of photocopy toners. *J Forensic Sci.* **38** (4) 843-863.
105. Sparkman, OD and JA Sparkman (1995). *NIST Mass Spectral Search Program and The NIST/EPA/NIH Mass Spectral Library Version 1.0; Users' Guide*, Gaithersburg: National Institute of Standards and Technology.
106. Parrish, JA (1983). Responses of skin to visible and ultraviolet radiation, In: *Biochemistry and physiology of the skin*, LA Goldsmith and JH Sterner, eds., New York: Oxford University Press. 713-733.

107. Gruijl, Fd, H Sterenborg, P Forbes, *et al*(1993). Wavelength dependence of skin cancer induction by ultraviolet irradiation of albino hairless mice. *Cancer Res.* **53** 53-60.
108. Woods, C (1988). Life without a sunscreen. *New scientist.* **120** (ZZZ) 46-49.
109. Kligman, LH, FJ Akin, and AM Kligman (1985). The contributions of UVA and UVB to connective tissue damage in hairless mice. *J Invest Dermatol.* **84** (4) 272-276.
110. Kumakiri, M, K Hashimoto, and I Willis (1977). Biologic changes due to long-wave ultraviolet irradiation on human skin: ultrastructural study. *J Invest Dermatol.* **69** (4) 392-400.
111. Bernstein, EF, DB Brown, F Urbach, *et al*(1995). Ultraviolet radiation activates the human elastin promoter in transgenic mice: a novel in vivo and in vitro model of cutaneous photoaging. *J Invest Dermatol.* **105** (2) 269-273.
112. Ullrich, SE (1995). Potential for immunotoxicity due to environmental exposure to ultraviolet radiation. *Hum Exp Toxicol.* **14** (1) 89-91.
113. Swerdlow, AJ, JS English, RM MacKie, *et al*(1988). Fluorescent lights, ultraviolet lamps, and risk of cutaneous melanoma. *BMJ.* **297** (6649) 647-650.

[published erratum appears in BMJ 1988 Nov 5;297(6657):1172]

114. Rivers, JK, PG Norris, GM Murphy, *et al* (1989). UVA sunbeds: tanning, photoprotection, acute adverse effects and immunological changes. *Br J Dermatol.* **120** (6) 767-777.
115. Ramsay, CA (1989). Ultraviolet A protective sunscreens. *Clin Dermatol.* **7** (3) 163-166.
116. AS/NZS-2604 (1993). *Sunscreen products-Evaluation and classification AS/NZS 2604:1993*. Joint Technical Committee CS/42, Australian/New Zealand Standard AS/NZS 2604.
117. Urbach, F (1989). Testing the efficacy of sunscreens: effect of choice of source and spectral power distribution of ultraviolet radiation, and choice of endpoint. *Photodermatol.* **6** (4) 177-181.
118. Lowe, NJ (1990). Sun Protection Factors: Comparative techniques and selection of ultraviolet sources, In: *Sunscreens, development, evaluation, and regulatory aspects. Vol 10*, NJ Lowe and NA Shaath, eds., New York: Marcel Dekker, inc. 379-393.
119. Pearse, AD and C Edwards (1993). Human stratum corneum as a substrate for *in vitro* sunscreen testing. *Int J Cos Sci.* **15** (6) 234-244.
120. Lavker, RM, GF Gerberick, D Veres, *et al* (1995). Cumulative effects from repeated exposures to suberythemal doses of UVB and UVA in human skin. *J Am Acad Dermatol.* **32** (1) 53-62.

121. Skolnick, AA (1991). Revised regulations for sunscreen labeling expected soon from FDA. *JAMA*. **265** (24) 3217.
122. Skolnick, AA (1991). Melanoma epidemic yields grim statistics. *JAMA*. **265** (24) 3217-3218.
123. Skolnick, AA (1991). Is ozone loss to blame for melanoma upsurge? [news]. *JAMA*. **265** (24) 3218.
124. Skolnick, AA (1991). Sunscreen protection controversy heats up. *JAMA*. **265** (24) 3218-3220.
125. Stockdale, M (1987). A novel proposal for the assessment of sunscreen product efficacy against UVA. *Int J Cosmet Sci*. **9** 85-98.
126. Groves, G and P Forbes (1982). A method for evaluating the photoprotective action of sunscreens against UV-A radiation. *Int J Cosmet Sci*. **4** 15-24.
127. Cole, C (1994). Multicenter evaluation of sunscreen UVA protectiveness with the protection factor test method. *J Am Acad Dermatol*. **30** (5) 729-736.
128. Furukawa, RD, WR Brown, GM Shivji, *et al* (1989). Assessment by mouse model of the ultraviolet A protective effect of topical sunscreens. *J Am Acad Dermatol*. **20** (6) 1031-1037.

129. Stanfield, JW, PA Feldt, ES Csortan, *et al* (1989). Ultraviolet A sunscreen evaluations in normal subjects. *J Am Acad Dermatol.* **20** 744-748.
130. Roelandts, R, N Sohrabvand, and M Garmyn (1989). Evaluating the UVA protection of sunscreens. *J Am Acad Dermatol.* **21** (1) 56-62.
131. Diffey, BL and J Robson (1989). A new substrate to measure sunscreen protection factors throughout the sunscreen spectrum. *J Soc Cosmet Chem.* **40** 127-133.
132. Sayre, RM, PP Agin, EM Desrochers, *et al* (1980). Sunscreen testing methods: *In vitro* predictions of effectiveness. *J Soc Cosmet Chem.* **31** 133-143.
133. Sayre, RM and PP Agin (1984). Comparison of human sun protection factors to predicted factors using different lamp spectra. *J Soc Cosmet Chem.* **35** 439-445.
134. Kahn, G and G Wilcox (1969). Comparison of *in vitro* and *in vivo* sunscreen testing methods. *J Soc Cosmet Chem.* **20** 807-824.
135. O'Neill, JJ (1984). Effect of film irregularities on sunscreen efficacy. *J Pharm Sci.* **73** (7) 888-891.
136. Brown, S and BL Diffey (1986). The effect of applied thickness on sunscreen protection: *in vivo* and *in vitro* studies. *Photochem Photobiol.* **44** (4) 509-513.

137. Sayre, RM, PP Agin, GJ LeVee, *et al* (1979). A comparison of *in vivo* and *in vitro* testing of sunscreens formulas. *Photochem Photobiol.* **29** (3) 559-566.
138. Diffey, BL and PM Farr (1991). Sunscreen protection against UVB, UVA and blue light: an *in vivo* and *in vitro* comparison. *Br J Dermatol.* **124** (3) 258-263.
139. Kaidbey, KH and AM Kligman (1978). Laboratory methods for appraising the efficacy of sunscreens. *J Soc Cosmet Chem.* **29** 525-536.
140. Bruls, WAG and JC van der Leun (1982). The use of diffusers in the measurement of transmission of human epidermal layers. *Photochem Photobiol.* **36** 709-713.
141. Marks, R and PR Dawber (1971). Skin surface biopsy: an improved technique for the examination of the horny layer. *Br J Derm.* **84** 117-123.
142. Gray, A, M Archard, and M Ward (1991). Operation manual for the Cary 1 and Cary 3 spectrophotometers: release 3, Varian: Melbourne; Australia.
143. McKinlay, AF and BL Diffey (1987). A reference action spectrum for ultraviolet induced erythema in human skin. *CIE Journal.* **6** (1) 17-22.

144. Schleider, NR, RS Moskowitz, DH Cort, *et al* (1979). Effects of emollients on ultraviolet-radiation-induced erythema of the skin. *Arch Dermatol.* **115** (10) 1188-1191.
145. Lebwohl, M, J Martinez, P Weber, *et al* (1995). Effects of topical preparations on the erythemogenicity of UVB: implications for psoriasis phototherapy. *J Am Acad Dermatol.* **32** (3) 469-471.
146. Cole, CA and RL Van Fossen (1990). In vitro models for UVA and UVB photoprotection, In: *Sunscreens: development, evaluation, and regulatory aspects. Vol 10*, NJ Lowe and NA Shaath, eds., New York: Marcel Dekker Inc. 395-404.
147. Takiwaki, H, S Shirai, Y Kanno, *et al* (1994). Quantification of erythema and pigmentation using a videomicroscope and a computer. *BrJ Dermatol.* **131** (1) 85-92.
148. Bjerring, P and PH Andersen (1987). Skin reflectance spectrophotometry. *Photodermatol.* **4** (3) 167-171.
149. MacAdam, DL ed. (1981). *Color measurement: theme and variations.* Springer Series in Optical Sciences, Berlin: Springer-Verlag. .
150. Minolta Camera Co., L (1993). *Precise color communication: color control from feeling to instrumentation*, , Minolta Camera Co., Ltd: Japan.

151. Andersen, PH, K Abrams, P Bjerring, *et al* (1991). A time-correlation study of ultraviolet B-induced erythema measured by reflectance spectroscopy and laser Doppler flowmetry. *Photodermatol Photoimmunol Photomed.* **8** (3) 123-128.
152. Takiwaki, H and J Serup (1994). Measurement of color parameters of psoriatic plaques by narrow band reflectance spectrophotometry and tristimulus colorimetry. *Skin Pharmacol.* **7** (3) 145-150.
153. Andersen, PH, PW Broichmann, and H Maibach (1993). A corticosteroid, a non-steroidal anti-inflammatory drug and an antihistamine modulate *in vivo* vascular reactions before and during post-occlusive hyperaemia. *Br J Dermatol.* **128** (2) 137-142.
154. Andersen, P, K Milioni, and H Maibach (1993). The cutaneous corticosteroid vasoconstriction assay: a reflectance spectroscopic and laser-Doppler flowmetric study. *Br J Dermatol.* **128** (6) 660-665.
155. Bjerring, P, PH Andersen, and L Arendt-Nielsen (1989). Vascular response of human skin after analgesia with Emla cream. *Br J Anaesth.* **63** 655-660.
156. Feather, JW, DJ Ellis, and G Leslie (1988). A portable reflectometer for the rapid quantification of cutaneous haemoglobin and melanin. *Phys Med Biol.* **33** (6) 711-722.
157. Smith, DS, W Levy, M Maris, *et al* (1990). Reperfusion hyperoxia in brain after circulatory arrest in humans. *Anesthesiology.* **73** (1) 12-19.

158. Ferguson-Pell, M and S Haggisawa (1995). An empirical technique to compensate for melanin when monitoring skin microcirculation using reflectance spectrophotometry. *Med Eng Phys.* **17** (2) 104-110.
159. Kollias, N and A Baqer (1985). Spectroscopic characteristics of human melanin *in vivo*. *J Invest Dermatol.* **85** (1) 38-42.
160. Robertson, A (1977). The CIE 1976 Color-Difference Formulae. *Color Res Appl.* **2** (1) 7-11.
161. Storer, RA, JL Cornillot, DF Savini, *et al* eds. ( 1987). *ASTM Standards on color and appearance measurement*. Second ed. , Philadelphia: ASTM. .
162. Tuchin, VV, SR Utz, and IV Yaroslavsky (1994). Tissue optics, light distribution, and spectroscopy. *Optical Engineering.* **33** (10) 3178-3188.
163. Anderson, RR and JA Parrish (1981). The optics of human skin. *J Invest Dermatol.* **77** (1) 13-19.
164. Dwyer, T, H Muller, L Blizzard, *et al* (1998). The use of spectrometry to estimate melanin density in Caucasians. *Cancer Epidemiol Biomarkers Prev.* **7** (3) 203-206.
165. Takiwaki, H, L Overgaard, and J Serup (1994). Comparison of narrow band reflectance spectrophotometric and tristimulus colorimetric measurements of skin color - twenty three anatomical sites evaluated

by the Deraspectrometer<sup>®</sup> and the chroma meter CR-200<sup>®</sup>. *Skin Pharmacol.* **7** (4) 217-225.

166. Springsteen, W, J Leland, and TM Ricker Techguide: a guide to reflectance materials and coatings, Labsphere: North Sutton.
167. Ishihara, S (1954). *Test for color-blindness*. 11th ed, Tokyo: Kenehara Shuppan.
168. Arecchi, AV (1994-1995). Integrating sphere applications, In: *Labsphere -product catalogue*, North Sutton, NH 03260140-142.
169. Zeng, HS, C Macaulay, B Palcic, *et al* (1993). A computerized autofluorescence and diffuse reflectance spectroanalyzer system for in vivo skin studies. *Phys Med Biol.* **38** (2) 231-240.
170. Andersen, PH and P Bjerring (1990). Noninvasive computerized analysis of skin chromophores in vivo by reflectance spectroscopy. *Photodermatol Photoimmunol Photomed.* **7** (6) 249-257.
171. Archard, M (1990). Producing an ASCII two column data table, In: *ADL News*, Melbourne: Varian Australia Pty Ltd. .